Digital Signal Processing Techniques for Peak-to-Average Power Ratio Mitigation in MIMO-OFDM Systems

Thesis submitted to Loughborough University in candidature for the degree of Doctor of Philosophy.

Faisal Shaji Alharbi

Loughborough University

Advanced Signal Processing Group
Loughborough University

ABSTRACT

The focus of this thesis is to mitigate the very large peak-to-average transmit power ratios (PAPRs) inherent to conventional orthogonal frequency division multiplexing (OFDM) systems, particularly in the context of transmission over multi-input multi-output (MIMO) wireless broadband channels. This problem is important as a large PAPR generally needs an expensive radio frequency (RF) power amplifier at the transmitter due to the requirement for linear operation over a wide amplitude range and such a cost would be compounded when multiple transmit antennas are used. Advanced signal processing techniques which can reduce PAPR whilst retain the integrity of digital transmission therefore have considerable potential for application in emergent MIMO-OFDM wireless systems and form the technical contributions of this study. A literature review of key schemes for the mitigation of PAPR in single-input single-output (SISO) OFDM is provided together with comparative simulations based upon the complementary cumulative density function (CCDF). A discussion of the computational complexities of the schemes is also given. The selective mapping (SLM) technique is thereby identified as the preferred approach to overcome PAPR as it introduces no signal distortion. The SLM technique is then used for overcoming the PAPR problem in quasi-orthogonal space-time block coded (QO-STBC) MIMO-OFDM systems with four transmit antennas. Simulation studies based on the CCDF confirm the utility of the method. A combined concurrent SLM and closed-loop QOSTBC approach is then proposed for mitigating PAPR in MIMO-OFDM systems and its performance is verified by CCDF simulations. Practical issues within the feedback necessary for the closed-loop realization are also discussed. Exploitation of techniques based on cross-antenna rotation and inversion (CARI) are then studied in the context of closed-loop QO-STBC MIMO-OFDM systems. In particular, three methods are examined, successive suboptimal (SS) CARI, random suboptimal (RS) CARI and a new approach, scrambling and CARI. These techniques are again compared in terms of CCDF simulations and the novel scrambling and CARI method yields the best performance. Finally, SLM-based PAPR mitigation is proposed for the first time for use in the context of broadband multi-hop MIMO-OFDM systems. The need to use the SLM-based scheme both in the source and relay nodes is studied. Performance evaluations both in terms of CCDF and end-to-end bit error rate are presented.

Keywords: peak-to-average power ratio (PAPR), orthogonal frequency-division multiplexing (OFDM), selective mapping (SLM), cumulative complementary distribution functions (CCDFs), side information (SI), quasi-orthogonal space-time block coded (QO-STBC), multi-input multi-output (MIMO).

To the memory of my children

Khaled and Renad

ACKNOWLEDGEMENTS

I wish to express my gratitude to my supervisor, Prof. Jonathon Chambers who was abundantly helpful and offered invaluable assistance, guidance and support throughout my research and the writing of this thesis. It has been an honour to work with so highly dedicated a scientist and outstanding group leader.

I also wish to express my warmest gratitude to my mother as well as my brothers and sisters in Saudi Arabia for their permanent encouragement and support despite the long distances that separate us.

Foremost, I would like to give my special thanks to my wife and my daughter whose patient love has enabled me to complete this thesis.

STATEMENT OF ORIGINALITY

The contributions of this thesis are concerned with peak-to-average power ratio mitigation in multiple transmit antenna based wireless communication systems with particular emphasis on systems which exploit space-time block codes and collaborative relay networks. The contributions are supported by three published conference papers, one submitted conference paper and one submitted journal paper. The contributions can be summarized as follows:

In Chapter 4, a study of a PAPR reduction scheme for quasi-orthogonal space-time block-coded (QO-STBC) multi-input multi-output (MIMO) orthogonal frequency division multiplexing (OFDM) systems based on selective mapping (SLM) is presented. The reduction technique is focused upon combining the PAPRs of the transmission blocks from four antennas and exploits the associated antenna diversity gain to mitigate errors in the transmission of the side information (SI) necessary for SLM. The results have been published in:

- F. S. Alharbi and J. A. Chambers, "Peak-to-average power ratio mitigation in quasi-orthogonal space time block coded MIMO-

OFDM systems using selective mapping", Proceeding of Antennas and Propagation Conference, LAPC 2008, Loughborough, pp.157-160, 2008.

Chapter 5, builds upon the results of Chapter 4 by practically choosing the feedback angles in closed-loop QO-STBC together with the appropriate sequences within the SLM scheme. The number of bits needed to represent the feedback phase angles is reduced by exploiting the correlation across frequencies of the required rotation angles. Two symbols within the OFDM frame are either used for transmitting selected mapping SI or for PAPR mitigation, thereby retaining the diversity gain of the multiple antennas whilst being able to perform the PAPR mitigation. The results have been published in:

- F. S. Alharbi and J. A. Chambers, "A combined SLM and closed-loop QO-STBC for PAPR mitigation in MIMO-OFDM transmission", EUSIPCO 2008-16th European Signal Processing Conference, Lausanne, Switzerland, 2008.

The work in Chapter 6 is an extension to a technique called successive suboptimal cross-antenna rotation and inversion (SS-CARI) and random suboptimal (RS) CARI for the reduction of PAPR for STBC MIMO-OFDM. In SS-CARI, the input OFDM frame is partitioned into M subblocks of equal size, then subblockwise rotations and inversions across two antennas are performed. Starting from the first subblock, four different OFDM sequence sets are formed where all the other subblocks remain unchanged, then the sequence set which yields the minimum maximum (minimax) PAPR is selected and by doing this for all M subblocks successively the resulting PAPR shows better performance and similar complexity compared with the minimax SLM scheme. While in RS-CARI the sequences for each of the M subblocks are chosen randomly from amongst those used in SS-CARI, for a prescribed number of times P, and the symbol with the minimax PAPR performance is then selected for transmission. In this chapter, the application of the CARI scheme with closed loop QO-STBCs is investigated. In particular, the complexity of the CARI scheme is reduced by only considering four permutations per subblock in the context of four antennas. This consideration is also applied to the suboptimal scheme and provided a lower amount of SI while maintaining a similar level of complexity with the STBC MIMO-OFDM transmission. Furthermore, a novel algorithm called scrambling and CARI scheme is presented. It has achieved further reduction in PAPR performance than the SS and RS-CARI schemes. The results have been published and submitted respectively in:

- F. S. Alharbi and J. A. Chambers, "PAPR mitigation in closed-loop QO-STBCs using the cross-antenna rotation and inversion scheme", 8th International Conference on Mathematical in Signal Processing, Cirencester, UK, 2008.
- F. S. Alharbi and J. A. Chambers, "A new scrambled SS-CARI scheme for PAPR mitigation in closed-loop QO-STBC-MIMO-OFDM systems", submitted to the Hindawi Advances in Signal Processing journal, March, 2009.

In Chapter 7, the SLM scheme is studied to reduce the PAPR of OFDM transmission over cooperative networks with one source, one/two intermediate stage(s) and one destination. The study presents a comparison between applying the SLM scheme only on the source node and on both the source node and the intermediate stages and the effects on SI relative to the number of stages. Moreover, a simulation which shows the degradation in end-to-end bit error rate along with SI detection is presented. The results have been submitted to:

- F. S. Alharbi and J. A. Chambers, "A study of SLM PAPR mitigation in a broadband multi-hop network", submitted to the 17th European Signal Processing Conference, Glasgow, Scotland, March, 2009.

Acronyms

ASDL	Asymmetric Digital Subscriber Line
BER	Bit-Error-Rate
CCDF	Complementary Cumulative Density Function
CP	Cyclic Prefix
CSI	Channel State Information
DAB	Digital Audio Broadcasting
DAC	Digital-to-Analog Converter
DAF	Decode And Forward
DMT	Discrete Multitone Modulation
DSP	Digital Signal Processing
DVB	Digital Video Broadcasting
FDD	Frequency Division Duplex
HDSL	High-bit-rate Digital Subscriber Line
IFFT	Inverse Fast Fourier Transform

ISI	Inter-Symbol-Interference
LAN	Local Area Network
LSBs	Least Significant Bits
MIMO	Multi-Input Multi-Output
MSBs	Most Significant Bits
OFDM	Orthogonal Frequency Division Multiplexing
PAPR	Peak-to-Average Power Ratio
PAs	Power Amplifiers
PEPs	Peak Envelope Powers
PV	Power Variance
QAM	Quadrature Amplitude Modulation
QO-STBC	Quasi-Orthogonal Space-Time Block Code
RF	Radio Frequency
SI	Side Information
SISO	Single-Input Single-Output
STD	STandard Deviation
TDD	Time Division Duplex
VAA	Virtual Antenna Array
VHDSL	Very High speed Digital Subscriber Line

LIST OF SYMBOLS

$\Re(.)$	Real part of (.)
j	$\sqrt{-1}$
$s(t)$	continuous-time samples of an OFDM symbol
$s[n]$	discrete-time samples of an OFDM symbol
γ	threshold level
$(.)^*$	complex conjugation
$max[\cdot]$	maximum element
$avrg[\cdot]$	average element
$E\{\cdot\}$	expected value
$\lvert \cdot \rvert$	absolute value
N	number of subcarriers
f_c	carrier frequency
L_t	number of transmit antennas

CONTENTS

List of Figures

List of Tables

Chapter 1

INTRODUCTION

The amplitude fluctuations of a signal are commonly quantified by a scalar parameter called peak-to-average power ratio (PAPR). This quantity is defined as the ratio of the peak power relative to its mean value. For a continuous-time signal s(t) defined over $[0, T]$, its PAPR, is given by:

$$PAPR(s(t)) = \frac{P_{max}}{P_{av}} = \frac{\max\limits_{t \in [0,T]} |s(t)|^2}{E\{|s(t)|^2\}} \tag{1.0.1}$$

where max and $E\{\cdot\}$ denote respectively the maximum value and statistical expectation operator.

Figure 1.1 illustrates examples of signals having relatively high (15.38 dB) and low (6.68 dB) PAPR. At transmitters within wireless communication systems, RF power amplifiers (PAs) and digital-to-analog converters (DACs) are power limited and only perform effectively when signals passed through them are within their dynamic range (linear region). To accommodate high PAPR signals, these devices must have a large range of dynamic linearity which can result in the need for expensive devices and higher power consumption (low efficiency). Otherwise,

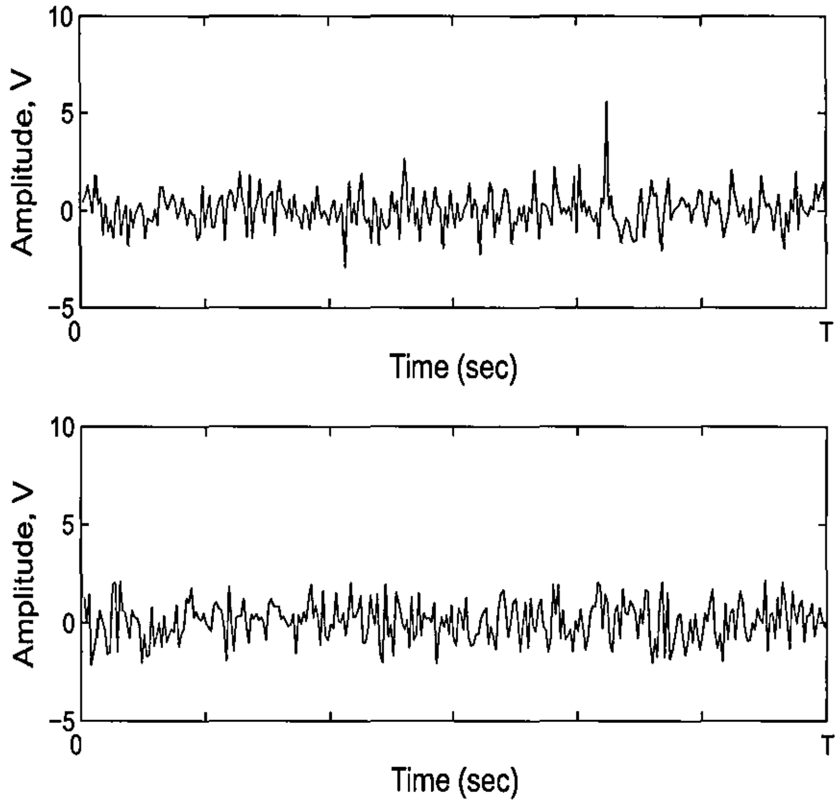

Figure 1.1. (a): Signal with a relatively high PAPR (15.38 dB). (b): and with a relatively low PAPR (6.68 dB) quantity.

they are then forced to operate in a non-linear region creating in-band distortion which induces increased bit-error rate (BER) within the in-band transmission and out-of-band noise which causes adjacent channel interference [2]. To avoid non-linearity effects, the input signals have to be backed-off to the linear region of PAs. Figure 1.2 shows a typical input-output power response for a PA, with the associated input and output back-off regions [1] (IBO and OBO, respectively).

The goal of this thesis is to mitigate the problem of high PAPR whilst

[1]An example $P_{out,max}$ for a 3G power amplifier used in the handset is 120mW and the output back-off (OBO) would be 10 dB down relative to this maximum value.

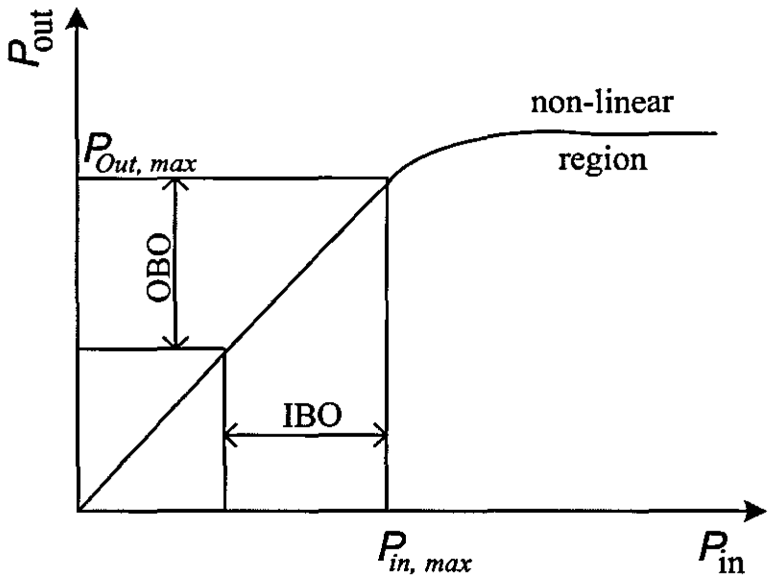

Figure 1.2. A typical radio frequency power amplifier response, typical units in mW .

retaining the integrity of the digital transmission by applying advanced digital signal processing (DSP) techniques as depicted in Figure 1.3.

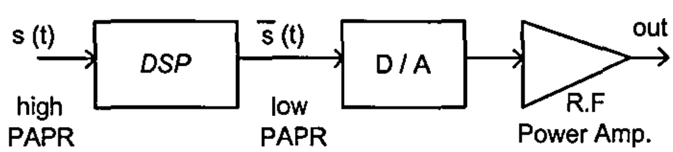

Figure 1.3. Proposed PAPR mitigation model.

Figure 1.3 only shows a single channel situation, however, the multi-channel context is the focus of this thesis.

1.1 Multiple-input multiple-output systems

Wireless communications have grown tremendously in recent years, the exploitation of wireless local area networks (LAN) and mobile telephones have been two major drivers for the growth [3]. Traditionally, wireless communication systems use a single transmitter and a single receiver to create a single-input single-output (SISO) system. The received wireless signal is however typically formed as a result of many time-varying paths between the transmitter and the receiver. These multipaths are due to reflection, refraction, diffraction and scattering mechanisms within the radio environment. Time-variation is a consequence of the relative motion between the transmitter and the receiver. If the multipath signals are merged in phase, the resultant signal would be intensified, otherwise, the resultant signal is weakened due to out of phase combination. This generally time-varying phenomenon is called channel fading. In digital communication systems, fading can increase the bit-error rate (BER) which has a direct impact on system performance and ultimately the quality of service provided to the user.

In recent years, significant progress has been made to overcome the effect of fading in communication systems [4]. Multiple-input multiple-output (MIMO) technology, as an example of this advancement, uses multiple antennas at the transmitter and multiple antennas at the receiver to theoretically take advantage of independent multi-path and fading to improve communication performance and enhance the spectral efficiency (bits/s/Hz). Inter-antenna correlation in practical point-to-point MIMO systems can reduce the performance advantage. Moreover, the need for higher speed wireless LANs and multimedia services has led to the demand for wireless technologies, in particular MIMO, to deliver higher capacities [5]. Typical MIMO-type configurations for wireless links along with a SISO link are illustrated in Figure 1.4. The presence of multiple independent links introduces spatial diversity and thereby the potential for improved end-to-end performance.

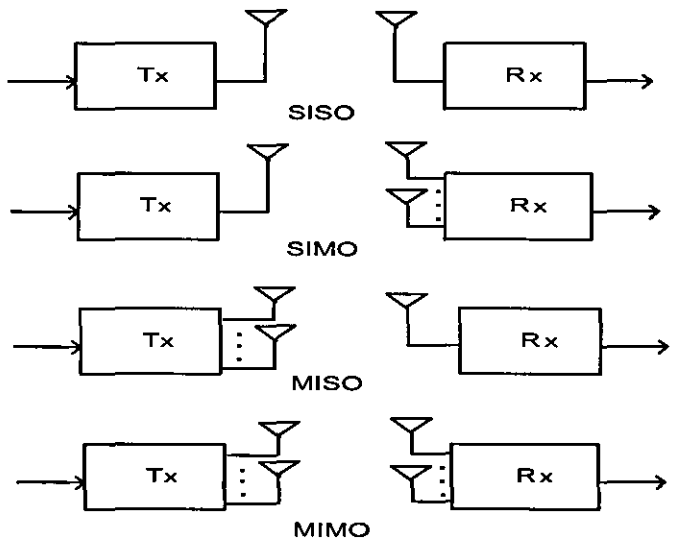

Figure 1.4. Antenna configurations in wireless systems (SISO: single-input single-output, SIMO: single-input multiple-output, MISO: multiple-input single-output, MIMO: multiple-input multiple-output).

The implementation of one part of a MIMO system on small devices may not be practical due to the limited size of these devices. Cooperative diversity [6] is another way to provide the benefits of diversity without implementing multiple antennas on one terminal. In such distributed systems surrounding terminals collaborate to form a virtual MIMO antenna array [7].

Multicarrier modulation such as orthogonal frequency division multiplexing (OFDM) is a powerful technique to handle impairments specific to frequency selective wireless communication channels [8]. OFDM modulation divides a broadband channel into many parallel sub channels, each of them is centered at a frequency which is an integer multiple of a fundamental frequency and the symbol rate within each sub channel is reduced. This ensures that even though the subcarriers overlap they do not interfere with each other provided the channel is static over the OFDM symbol and there is perfect synchronization between the transmitter and receiver. This results in a high spectral efficiency. Moreover, channel equalization is simple as OFDM may be viewed as using many parallel low symbol rate channels for transmission.

MIMO systems combined with the OFDM method provide a feasible physical layer technology for the next generation of communication systems, particularly due to the low computational complexity of the fast Fourier transform (FFT). The promise of higher data rates with increased spectral efficiency makes MIMO-OFDM especially attractive in wireless communications when systems operate in multi-path environments. For this reason, wireless standards such as IEEE 802.16 WiMAX (OFDM symbol size 256) and IEEE 802.11a,g WiFi (OFDM symbol size 64) [9] have recently been adopted and are in use. The IEEE 802.16j working group is also considering collaborative operation for future WiMax systems. OFDM is also exploited in most wideband transmissions such as digital audio broadcasting (DAB) [10], digital video broadcasting (DVB) [11], high-bit-rate digital subscriber line (HDSL), asymmetric digital subscriber line (ADSL) and very high speed digital subscriber line (VHDSL).

1.2 Research Objective

OFDM technology has gained considerable interest for high data rate transmission application due to its high spectral efficiency achieved by a large number of subcarriers and its robustness against frequency fading channels with a moderate system complexity. However, beyond all these advantages, one of the major limitations of OFDM is the high PAPR of its transmitted signals. These large peaks occasionally reach the power amplifier saturation region resulting in in-band and out-of-band distortions. To avoid this problem, very efficient and expensive amplifiers and DACs with wide amplitude linear operation range can be required.

In MIMO-OFDM systems PAPR becomes even more important since there are multiple transmit antennas each of which would require its own RF power amplifier and DAC. Therefore, methods to reduce the overall PAPR across all the antennas will be considered in this thesis. The main objective of this thesis is to propose PAPR reduction algorithms suitable for quasi-orthogonal space-time block coded (QO-STBC) MIMO-OFDM systems with four transmit antennas. This number of transmit antennas is appropriate for a practical system, and previous work has generally only considered two antenna open-loop systems. A quasi-static channel means that the path gains are constant within the OFDM block and only vary from block-to-block. The proposed algorithms will be implemented in the frequency-domain so that they do not introduce in-band or out-of-band distortion, as simple time-domain clipping would. Since these techniques require side information (SI) to be sent to the receiver in order to recover the original signal and maximize diversity performance, it is very important to protect the SI as an error in the SI will result in losing the whole information block.

Therefore, utilizing the spatial diversity properties of MIMO systems will be a major issue.

Finally, a study on how to mitigate the PAPR in the context of emerging broadband multi-hop MIMO-OFDM systems will be included.

1.3 Organization of the thesis

The chapters in this thesis are organized as follows:

Chapter 2 introduces OFDM systems and presents a detailed overview of the PAPR problem for OFDM signals. The chapter outlines the statistical description of PAPR as well as its theoretical bounds.

Chapter 3 discusses and compares a broad range of techniques for the mitigation of PAPR studied in the literature and used in SISO-OFDM; such techniques are organized into three classes: probabilistic techniques, clipping and filtering, and coding techniques. These three distinct classes of methods can be identified; each with their respective advantages, disadvantages and complexities. The study is also carried out with the aid of extensive simulations of their operation, performed based upon the complementary cumulative density function (CCDF). This chapter has been designed to be open enough to allow new researchers and engineers to select the appropriate PAPR method based on their requirements and specific constraints.

Next, in Chapter 4 a study of PAPR reduction schemes for open-loop quasi-orthogonal space-time block coding is presented. Such reduction techniques are based upon combining the PAPRs of the transmission blocks from four antennas and exploiting the associated antenna diversity gain to mitigate errors in the transmission of the necessary side information. Comparisons are made with single antenna and conventional OFDM schemes. In this chapter a method for positioning the SI to maximize frequency diversity over the four transmit antennas is also suggested. Furthermore, performance improvement is demonstrated in terms of comparison with a conventional OFDM SLM-based scheme in terms of average BER and probability of SI detection.

Chapter 5 presents an extension of the work proposed in [12] to closed-loop QO-STBCs and analyzes the PAPR over four transmit antennas. This chapter illustrates that combining SLM with QO-STBCs can improve the overall bit-error rate (BER) performance and increase the reliability of side-information (SI) at the expense of the PAPR reduction gain. In addition, it discusses for the first time the major challenges in PAPR mitigation in closed loop QO-STBCs.

In Chapter 6, two conventional algorithms based on the cross-antenna rotation and inversion (CARI) approach are presented in combination with closed loop QO-STBCs. These proposed schemes perform PAPR mitigation whilst maintaining the diversity gain of the multiple antennas. It is also shown that by considering only four permutations the PAPR can be decreased with limited complexity. What is more, a new scrambling SS-CARI scheme for closed loop operation is proposed and represented in pseudo-code form to clarify the algorithm within the chapter.

Chapter 7 introduces a study to minimize the PAPR in cooperative networks by using the SLM technique. It investigates PAPR mitigation when this technique is applied only to the source node, as compared to when the full technique is utilized in both the source and relay nodes. Both BER and complexity performances are considered.

Finally, Chapter 8 summarizes what was achieved in the thesis study and gives some suggestions for future research direction.

Chapter 2

FUNDAMENTALS OF OFDM SYSTEMS AND PAPR MITIGATION

The present chapter consists of a brief introduction to orthogonal frequency division multiplexing (OFDM). Next, a further study of peak-to-average power ratio (PAPR) and the cause of this problem is presented. Additionally, the statistical properties of PAPR and its theoretical bounds are given in this chapter. Finally, a chapter summary is provided.

2.1 OFDM systems

OFDM is a relatively new digital modulation technique which divides the available spectrum into many subcarriers, instead of using only one carrier, and each one is modulated by a low rate data stream. The peak power of the OFDM signal is increased according to the number of subcarriers. OFDM is selected for practical systems due to its high spectral efficiency and immunity to multipath fading and impulsive noise. The general concept was first introduced in 1971 [13], but it is only in the last decade, with the development of digital signal processing (DSP) that applications have appeared [14], in particular through the use of the FFT.

The uncoded OFDM transmit signal is generated by the process shown in Figure 2.1. In this process, the input data go through a serial to parallel converter, then there is a mapping from the original symbols to the input to the inverse Fourier transform (IFFT). This mapping is typically to a complex quadrature amplitude modulation (QAM) constellation to enhance spectral efficiency. The normalized frequency spacing between any adjacent subcarriers is $2\pi/N$, where N is the number of subcarriers. This can be achieved by using the IFFT. The reason for using the IFFT is related to the fact that the bandwidth is divided into a number of orthogonal sub channels and its low computational complexity. Then, the input data are converted to a time domain signal through the IFFT and in order to mitigate inter symbol interference (ISI) in OFDM a cyclic prefix (CP) is added which is a repeat of the last few symbols of the output of the IFFT. The addition of the CP also forces the effective channel convolution matrix to be cyclic so that the FFT matrix diagonalizes the channel. The output data from the IFFT go through a parallel-to-serial converter and then form the input to a DAC. The analog signal is then amplified and converted to the radio frequency (RF) before being transmitted from the transmitting antenna into the channel. As a result, the OFDM symbol in the time domain is generated as an N-subcarrier system by adding the weighted subcarrier components represented as:

$$s(t) = \frac{1}{\sqrt{N}} \sum_{k=0}^{N-1} c_k e^{j2\pi tk/N} \ , 0 \leq t \leq N-1 \qquad (2.1.1)$$

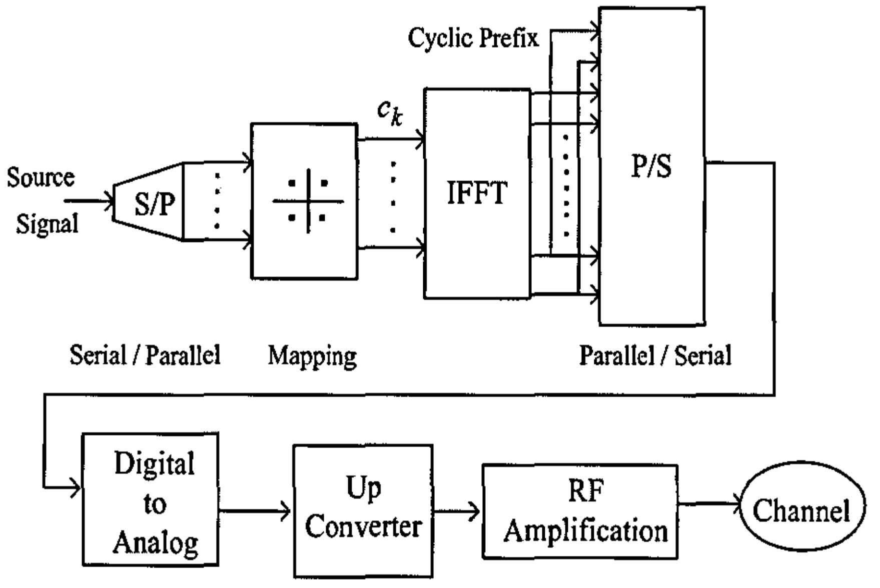

Figure 2.1. Basic OFDM transmitter architecture.

where c_k is the complex symbol in the frequency domain, and t denotes continuous-time.

The signal s(t) is real only when the c_k coefficients have conjugate symmetry, i.e. $c_k = c^*_{N-k}$; no such assumption is made in this thesis, however, so s(t) is assumed complex. In practice, the baseband modulation is applied in the digital domain using an oversampling version of s[n] which is given by:

$$s[n] = \frac{1}{\sqrt{N}} \sum_{k=0}^{N-1} c_k e^{j2\pi nk/LN} \ , n \in [0, LN-1] \qquad (2.1.2)$$

where L is the oversampling factor typically four, and n is the normalized discrete time index. Notice that when $L = 1$ s[n] is the Nyquist sampling version of s(t).

The channel in the wireless environment is typically characterised by multi-path propagation, so that in the frequency domain the channel response will be frequency selective. However, in reality the mobile might be moving and therefore the shape of the frequency response can be changing, as a result of fading. In this work, the channel is assumed to be quasi-static, so that within an OFDM symbol the channel coefficients remain fixed; perfect synchronization is also assumed between the transmitter and receiver.

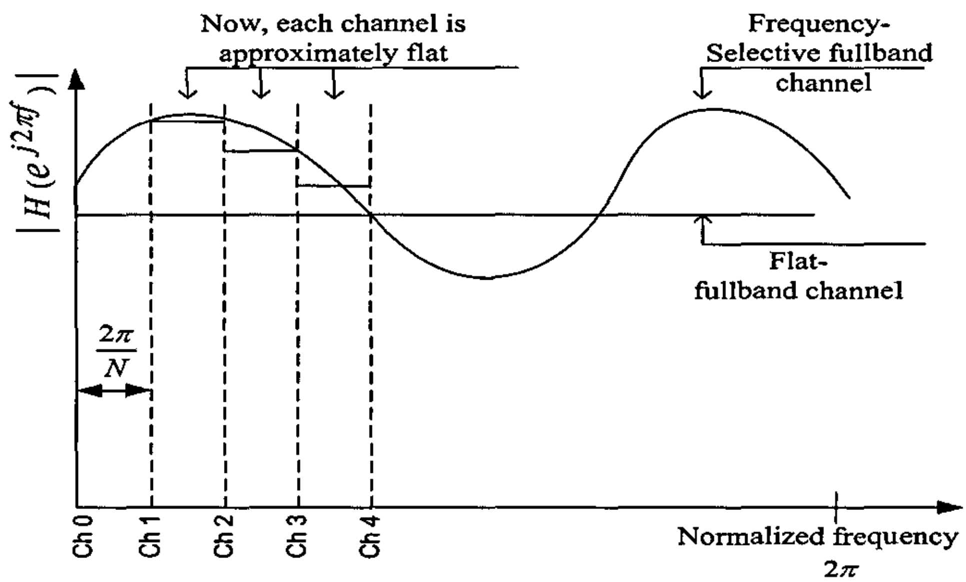

Figure 2.2. The magnitude response of a frequency selective channel in OFDM divided into a number of channels with small bandwidth, which can be assumed to have flat frequency response.

The OFDM system is designed to deal with a frequency selective channel, where the channel is divided into a number of much narrower bandwidths as shown in Figure 2.2. Assume $N = 64$ symbols, and that these symbols are generated at a single time instead and all 64 values form the input to the IFFT with the user data transmitted simultaneously on the sub channels. Effectively, symbol one goes through the first subchannel (Ch 0, as shown in Figure 2.2) of the original wideband frequency selective channel which is centered at DC (zero frequency); symbol two goes through the second channel (Ch 1) centered at the fundamental frequency and so on, with each symbol passing through individual narrow channels, which are harmonically related because of the IFFT.

The spectra of the subcarriers overlap each other as shown in Figure 2.3 which makes OFDM more spectrally efficient as compared to conventional multicarrier communication systems. In particular, in the frequency domain plots Figure 2.3 (b), (d) and (f) show the peaks of one frequency correspond to the zeros of other frequencies so that no interference is caused, this is crucially dependent upon perfect synchronization between the transmitter and the receiver.

In Figure 2.4, the assumption is that there are two paths between the transmitter and the receiver. The delay through path one is given by T_1 while the delay through path two is given by T_2. The CP is chosen to be of length equal to T_2 which because the two signals are of the same frequency means the phase of the top one at time T_1 is identical to the phase of the second one at T_2. The purpose of using the CP between OFDM frames is to eliminate intersymbol interference (ISI), thereby mitigating the effect of the wireless channel delay spread.

The symbol c_1 in Figure 2.5 can be regarded as passing through a complex scalar channel of $H(e^{j2\pi f_1})$, where y_1 is obtained at the output. In the noise free case, this must be multiplied by the inverse of this channel in order to obtain the same symbol that had been transmitted. A minimum mean square error equalizer can be used in the presence of noise.

From Figure 2.5 it can be said that the equalisation or the removal of the effect of the channel is simply based upon multiplication at the receiver by the inverse of the channel at that particular frequency which is importantly computational simple. The formal definition of PAPR is next considered.

2.2 Definition of Peak-to-Average Power Ratio (PAPR)

An important limitation of OFDM is that it suffers from a high peak-to-average power ratio (PAPR)[1] resulting from the coherent sum of several carriers. This implies that the RF power amplifier (PA) in the transmitter requires a large input back off, see Figure 1.2, to operate efficiently in its linear region and thereby avoid distortion effects, including non orthogonal intermodulation terms [15]. High PAPR also affects DACs negatively and may lower the range of transmission. PAPR can be defined for a sampled signal as follows [16]:

$$PAPR(s[n]) = \frac{\max\limits_{0\leq n\leq LN-1} |s[n]|^2}{E\{|s[n]|^2\}} \tag{2.2.1}$$

[1]PAPR is also called *peak-to-mean envelope power ratio* (PMEPR) [1].

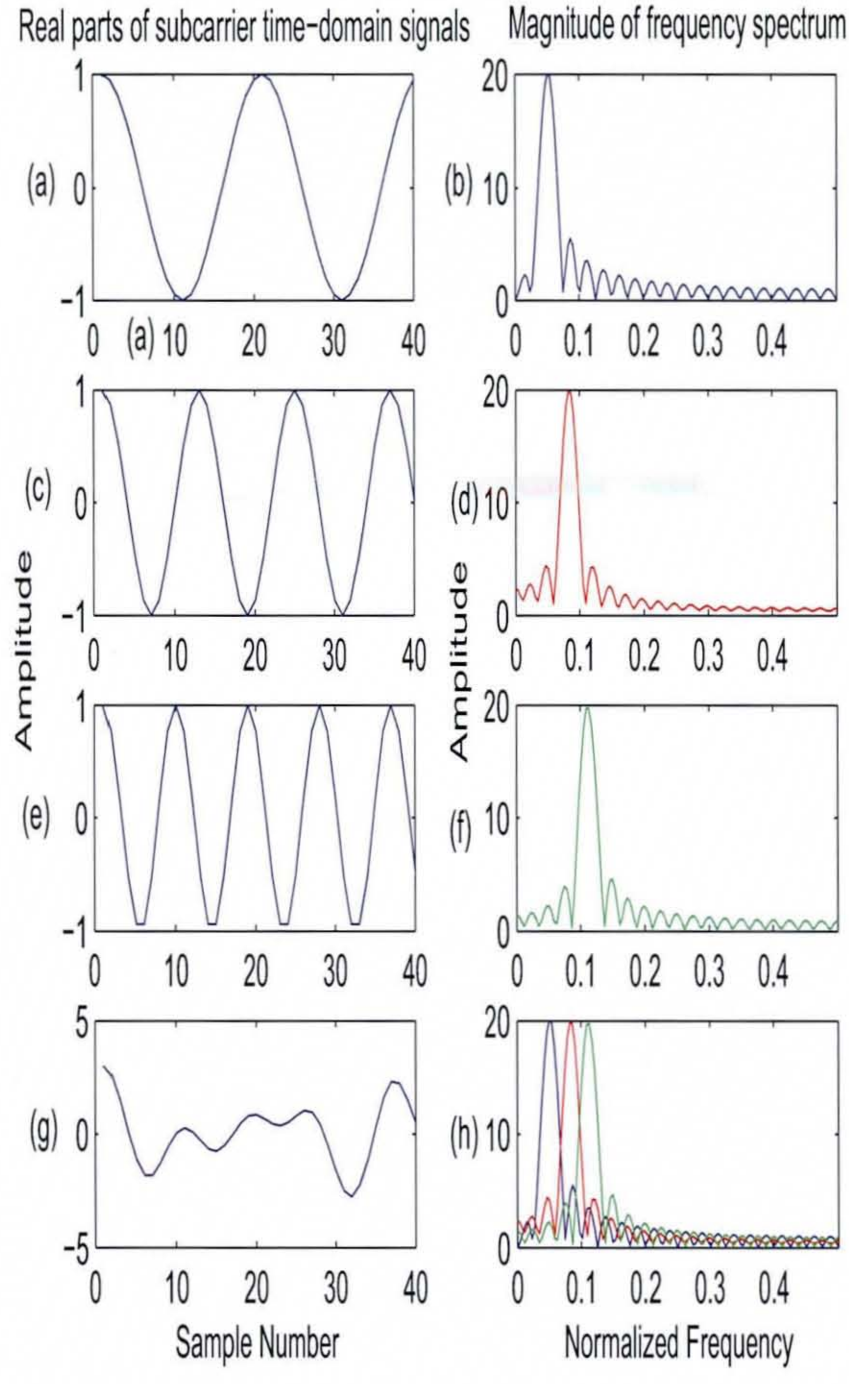

Figure 2.3. (a,c,e): The real parts of three subcarrier signals in the time domain. (b,d,f): Three corresponding magnitude frequency specta. (g): Addition of the three subcarriers. (h): Common display of the three magnitude frequency spectra.

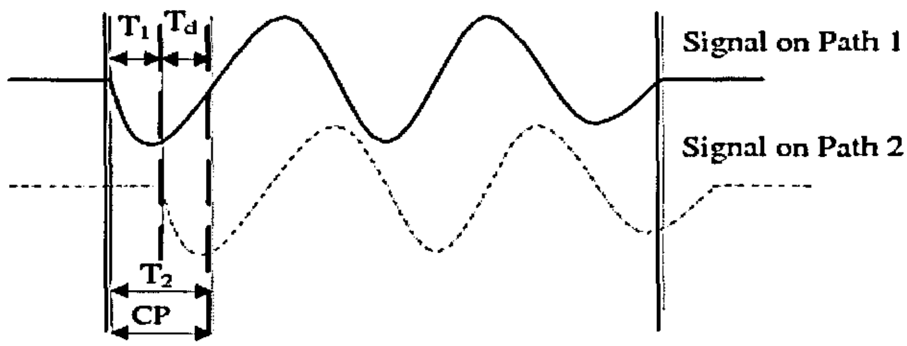

Figure 2.4. The signal measurements over a two path channel as a function of time showing the path delays together with a $CP = max(T_2)$.

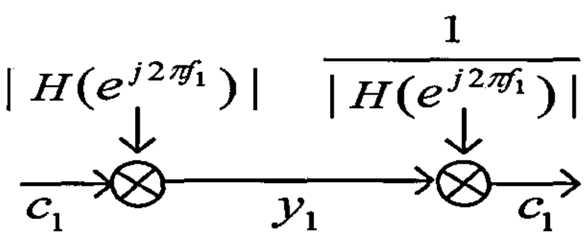

Figure 2.5. The processing of a symbol in a noise free model of a single subcarrier of an OFDM system.

where max[·], $E\{\cdot\}$ and $|\cdot|$ represent respectively the maximum element, the statistical expected value operator and the absolute value of the input symbols. Since nonlinear distortion occurs in the analog domain (passband domain), PAs have therefore to be designed around the PAPR of the passband signal. So, it is desirable to describe the passband PAPR from the mathematical point of view. Given that the passband signal is:

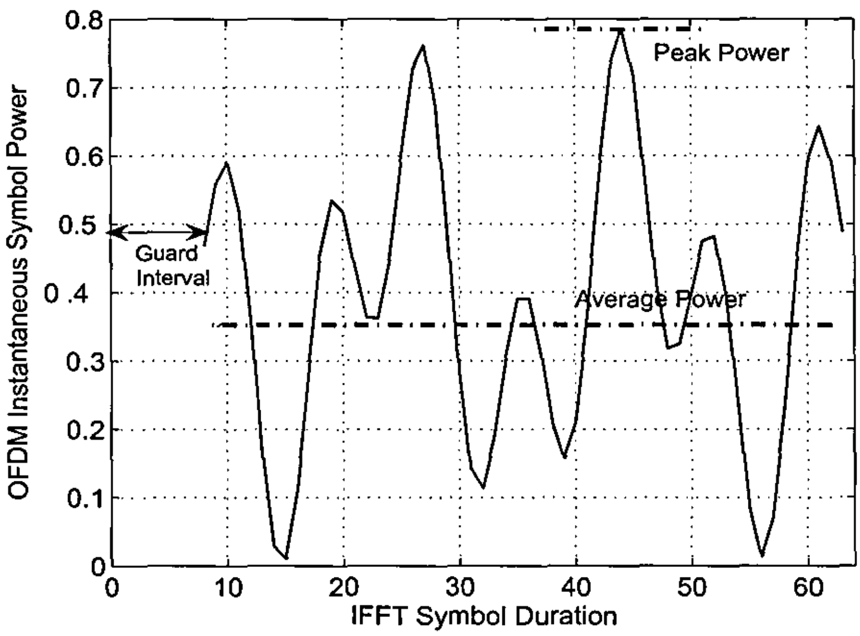

Figure 2.6. Typical instantaneous power profile of a time-domain signal highlighting the average and peak values.

$$\begin{aligned} s_{PB}(t) &= \Re\{s_{BB}(t)e^{j2\pi f_c t}\} \\ &= \Re\{s_{BB}(t)\}\cos(2\pi f_c t) - \Im\{s_{BB}(t)\}\sin(2\pi f_c t) \\ &= \{s_I(t)\}\cos(2\pi f_c t) - \{s_Q(t)\}\sin(2\pi f_c t) \end{aligned} \tag{2.2.2}$$

where $\Re\{\cdot\}$ is the in-phase (real part) component and $\Im\{\cdot\}$ is the quadrature (imaginary part) component.

Since the center frequency, f_c, is always higher than the signal bandwidth, the passband maximum coincides with the baseband maximum [17]:

$$\max|s_{PB}(t)| \approx \max|s_{BB}(t)| \tag{2.2.3}$$

The average power of the passband signal is:

$$\begin{aligned} E\left[|s_{PB}(t)|^2\right] &= E\left[|\Re\{s_{BB}(t)e^{j2\pi f_c t}\}|^2\right] \\ &= E\left[|\{s_I(t)\}\cos(2\pi f_c t) + \{s_Q(t)\}\sin(2\pi f_c t)|^2\right] \\ &= 0.5\ E\left[\{s_I(t)\}^2 + E\{s_Q(t)\}^2\right] \\ &= 0.5\ E\left[|s(t)|^2\right] \end{aligned} \tag{2.2.4}$$

From (2.2.3) and (2.2.4) the passband PAPR is approximately 3 dB higher than that of the baseband signal, i.e.

$$PAPR\{s_{PB}(t)\} \approx 2PAPR\{s_{BB}(t)|\} \tag{2.2.5}$$

It should be noted that throughout the proceeding chapters, all PAPR quantities will be given for the baseband signal.

2.3 Statistical Properties of PAPR

Assume that $\{c_k\}_{k=0}^{N-1}$ are stationary with variance σ^2 and that c_k and c_m are uncorrelated for $k \neq m$. Based on the central limit theorem, $\{s[n]\}_{n=0}^{N-1}$ are approximately independent and identically distributed complex Gaussian when N is large [1], each with zero mean and variance 0.5. In this case, the amplitude of c_k has a Rayleigh distribution, where for convenience c_k is denoted as s:

$$f(s) = \frac{2s}{\sigma_s^2} e^{-s/\sigma_s^2} \tag{2.3.1}$$

The probability that the magnitude of one value of the OFDM symbol, $|s[n]|$, does not exceed a certain amplitude threshold T_h can therefore be calculated as:

$$\begin{aligned} Pr\{|s[n]| \leq T_h\} &= \int_0^{T_h} f(s)ds \\ &= 1 - e^{(\frac{-T_h^2}{\sigma_s^2})} \end{aligned} \tag{2.3.2}$$

The probability that at least one value of an entire OFDM symbol exceeds a certain threshold can be given by:

$$\begin{aligned} Pr\{|\mathrm{s}[n]| > T_h\} &= 1 - Pr\{\max_{0 \leq n \leq N-1} |s[n]| \leq T_h\} \\ &= 1 - (Pr\{|s| \leq T_h\})^N \\ &= 1 - (1 - e^{(\frac{-T_h^2}{\sigma_s^2})})^N \\ &= 1 - (1 - e^{-\gamma})^N \end{aligned} \tag{2.3.3}$$

In Figure 2.6, the guard interval corresponds to the time-domain region where the CP has been removed[2]. It should be noted that the PAPR of

[2]Note that CP does not affect the PAPR, since it is a repetition of the last part of the time-domain signal.

a continuous time OFDM signal cannot be computed precisely by using an ordinary IFFT in the optimization. In this case, signal peaks can be missed and PAPR reduction estimates are unduly optimistic. Using a longer IFFT, i.e. interpolation, with typically four times oversampling is effective in ensuring that PAPR is actually estimated. This is confirmed in Figure 2.7 where it shows that the maximum peak of the output of the longer IFFT is higher than that for the non interpolated IFFT. This higher value of PAPR is a more accurate representation of the true PAPR of the underlying continuous time OFDM signal. Representation of interpolation in the frequency-domain is depicted in Figure 2.8. In this figure the length of the IFFT is assumed to be 16 and the original samples are shown on the right-hand side with solid dots; the extra zeros are added on the left-hand side with clear dots. From (2.3.3), it is evident that PAPR occurrence grows as the number N of subcarriers grows. Figure 2.9 is a plot which shows that as the number of subcarriers increases the probability level of the PAPR increases. In this plot, the y-axis corresponds to the complementary cumulative density function (CCDF) which is the probability that the PAPR is greater than a particular γ as in (2.3.3). The x-axis is the particular value of γ in dB. In this figure, these plots for N = 64, 128 and 512 are shown and it reveals that as N increases the CCDF moves to the right in the plot. Methods to perform PAPR reduction are next considered.

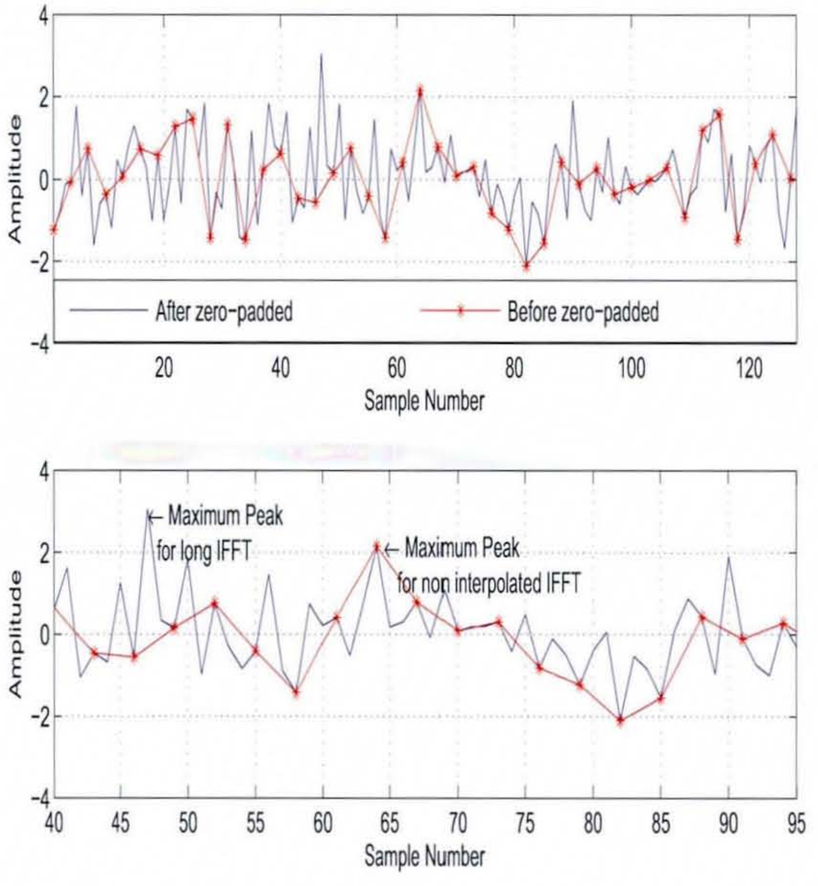

Figure 2.7. (a): OFDM symbol sampled at the Nyquist frequency and oversampled by factor of four. (b): zoom in of (a) over the range 40 to 95.

2.4 PAPR Reduction

The simplest way of removing PAPR is by using time-domain clipping. Therefore, if the maximum amplitude of the signal which is allowed is known then any amplitude which is bigger than that level is just clipped. Clipping is the simplest technique in the sense of having lowest complexity but it is very crude in terms of overall bit-error-rate (BER) performance. This is because by performing the clipping in the

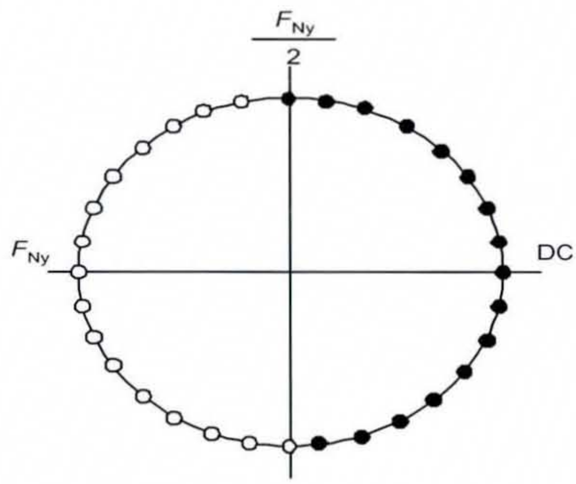

Figure 2.8. Representation of interpolation in the frequency-domain, where DC is zero frequency and F_{Ny} is Nyquist frequency.

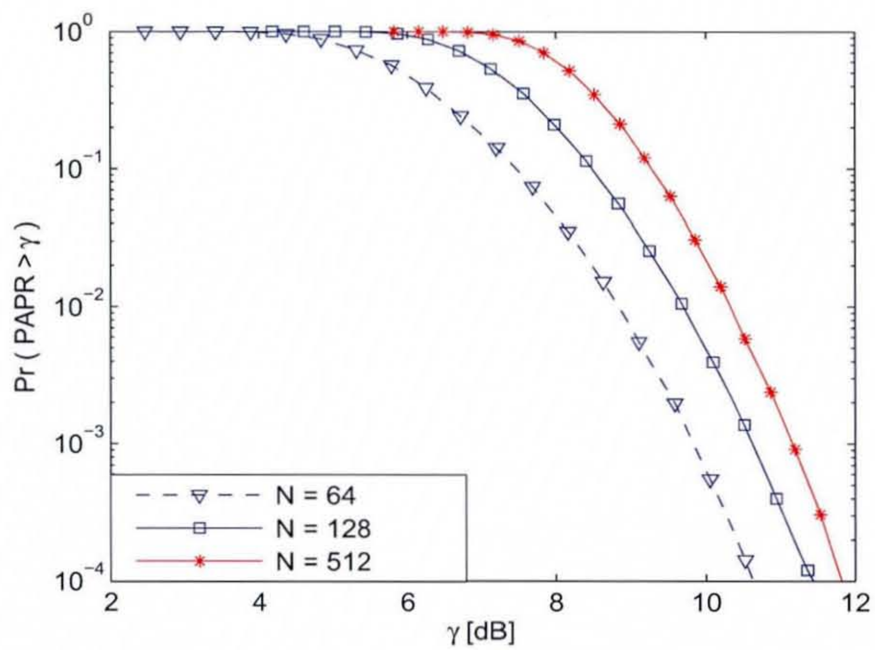

Figure 2.9. CCDF of PAPR for a QPSK modulated OFDM system for different values of N.

time-domain, it will introduce extra frequencies or degradation in the frequency-domain which makes the decoding of the original symbols more difficult.

In general, the larger the constellation becomes the bigger the effect that the degradation is likely to have due to the reduction in inter symbol amplitude spacing. However, the spectrum distortion can be

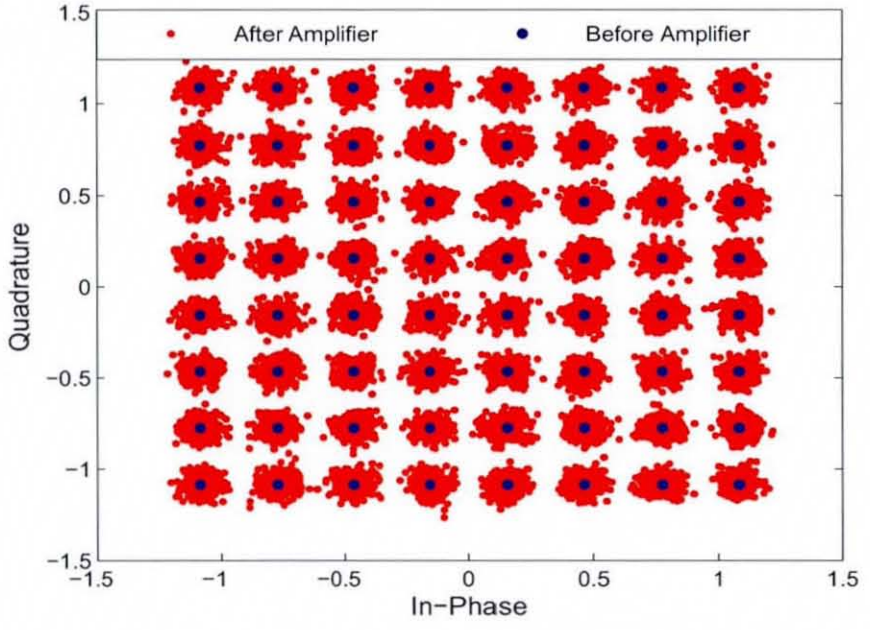

Figure 2.10. Effect of 3 dB clipping for 1000 OFDM symbols of length 512 with 64 QAM, notice the perturbations in the received constellation. Note, the length of the transmitted sequence was such that not all members of the 64 QAM constellation were transmitted.

mitigated either by filtering or by moving the spectrum from DC to Nyquist [2] and then by implementing the distortion or the processing at that point and thereby ensuring that the impact will be less than that performed around the DC frequency. In Figure 2.10 the constellations of the original and the clipped signal are shown. It is clear that with performing clipping 3 dB down relative to the peak of the original signal amplitude, the effect in the time domain has shifted the position of the points in the constellation away from their ideal location and as the clipping level increases, the movement away from these values will generally increase. This would impact upon decoding performance particularly in the presence of channel noise.

2.5 Theoretical Bounds on PAPR

As outlined in Section 2.1, PAPR occurs due to the large number of independent subcarriers with random phase that add together at the modulator. Thus, it is desirable to know the bounds of this phenomenon. In this section, a theoretical analysis for the upper and lower bounds achieved by the most common modulation techniques used in OFDM systems is given.

M-ary PSK-OFDM: In the case of an M-ary PSK-OFDM modulated signal, the output signal has the same energy constellation. Thus, the $|c_k|s$ in (2.1.2) are equal and the peak power can be written as:

$$\max_{0\leq n\leq LN-1} |s[n]|^2 = \max_{0\leq n\leq NL-1} \left| \frac{1}{N} \sum_{k=0}^{N-1} c_k e^{j2\pi nk/LN} \right|^2 \tag{2.5.1}$$

However, the maximum peak can be upper bounded as follows:

$$\begin{aligned} \max_{0\leq n\leq LN-1} |s[n]|^2 &\leq \left(\frac{1}{N} \sum_{k=0}^{N-1} |c_k|^2 \right)^2 &(2.5.2)\\ &\leq A^2 &(2.5.3) \end{aligned}$$

while with Parseval's theorem [18]:

$$\sum_{n=0}^{N-1} |s[n]|^2 = \frac{1}{N} \sum_{k=0}^{N-1} |c_k|^2 \tag{2.5.4}$$

and if both sides are divided by N, the average power of the OFDM signal becomes:

$$\begin{aligned} E\{|s[n]|^2\} &= \frac{1}{N}\{E|c_k|^2\} \\ &= \frac{A^2}{N} \end{aligned} \tag{2.5.5}$$

Finally, the PAPR of s[n] can be easily computed as follows:

$$\begin{aligned} PAPR(s[n]) &= \frac{\max\limits_{0 \le n \le LN-1} |s[n]|^2}{E\{|s[n]|^2\}} \\ &\le \frac{A^2}{A^2/N} \\ &\le N \end{aligned} \tag{2.5.6}$$

The importance of this result is that the PAPR of an M-ary PSK-OFDM symbol is always less than or equal to the number of subcarriers.

M-ary QAM-OFDM: Since the M-ary QAM modulated OFDM signal has different power levels over its constellation points, the worst case of PAPR value depends upon the choice of the signal points over different subcarriers. Defining the constellation points as $(\pm\sqrt{m}A, \pm\sqrt{m}A)$, where m = 1,...,$M$-1 and assuming data symbols occur with equal probability, the variance σ_s^2 for an M-ary QAM constellation is given by [4]:

$$\sigma_s^2 = \frac{2A^2(M-1)}{3} \tag{2.5.7}$$

and repeating the derivation in (2.5.4), the ensemble average power for MQAM is given by:

$$E\{|s[n]|^2\} = \frac{2A^2(M-1)}{3N} \tag{2.5.8}$$

Since the highest power is considered as the worst case, the maximum peak in MQAM is expressed as:

$$\overline{P}_{max} = 2A^2(\sqrt{M}-1)^2 \tag{2.5.9}$$

and hence the minimal envelope power becomes:

$$\overline{P}_{min} = 2A^2 \tag{2.5.10}$$

From (2.5.8), (2.5.9) and (2.5.10), the boundaries of the PAPR can be written as:

$$\frac{3N}{M-1} \leq PAPR(s[n]) \leq \frac{(3N\sqrt{M}-1)^2}{M-1} \tag{2.5.11}$$

and similar to M-ary PSK, the PAPR for the M-ary QAM is proportional to the number of subcarriers, N. However, it was shown in Figure 2.9 that the statistical distribution is not very sensitive to this relationship. Furthermore, the CCDF for a large number of N is less sensitive to an M-ary QAM modulation scheme, as shown in Figure 2.11. Notice that QPSK will be the modulation method used throughout this thesis as it is commonly adopted within wireless systems due to its spectral efficiency and simple decoding.

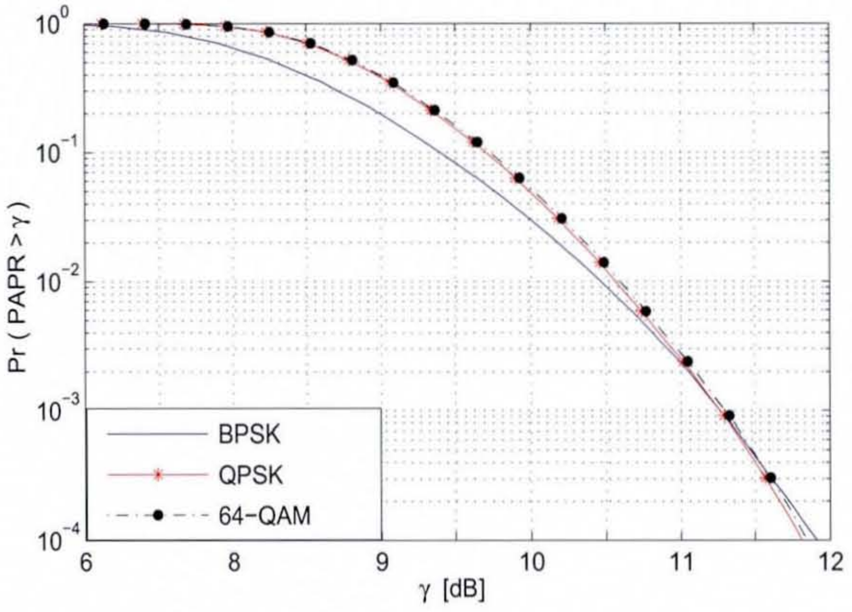

Figure 2.11. CCDF for N = 256 and different modulation schemes.

Lower Bound: The minimum theoretical PAPR is achieved only when the peak power becomes equal to the mean power, i.e., unity. Many studies [19] have shown that complex OFDM signals with PAPR close to unity exist if the number of subcarriers, N, is large. The lower bound on PAPR is given by [19]:

$$PAPR_{min} = 1 + 2/N \tag{2.5.12}$$

The choice of phases which yield a nearly minimal PAPR for a multitone signal has been studied by several researchers such as Rudin phases [20], Newman phases [21] , Schroeder phases [22], and Narahashi phases [23]. Nevertheless, none of these studies approach the optimal minimal value. However, the work in [19] showed a result close to the theoretical minimum at the cost of using several iterative algorithms. All algorithms have in common that they start with an initial phase vector which is modified through a number of optimization process iterations. This optimization differs from one algorithm to another depending on the cost function used. However, the iteration of these algorithms stops once the crest factor[3] (CF) cannot be reduced any further.

2.6 Summary

OFDM has become a popular technique for high speed data transmission in frequency-selective SISO radio channels. However, its time-domain signal suffers from large envelope variations which limited its applications. Single carrier frequency domain equalization schemes overcome this problem however their computational complexity is not symmetric between the transmitter and receiver so are not considered in this thesis. The definition of baseband and passband PAPR as well as the theoretical bounds on PAPR and its statistical characteristics were presented. It was shown that the most straightforward PAPR reduction method can be performed by clipping the high amplitudes

[3]The square root of the PAPR is often called the crest factor (CF).

of the OFDM signals. However, although this method is simple and low complexity, it causes distortion resulting in increased BER. Other methods to perform PAPR mitigation are therefore introduced in the next chapter.

Chapter 3

LITERATURE REVIEW

Chapter 2 explained the fundamentals of orthogonal frequency division multiplexing (OFDM) and defined the main drawback characterized by peak-to-average power ratio (PAPR). Moreover, statistical properties of the PAPR of an OFDM signal as well as its theoretical bounds were presented. This chapter provides a survey for up-to-date PAPR reduction techniques proposed in the literature for single-input single-output-OFDM (SISO-OFDM) systems. Such methods will be categorized and the various techniques are explained along with their potential drawbacks. However, more recent work in terms of applying PAPR mitigation in multiple-input multiple-output-OFDM (MIMO-OFDM) systems is given in [12], [24], [25] and [26]. A description of these works will be given in more detail in the later chapters.

3.1 Probabilistic Techniques

3.1.1 Partial Transmit Sequence (PTS) Technique

In the partial transmit sequence (PTS) technique [27], the input data frame of an OFDM symbol of length N is divided into M sub-blocks which are combined to minimize the PAPR. A PTS transmitter is shown in Figure 3.1. Define the data block vector $\mathbf{C} = [c_0, c_1, ...c_{N-1}]^T$ where

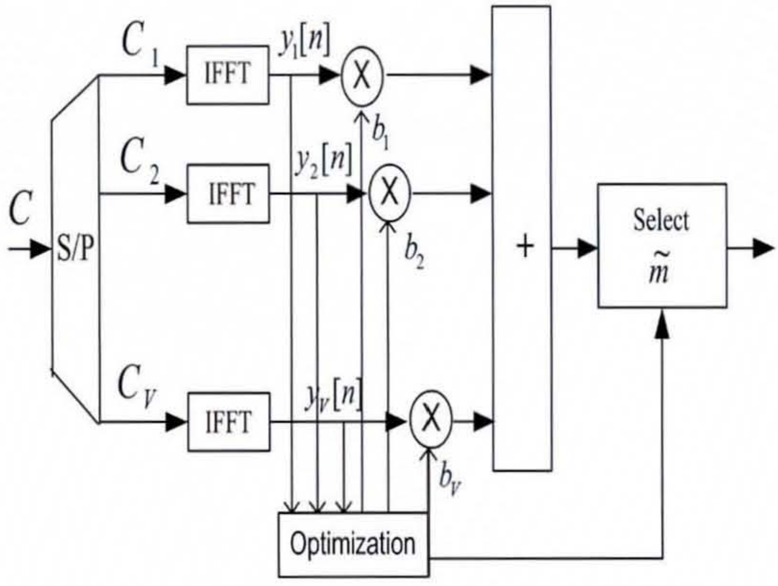

Figure 3.1. Diagram representation of the partial transmit sequence approach, $\tilde{m}$ corresponds to the index of the modified sequence with minimum PAPR.

$c_k, k = 0, 1, ..., N-1$ are the complex subcarrier symbols. Then, partition $\mathbf{C}$ into V sub-blocks, so that $\mathbf{C} = [\mathbf{C}_1, \mathbf{C}_2, ..., \mathbf{C}_V]$ contains the sub-blocks, represented by the vectors $\mathbf{C}_v, v = 1, 2, ..., V$. Here, all such sub-blocks apart from the first one are multiplied by a binary weighting factor b_v, where $v = 2, ..., V$, hence 2^{V-1} possible combination are searched such that the resultant PAPR is minimized. As the actual signal in the analog domain could have slightly higher PAPR than that predicted by the use of the Nyquist sampling rate in the digital domain, it is suggested in [27] that the 256 length transmitted signal has to be oversampled by a factor four. Using the linearity property of the IFFT, the optimal PAPR can be found as [28]:

$$PAPR = {}_{b_2,\ldots b_V}^{min}|_{b_1=1}[{}_{0<n\leq 4N}^{max}|\sum_{v=1}^{V} b_v y_v[n]|^2] \qquad (3.1.1)$$

where $b_v, v = 2, 3, ..., V$ are weighting factors which are assumed to be pure rotations and $y_v[n]$ is the partial transmit sequence in the time-domain.

However, finding the best weighting factor among those possible combinations is highly complex. For this reason, some attempts have been made to reduce the computationally complexity of the optimization:

(1) Adaptive partial transmit sequence (APTS) [27]: this establishes an early terminating threshold and the search is terminated as soon as the PAPR drops below the threshold. It assumes that $b_v = 1$ for all v and computes the PAPR. If the new PAPR is lower than a certain threshold then the optimization is stopped otherwise invert b_1 and recalculate the PAPR. If it is less than the threshold, b_1 is retained as part of the final phase sequence. The algorithm continues in this way until all the combinations of the signs of the phase factor have potentially been explored.

(2) Phase optimisation [29]: The total OFDM block of length N symbols, which are denoted by $(c_0, ..., c_{N-1})$, is divided into sub-blocks of length M. Each of these sub-blocks is multiplied by a rotation value, $e^{j\phi_k}$. To reduce the search complexity ϕ_k is restricted to $(0, \pi/2, \pi, 3\pi/2)$. The first block has to be multiplied by $e^{j\phi_1} = 1$, the next block by $e^{j\phi_2}$, the third by $e^{j\phi_3}$ and so on. The modified

symbols become $\hat{\mathbf{c}} = (\hat{c}_0, \hat{c}_1, ..., \hat{c}_{N-1})$ and the actual transmitted sequence is given by the following matrix multiplication :

$$\mathbf{s} = \Lambda\hat{\mathbf{c}} \tag{3.1.2}$$

where $[\Lambda]_{n,m} = \frac{1}{\sqrt{N}} e^{(j2\pi nm)/N}, (0 \leq n, m < N)$ and $\hat{\mathbf{c}}$ is the M-ary phase shift keying modulation symbol for the n^{th} carrier.

The resulting PAPR of $\mathbf{s}$ must then be estimated, and interpolation is generally necessary to accurately match the PAPR of the true underlying analogue transmitted signal. An example of measuring the minimum PAPR before and after interpolation is given in Figure 3.2. In this figure, a length 16 OFDM symbol is multiplied by 64 different combinations of rotation angles. Importantly, the minimum PAPR obtained was different. In the case of no interpolation, the minimum PAPR achieved was 3.2 dB. However, when extra zeros have been added to the original OFDM symbol, the new minimum PAPR changed to 5 dB. It is also noticeable that as the range of the PAPR increases, the interpolation becomes more important. In [30] it is shown that instead of dividing the OFDM block into contiguous symbols, there might be a case to split these sub-blocks for better PAPR, but that will cost extra complexity at the receiver. However, an optimum criterion can be found on the basis of having contiguous sub-blocks and instead of looking at the maximum value, looking at the auto-correlation function. Assuming $\Psi(k)$ is the aperiodic autocorrelation of $\hat{\mathbf{c}}$. The new

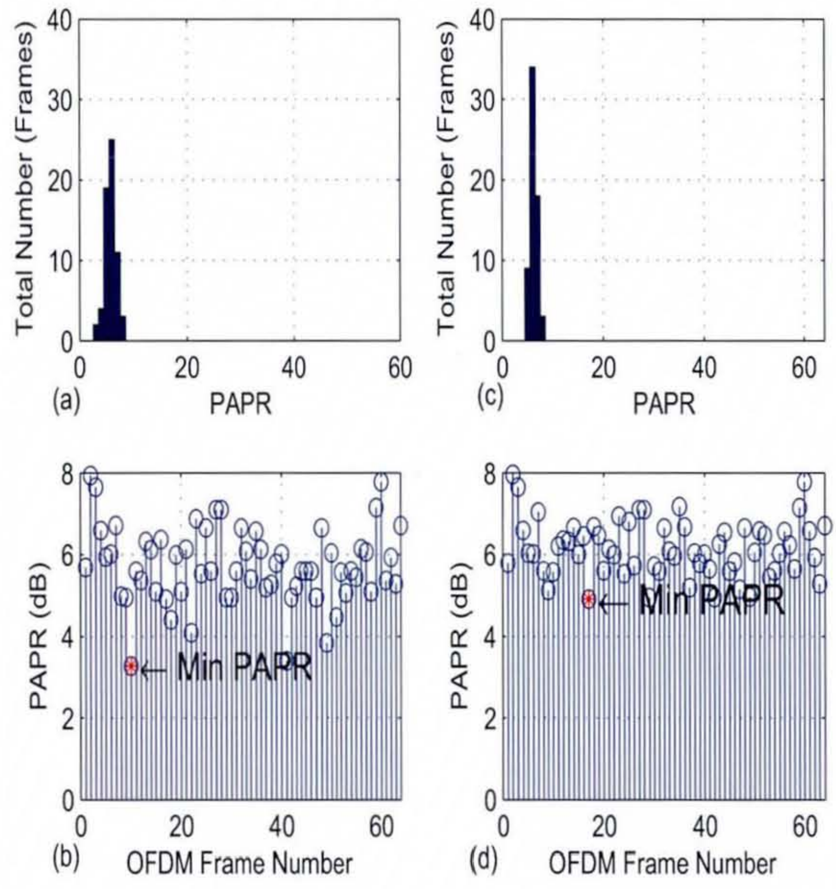

Figure 3.2. Histogram of different PAPRs for the same original OFDM symbol. (a): With no zero padding. (c): With interpolation by a factor of four. (b,d): Identifying the minimum PAPR in each case.

optimisation criterion can be written as [29]:

$$[\hat{\phi}_2, \hat{\phi}_3, ..., \hat{\phi}_M] = \underset{[\hat{\phi}_2, \hat{\phi}_3, ..., \hat{\phi}_M]}{\arg\min} \; \Sigma_{k=1}^{N-1} |\Psi(k)| \tag{3.1.3}$$

where $\Psi(k)$ is the aperiodic autocorrelation of $\hat{\mathbf{c}}$ as defined on page 40.

Calculating the auto-correlation values is more computationally complex because of the need to calculate all N correlation values, however, it achieves a PAPR improvement of approximately 2.5 dB (see Figure 3.3). The improvement is mainly due to the interrelationship between the auto-correlation function and the PAPR. The most important aspect when considering PAPR is to try to calculate what is occurring between the OFDM symbol time samples because the danger is if the peak in between is too high. The auto-correlation appears from the results in Figure 3.3 to be more efficient at finding how the signal behaves in these regions [29]. In order to avoid experiencing difficulties in

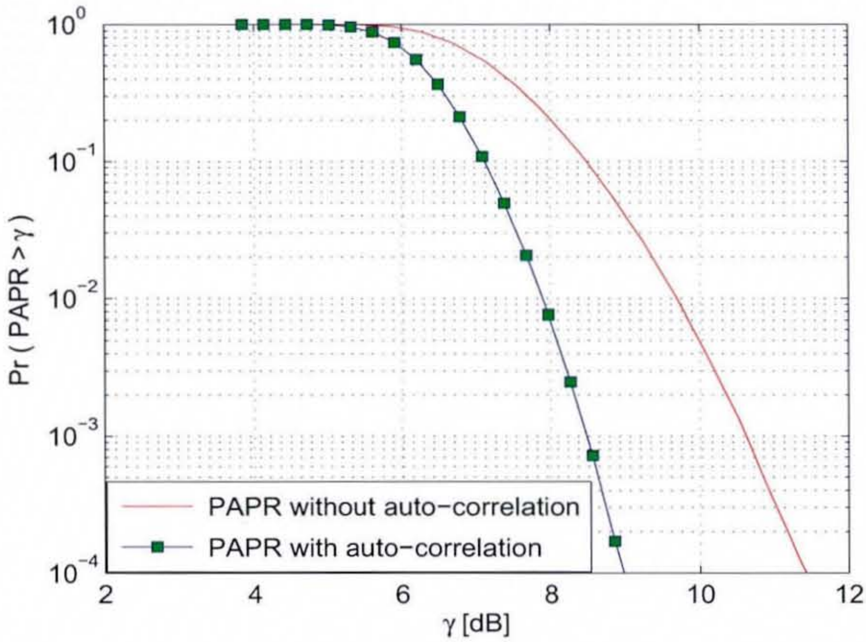

Figure 3.3. Probability that the PAPR exceeds γ for a 128 OFDM frame QPSK modulated carrier.

obtaining a peak value between the samples, the use of a raised-cosine filter could help with making the peak much smoother [2].

In the PTS approach, the receiver must have knowledge about the generation process of the transmitted OFDM signal. The weighting factor must then be sent as side information resulting in some loss of spectral efficiency.

3.1.2 Selective Scrambling

This technique suggests that if, for example, a BPSK symbol forms the input to the IFFT, then generally if the sequence of 1s and 0s has a fairly random pattern, then it is much more likely that the PAPR at the output will be smaller [31].

Therefore, if the data sequence that must be transmitted is c_1 through c_{126} but the sequence of 1s and 0s is not very random, what can be done is to take that sequence of values and scramble[1] it. Note, 128 values are not taken as two are used for transmitting side information as explained below. This means re-ordering those values and getting a new output with a much more random mixture and hopefully by using that new set of randomized 1s and 0s, the PAPR will be less. Clearly, however, if this system is to work at the receiver then the receiver must know which scrambler has been used.

In [31] four scramblers were used and the idea was to choose one of four different scramblers. When the data are transmitted to the receiver, as said previously, the receiver must know which scrambler has been used. However, how does the receiver know? A composite word of two binary bits has to be formed, with possible values (00,....,11), and these two binary bits inform the receiver which effective scrambler has been used. This means that the total word now has a length of 126-bits go-

[1]A scrambler can be designed by using an m-sequence generator which is made up of shift registers and modulo 2 additions [4].

ing into the IFFT to obtain a particular PAPR. Figure 3.4 shows that scrambled data give much lower PAPR, i.e. an average PAPR around 160 is dropped to approximately 5. Figure 3.5 illustrates the sample

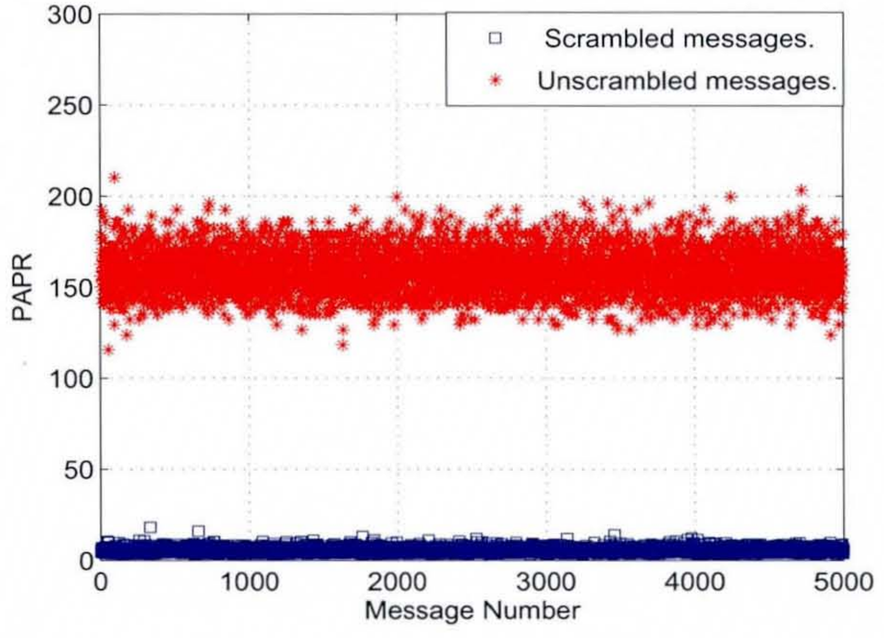

Figure 3.4. Comparison of PAPR for unscrambled and selected scrambled messages.

probability density function for the scrambled messages. It is clear from this figure that the mean PAPR is much lower than the unscrambled version and the standard deviation (STD) or the dispersion about the mean value is relatively low. This implies whichever scrambling example is used, the result of the PAPR is always going to be approximately somewhere between 3.5 and 7, which means very tightly distributed around the mean value of 5. In addition, in this method, the author discussed that codewords with a small power variance (PV) have a low

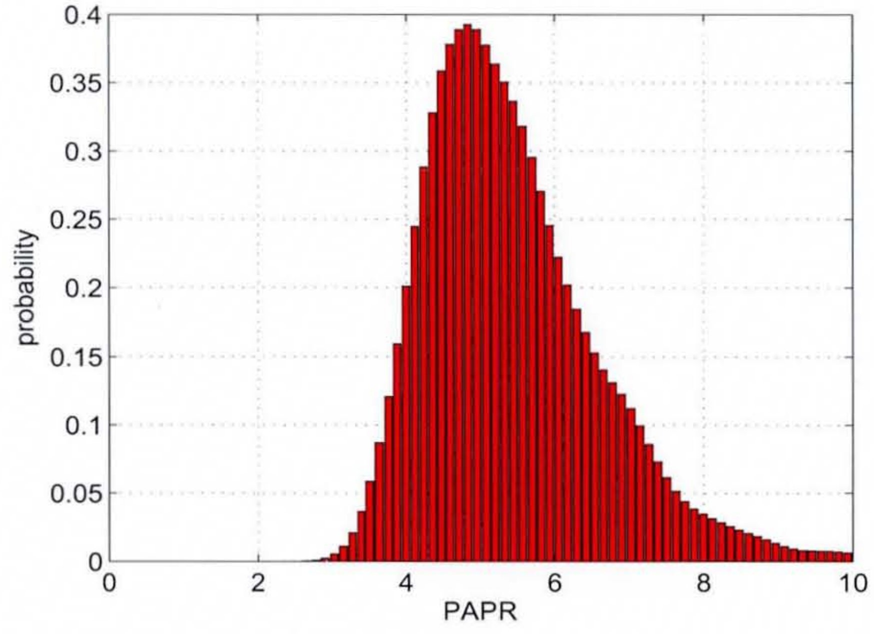

Figure 3.5. PAPR distribution for selected scrambled messages, mean = 5.49, and standard deviation = 1.13.

PAPR. This can be expressed as:

$$PV = \sum_{i=0}^{N-1} |R_i|^2 \tag{3.1.4}$$

where $R_i = \Sigma_{k=0}^{N-1} c_k c_{k+i}^*$ is the aperiodic autocorrelation function of the complex sequence.

Unfortunately, calculating all of the R_i values might be quite difficult particularly if the codeword length was 512, 1024 or larger. However, if the length of the code and the number of ones is known, then R_1 can be calculated very easily by using both Hamming weight W_H, i.e. the number of ones within the codeword, and R_1:

$$SF = [|W_H - N|^2 + |R_1|^2]/2N^2 \tag{3.1.5}$$

This was proposed in [31] and shown to yield a practical method for PAPR reduction.

3.1.3 Tone Injection

The main idea of the tone injection (TI) technique comes from the diagram shown in Figure 3.6.

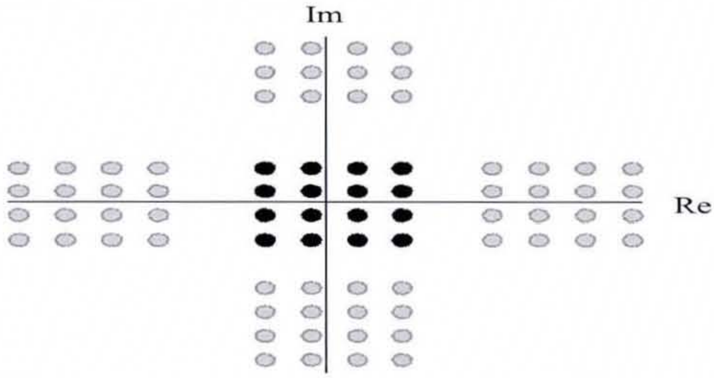

Figure 3.6. Constellation for 16 QAM together with images of the constellation used in the tone injection method [1].

Firstly, the basic QAM constellation as shown in Figure 3.6 is in the middle. From which, images of the constellation are generated at the particular points shown in Figure 3.6 where the structure of each of these images is identical. This can be done by generating a so-called *anti-peak* signal [1] which shifts the true signal to one of the image locations. The images are modified in such a way so as to avoid redundant information. The PAPR can be reduced by carefully choosing the *anti-peak* signal to give the right shift of moving that particular point. The drawback of this technique is an increasing average power and loss in throughput. This can be alleviated by using convolutional codes [4], but is not considered further in this thesis.

3.1.4 Selective Mapping Technique (SLM)

Selected mapping (SLM) was introduced in [32] for PAPR reduction in SISO transmissions. In SISO-SLM, the PAPR reduction is achieved by multiplying independent phase sequences with the original data such that the PAPR of each data combination is reduced. Then, the sequence with the lowest PAPR is chosen for transmission. In other words, the original source signal, in Figure 3.7, is converted into a vector $\hat{\mathbf{C}}$ of total length (MN) through a Kronecker product denoted by $\otimes$, i.e. $\hat{\mathbf{C}} = \mathbf{C} \otimes \mathbf{1}$, where $\mathbf{1}$ is an $M \times 1$ vector with unity elements and $\mathbf{C}$ is an $N \times 1$ vector containing the original signal information.

The M subvectors within C are weighted elementwise by the complex values b_i, $i = 1,..., M$ to form $\mathbf{C}^{(i)}$, $i = 1,..., M$. Note that all of the b_i values are chosen randomly among the set of $b_i \in (\pm 1, \pm j)$ to reduce complexity. Define the M complex valued time-domain transmitted symbols:

$$\mathbf{c}_L^m = IFFT_L\{\mathbf{C}^m\} \tag{3.1.6}$$

Here, the sampling frequency, L, plays an important role in PAPR evaluation (see Section 1.2). The PAPR of the transmitted signal of (3.1.6) is defined as:

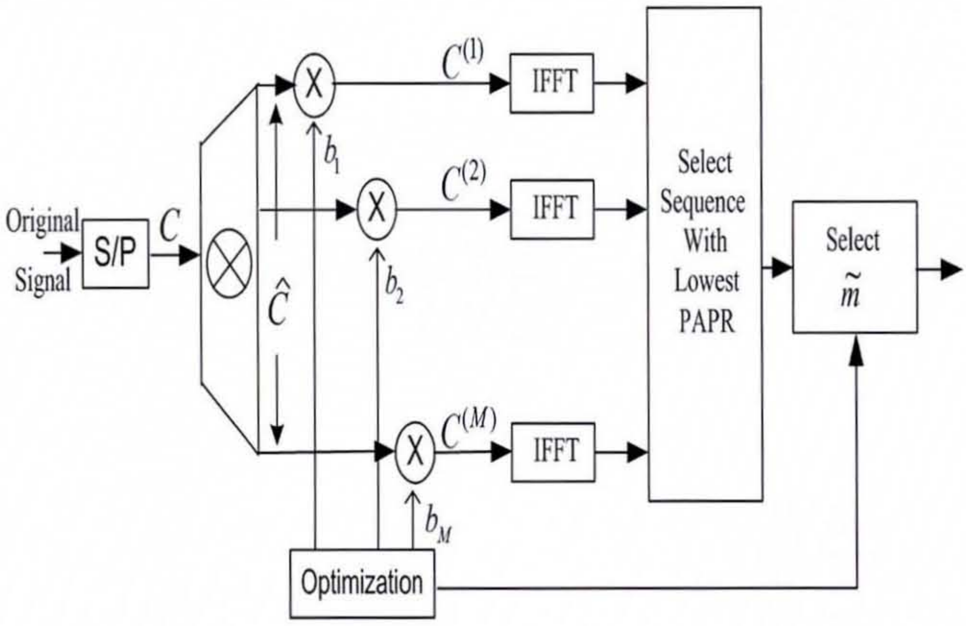

Figure 3.7. Selective mapping approach in SISO systems.

$$PAPR(\mathbf{c}_L^m) = \frac{\max\limits_{0 \le n \le NL-1} |c_L^m[n]|^2}{E\{|c_L^m[n]|^2\}} \tag{3.1.7}$$

where max[·], E{·}and |·| represent respectively the maximum element, the statistical expectation operator and the absolute value of the input symbols. Finally, the symbol with the lowest PAPR is transmitted:

$$\tilde{m} = \arg\min_{1 \le m \le M}\{PAPR(\mathbf{c}_L^m)\} \tag{3.1.8}$$

Although the definition of (3.1.7) is a good assessment for the signal power fluctuations relative to its mean, it takes no account of the probability of the peaks occurrence. This is derived by the complementary cumulative distribution function (CCDF) defined in (2.3.3).

In Figure 3.8 results are shown using M different transmit sequences, $M = 1, 2, 3$ and 4. The PAPR exceeds 10 dB at a probability of 0.001

only when M = 1. However, when the number of M is increased to four, the PAPR is improved by 2.5 dB at the same probability. In

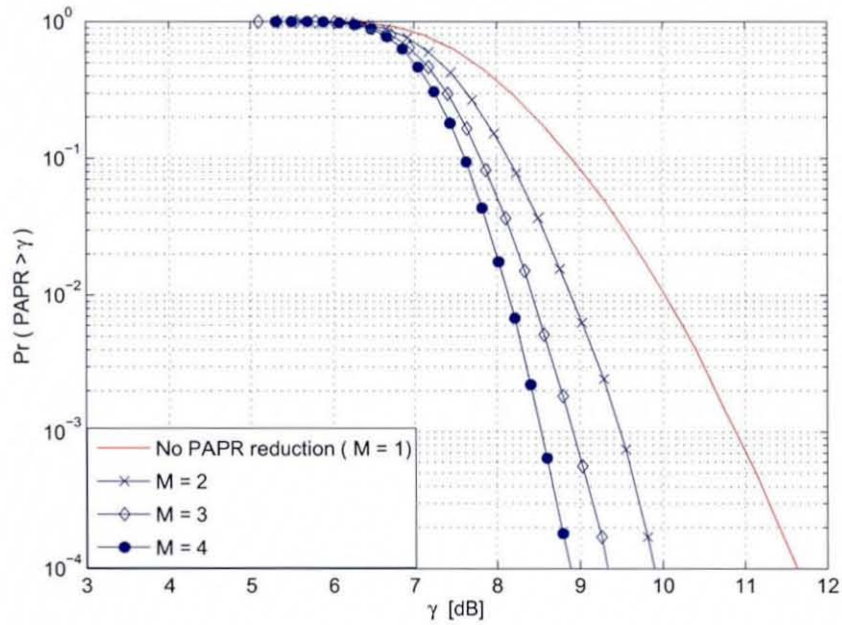

Figure 3.8. CCDF of PAPR, if the frame with lowest PAPR is selected out of N statistically independent frames.

Figure 3.9 results are shown for the case of using 256 subcarriers and $M = 1, 4$. The PAPR of this approach is identical to the prediction from theory given by the analytical curves shown on the same figure. It is also shown that at a probability of 0.001 the PAPR advantage for M = 4 is approximately 2 dB better than the case with M = 1. These results confirm the efficacy of the scheme.

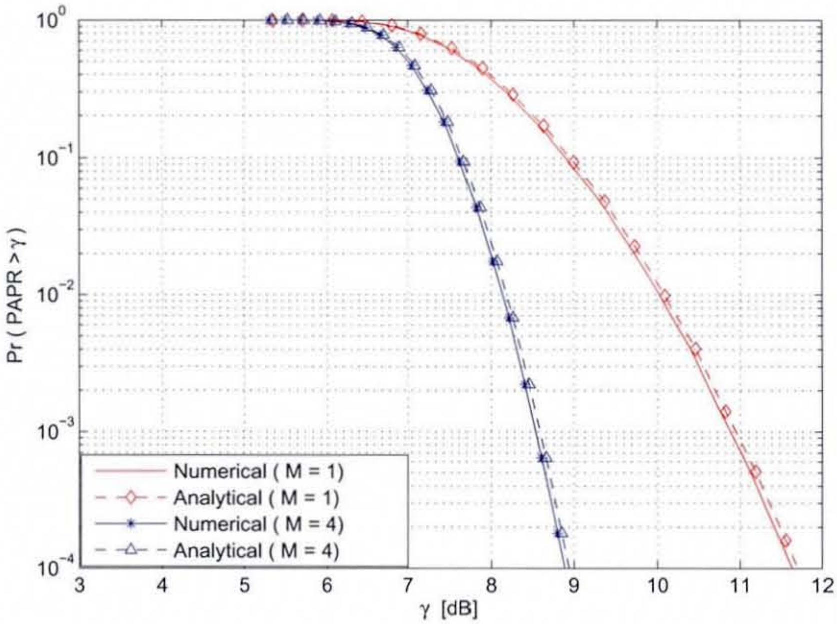

Figure 3.9. CCDF of $PAPR_{low}$ for QPSK when $M = 1$ and 4, $N =$ 256 subcarriers.

3.2 Clipping and Filtering

3.2.1 Clipping

The time-domain clipping operation is a non-linear method of reducing PAPR. If the digital signal is clipped directly, this will add extra frequency components and generate energy in the out-of-band region, see Figure 3.10. In-band components are also generated which can cause considerable confusion in the decoding process thereby increasing the bit error rate. Effectively, providing N is large enough, N>64 symbols, the in-band distortion is going to have a relatively broadband type of behaviour.

The researchers in [2] suggested a better way for clipping. Their idea of clipping was firstly oversampling each OFDM block and padding the original input signal with zeros, $L = 8$, then the frequency content was moved from being centered at DC to being centered at half of the Nyquist rate:

$$\begin{cases} c_{k+N/2} & 0 \leq k \leq N/2-1 \\ 0 & N/2 \leq k \leq LN - N/2 - 1 \\ c_{k-(LN/2)} & LN - N/2 \leq k \leq LN - 1 \end{cases} \tag{3.2.1}$$

As the signal after the IFFT is a complex signal, the clipping has to be performed with a real signal which is performed by the digital passband modulation operation [2]. Once the real signal has been received, the clipped signal must then go through a low pass filter to smooth the sharp edges but care must be taken during filtering not to degrade the performance.

Ultimately, at the receiving end the original values should be easily reconstructed. Thus, the comparison between clipping using the above process and clipping the signal directly is that there will be better control of the degradation than if the clipping is performed when all the signal energy is around the DC frequency where the decoding performance is going to be poor. The effect of clipping on the bit error rate (BER) of the OFDM signal is observed in Figure 3.11. Transmission over a frequency selective, length four, Rayleigh fading SISO channel is assumed. Independent, Gaussian white noise is added at the receiver to control the signal-to-noise ratio (SNR). This was performed by clipping the original signal and it was found that the peaks can be clipped up to 0.8 dB without any noticeable effect on BER. However, when 1.5

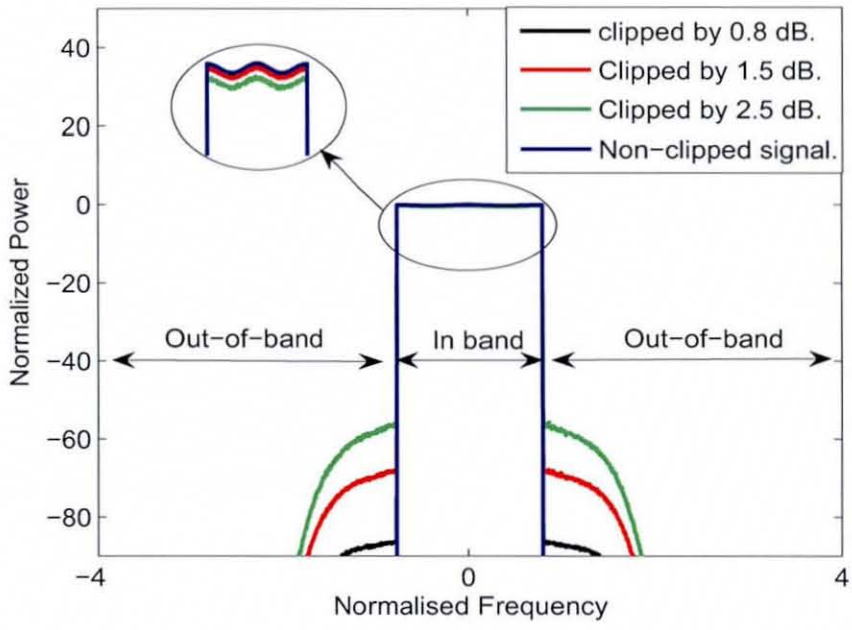

Figure 3.10. Power spectral density of an OFDM signal with frame length of 256.

dB clipping from the peak value was applied, the performance becomes worse by approximately 2 dB at the value of BER = 0.001. The degradation in BER due to clipping is considered in this thesis to render this approach unsuitable for further consideration.

3.2.2 Tone Reservation

The basic idea of the tone reservation (TR) technique introduced in [17] is that based on the information data, there are typically several subcarriers (tones) that carry data with low SNRs. If these tones are not used for data transmission, it is desirable to shape the clipping noise in those tones in a way to cancel any large peaks from the original data subcarriers. This technique is most commonly used in discrete

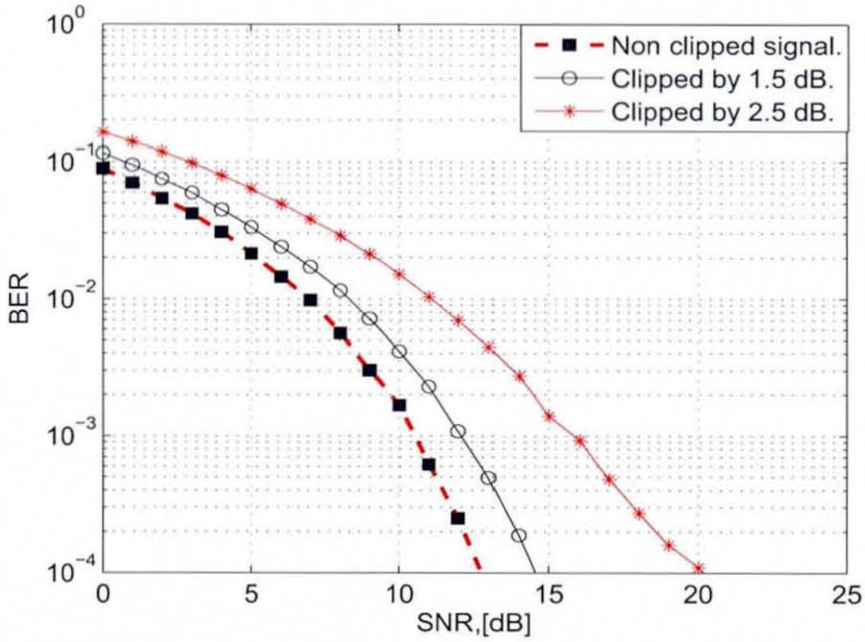

Figure 3.11. Effect of clipping on the BER for an OFDM frame of length 256, two levels of clipping relative to the original maximum value of the time-domain signal are used, 1.5 dB and 2.5 dB.

multitone modulation (DMT) systems such as ADSL, and is therefore, not adopted in this thesis, as the target is MIMO wireless systems.

3.3 Coding Technique

3.3.1 Block Coding

The idea of this method is to transmit words which are known to have low PAPR [33]. Some spectral efficiency is lost since the full OFDM symbol length N is subdivided. As a simple example, if $N = 4$, only three bits could be used for data and the remaining bit is chosen to ensure the full length four word has low PAPR. In Figure 3.12 the envelope power for all the possible four-bit words, 16 in total, is shown within these words, the peak envelope-powers (PEPs) form three sets of values: 16W, 12.29W and 10.45W. If each of these words is assumed to appear on the average with the same probability then the average PEP will add these up and divide by 16. Instead of four bits of useful

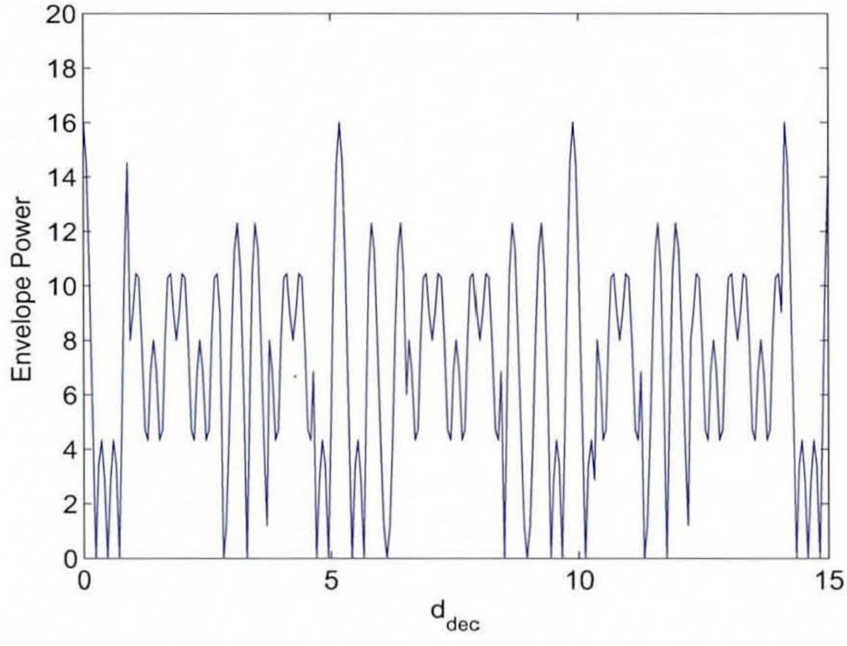

Figure 3.12. Possible OFDM symbols with N = 4 and BPSK modulated subcarriers.

information being transmitted, only three bits could be transmitted. Thus, there are eight possible combinations, but instead of transmitting those eight possible combinations, a mapping of three-bit numbers into four-bit numbers is designed so that those four-bit numbers selected have low PAPR. On average, therefore, the PAPR is reduced.

Indeed, a reduction of 3.54 dB in the PAPR was achieved when this method was used. However, this reduction was at the expense of an increase in bandwidth and a reduction in the SNR.

In addition, eight carrier signals were also considered and results showed that if half of the possible code words were permissible then a reduction of PAPR of 4.58 dB could be achieved and if a quarter were used the reduction could be 6.02 dB.

Implementation of such a technique is conceptually straightforward. If the overall word length is eight, or possibly ten, the method is computationally feasible, but by the time you get up to sixteen or sixty four it is impractical to go through this as it would need an exceedingly large look-up storage table. However, another way to perform this scheme would possibly to use different types of coding either the Golay code or the Reed-Muller code [34]. But the price for that is the extra redundancy, and therefore the reduction in code rate. For example, if the frame length is very large, N = 256, to guarantee the PAPR is going to be low, it might be necessary to operate at a redundancy rate of half or less.

3.3.2 Complementary Codes

The complementary sequence [35] is one way of generating a code which makes the properties of the IFFT input more effective in bringing the PAPR down at the output. When N = 64 subcarriers are combined with the same phase (PSK modulation), the normalized instantaneous power of the OFDM signal in time-domain is shown in Figure 3.13. This figure illustrates the envelope power variations of the OFDM signal over time, where the peak power of the signal is 1W and the mean power of the signal is 0.089W. As a result, the PAPR of the signal is 21 dB. Based on exhaustive search through all possible QPSK codewords it is claimed in [35] that for 8 subcarriers, a rate 3/4 code provides a maximum PAPR of 3 dB. Golay complementary sequences open the way to a structured approach to generating PAPR reduction codes. They are pairs of sequences for which the sum of the auto-correlation function is zero for all delay shifts unequal to zero [36], [37] and [38]. The type of

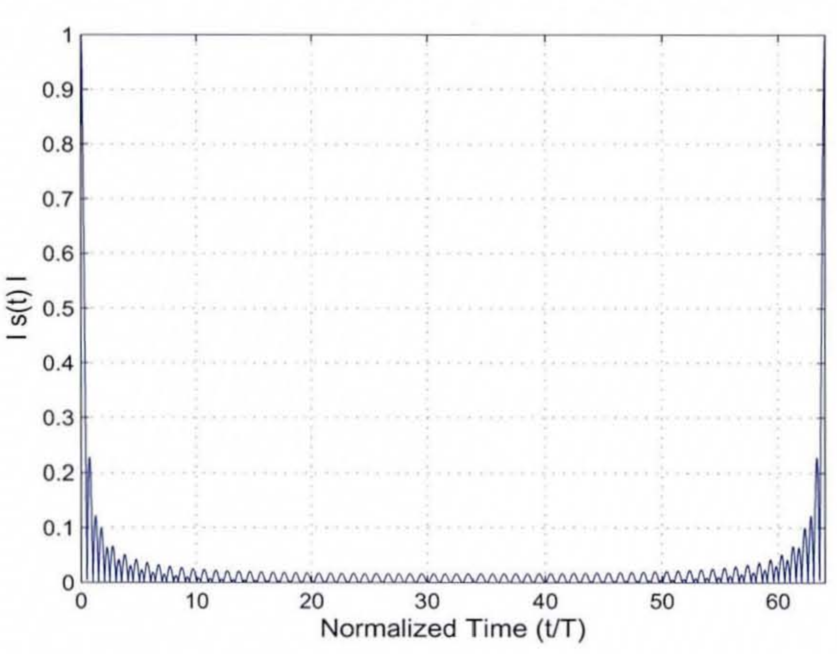

Figure 3.13. Normalized instantaneous power for 64-subcarriers before the complementary code was applied.

performance that can be achieved by using a complementary sequence is shown in Figure 3.14.

In this figure, the peak power of the signal is 0.845W and the mean power of the signal is 0.250W. As a result the PAPR of the new signal is 5.3 dB. Although such coding strategies are possible approaches for mitigating PAPR, due to the loss in coding rate they will not be

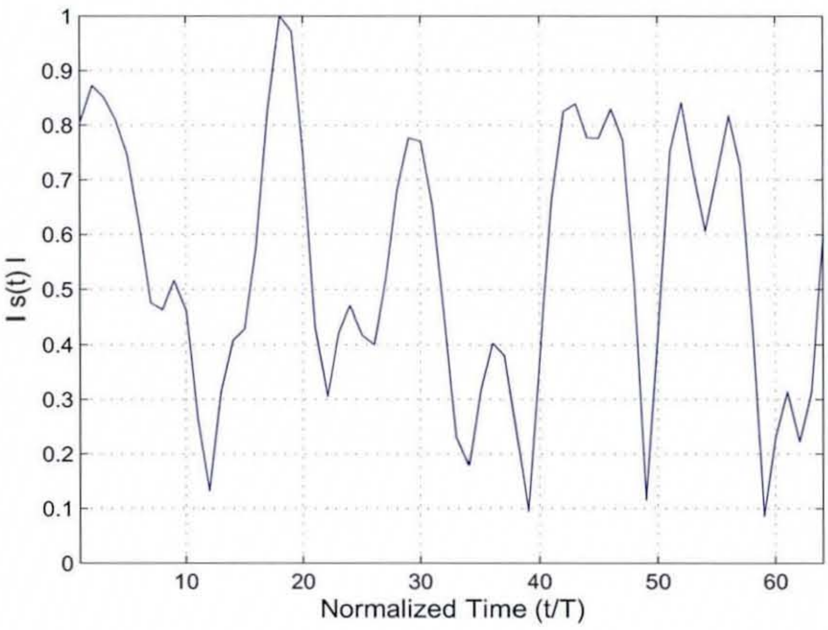

Figure 3.14. Normalized instantaneous power for 64-subcarriers modulated with a complementary code.

considered further in this thesis.

3.3.3 Trellis Shaping

Trellis shaping is a method of selecting a minimum weight sequence from an equivalence class of possible transmitted sequences by a search through the trellis diagram of a shaping convolutional code. Consider a mapping of 16 QAM depicted in Figure 3.15 with the number of individual symbols, N = 64, so if one QAM word for example is taken, there are two most significant bits (MSBs) and two least significant bits (LSBs) at each carrier. The underlying principle of this is that the LSBs have low effect on PAPR while the MSBs have high effect. For all 256 bits, a word vector **v** of length 128 length, for only the MSBs,

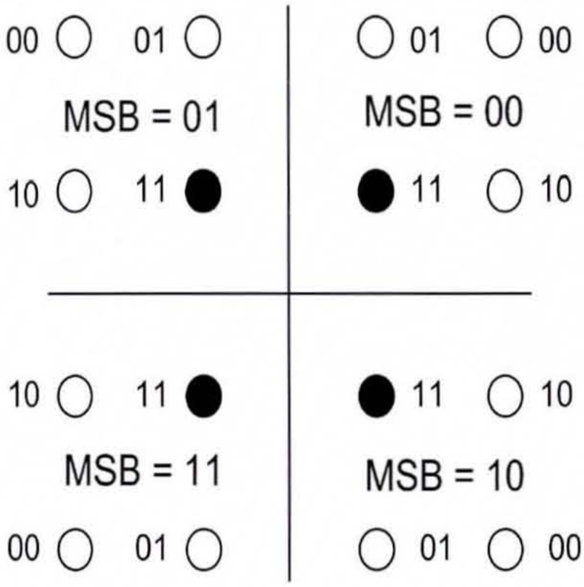

Figure 3.15. Constellation mapping for 16-QAM used in Trellis Shaping [1].

is created. The problem is using any points within the constellation could lead to a large PAPR. Therefore, the following coding matrix $\mathbf{G}$ is added :

$$\mathbf{V^c} = \mathbf{G} \times \mathbf{v} \tag{3.3.1}$$

This coding matrix can either be in the form of a linear code or it can be a convolutional code. By doing this coding the MSBs from the whole OFDM frame are connected together. Hence, this method is termed Trellis shaping. Then a special code $\bar{c}$ is added in order to improve the PAPR:

$$\mathbf{W} = \mathbf{V^c} + \bar{c} \tag{3.3.2}$$

Lastly, a new multicarrier (MC) symbol is formed on the basis of:

$$\mathbf{W} + LSB_{OLD} \tag{3.3.3}$$

where LSB_{OLD} is the vector containing the original LSB bits.

And if this process is designed well then the new MC symbol will have a much lower PAPR. This approach is not followed in this thesis due to the additional redundancy introduced.

3.3.4 Blind Selected Pilot Tone Modulation (BSPTM)

Blind selected pilot tone modulation (BSPTM) is proposed in [16] and reduces PAPR by multiplying the original symbols by a phase rotation sequence described by:

$$y_{n,m} = c_n e^{j\phi_n^{(m)}} \tag{3.3.4}$$

where $\phi_n^{(m)}$, $0 \leq n \leq N-1$, $0 \leq m \leq M-1$ is a set of M random phase sequences of length N each. This is the same as the previous method mentioned in Section 3.1.4 but this method extends it by eliminating the need to send side information.

This is a preferred method because only the phase of the signal is changed and the information amplitude is not affected. In order to obtain a maximum reduction of PAPR, the scheme selects the best sequence out of M possible sequences to be applied to the transmitted symbol. Therefore, control information needs to be sent to the receiver with the data information, to distinguish the sequence that has been transmitted.

The receiver examines the signal and performs Gray decoding on the sections that represent training data; the parts that represent real data can be differentiated based on their energy. Importantly, the decoded training data can be used to decide which rotation functions were actually used on the real data and the advantage is that there is no need to transmit extra information to indicate which rotation function position of the library was used, hence the term 'blind'. A non-blind scheme would need to receive extra bits for the index into the library and that would add an overhead to the bandwidth by an amount dependent on the length of the extra bits.

The good part of BSPTM is the combination of the training data with the phase sequence addressing, eliminating the need to transmit extra information [16].

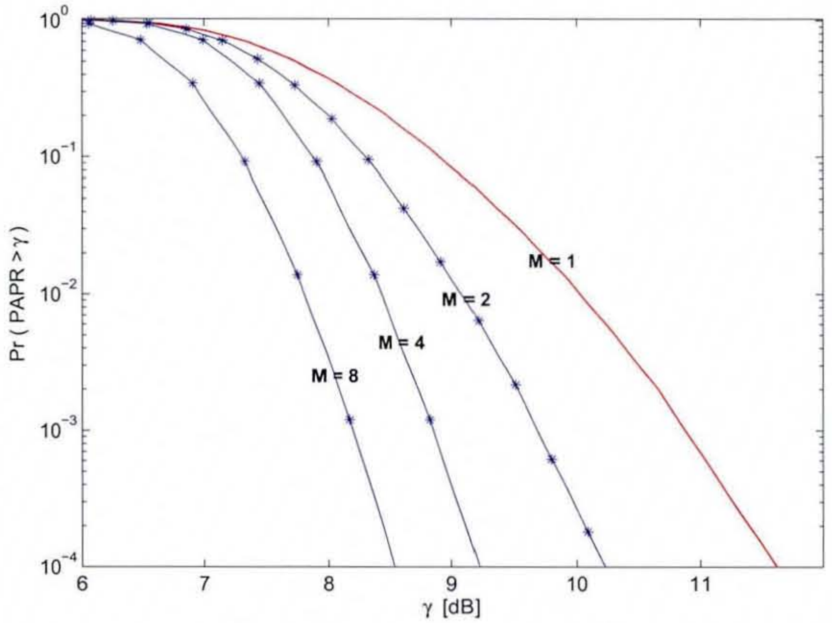

Figure 3.16. CCDF of the PAPR of the BSPTM signal for varying M values with $N = 256$.

Figure 3.16 shows the simulation for this scheme using 256 subcarriers and QPSK modulation. It illustrates different numbers of possible phase sequences, M, as a function of the probability, PAPR> γ. Four curves are shown from selecting one from one, two, four and eight possible sequences. It demonstrates that when $M = 8$, the proposed algorithm could achieve 2.5 dB of PAPR reduction as compared with the $M = 1$ case at the probability level of 0.001. It also shows that the larger the M, the smaller the resulting PAPR.

In [16], it is shown that some sequences give a very bad PAPR, but if the optimal sequence is chosen, then the PAPR can be improved. In [16], the relationship between BER and SNR is simulated. It is shown that if the proposed BSPTM scheme is closer to the known channel performance, an approximate 0.75 dB advantage is seen, compared to the old scheme.

3.4 Performance comparison and complexity analysis for SISO systems

Several PAPR reduction techniques for SISO-OFDM systems have been studied in this chapter; their effectiveness is a trade-off between complexity of implementation, data rate loss and BER degradation.

Probabilistic techniques aim to find the OFDM symbol that has small probability of peaks. These are classified into two known groups. One is the selective mapping (SLM) approach, in which an input sequence is multiplied by each of a set of predefined sequences, called phase rotations, to form new input sequences. Each of these new input sequences goes through the IFFT, and then, the one which yields the lowest PAPR is selected. The other scheme is partial transmit sequence (PTS), in which the input block is partitioned into disjoint subblocks. After that, the IFFT is applied to each subblock the outputs of which are then multiplied (except the first block) by phase sequences and combined to minimize the PAPR.

The coding technique is another distortionless technique, which not only reduces the PAPR, but also correct errors and hence improves the overall BER performance. However, codes which give a low PAPR can only be constructed at the expense of sacrificing the data rate.

The third type of PAPR reduction technique is amplitude clipping. Clipping the OFDM signal before amplification is a simple method to limit the maximum magnitude of the transmit signals, but it was found that it causes distortion resulting in increased BER and out-of-band spectral radiation (see Figure 3.10).

The performance comparisons of the above schemes were performed by Monte Carlo simulations with 10^5 OFDM symbols, the results of which are presented and analyzed in this section. For a fair comparison, it is necessary to consider an equal number of signal subcarriers and the same constellation modulation, i.e., QPSK, is used. The CCDF of PAPR is used to measure the performance, which is defined as the probability that the PAPR of the OFDM symbols exceeds a given threshold γ. Figure 3.17 shows a PAPR comparison for SLM, PTS, Tone injection (TI), clipping, Trellis shaping and Tone Reservation (TR).

In this figure, the unmodified OFDM signal has a PAPR which is approximately 11 dB for a probability of 0.001 of the blocks. Taking the example of M = 4 and 0.001 PAPR, the PTS technique improves the PAPR performance by approximately 3.7 dB which is better than the SLM scheme which is degraded by 1.2 dB, i.e. to a 2.5 dB improvement. As can be seen, both schemes make the probabilities decrease faster when the number of phase rotations is increased, yielding a more desirable performance improvement. It was shown in [39] that additional PAPR reduction becomes negligible by increasing the number of weighting factors greater than four. However, the gain can be reduced further with other schemes. For the same parameters, the unmodified signal can be reduced by 4.2 dB using the TI scheme and by approximately 4.5 dB when Trellis shaping is used. It also can be seen that when the maximum peaks are clipped by 1.5 dB, the clipping approach shows better performance at a lower value of γ and equal to the PTS, with M = 3, at a higher value of γ. However, it should be emphasized that this gain improvement can be obtained only at the expense of causing both out-of-band noise and in-band distortion.

In the case of the TR approach, the OFDM peak signals can be reduced without introducing any additional distortion to the information data. Increasing the number of reserved tones (subcarriers), results in increasing slope and lower PAPR. In Figure 3.17, two numbers of reserved tones were considered. As one can see, the PAPR improved by between 6.5 dB and 4.9 dB with increasing the number of tones from 5% to 20% respectively; but this would reduce the spectral efficiency.

It must be said that an analytical comparison is not always enough, because great differences in scheme methodology make the direct com-

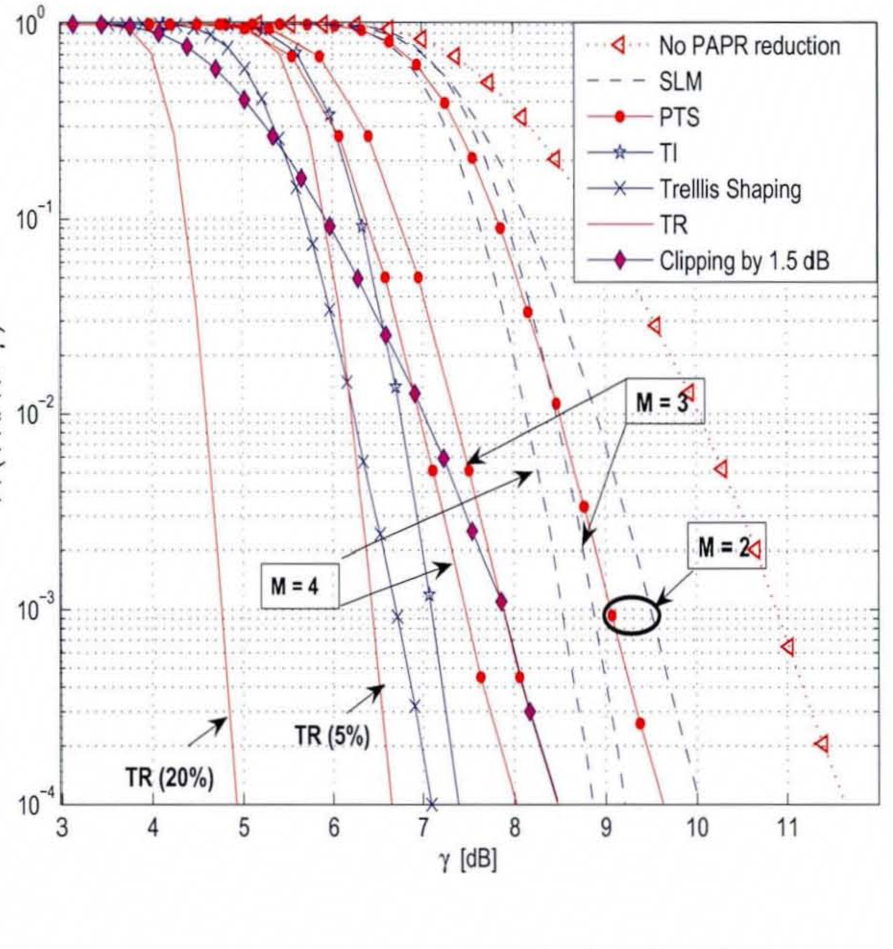

Figure 3.17. Performance comparison of SISO-OFDM PAPR mitigation techniques with N = 256 employing QPSK and an oversampling of unity.

parison of some parameters difficult. Therefore, the implementation complexity of the different techniques is a major issue when selecting the technique to be used. Table 3.1 summarises the main parameters and the order of complexity for PAPR reduction techniques studied in this chapter.

Technique	Data Rate Loss	BER increased?	Complexity per OFDM symbol
PTS	Yes	No	$\mathcal{O}(MN\log_2 N)$
TI	No	No	$\mathcal{O}(N^2 + N^{3/2})$
SLM	Yes	No	$\mathcal{O}(VN\log_2 N)$
Clipping	No	Yes	$\mathcal{O}(N)$
TR	No	No	$\mathcal{O}(N)$
Trellis shaping	No	No	$\mathcal{O}(N^2)$

Table 3.1. Comparison of SISO-OFDM PAPR mitigation techniques.

From Table 3.1, it can be seen that clipping, TR, Trellis shaping and TI do not transmit side information (SI) which is recognized as a positive feature for these schemes. However, they have their own drawbacks in terms of implementation which make them less preferable than other schemes. Clipping and TR have a similar complexity, however, clipping introduces in-band and out-of-band distortion which increase the error probability. While TR is not very implementable for systems such as IEEE 802.11a/g as these have a relatively small number of data carriers, e.g. 64. This technique could be useful in wireline systems implementation as there are typically subchannels with low SNRs that can be used for PAPR reduction. In wireless systems, however, there is no fast and reliable channel state feedback to dictate whether some tones should go unused. Instead, a set of subchannels must be reserved regardless of the received SNRs. Therefore, this technique is not always possible for wireless systems.

Unlike clipping, Trellis shaping does not cause any distortion, but it reduces the information rate for a given constellation size as it only selects the constellation which results in a lower envelope variance or peak power.

In TI selecting the optimum subcarriers that achieve a lower PAPR from the extended signal constellation is very complex and requires extensive calculation. In addition, it has a larger transmission power since it uses a larger constellation size, hence its implementation in practical systems can be prohibitive.

In general, coding techniques significantly reduce the information rate of the system and require a complex implementation and specific dedicated encoding and decoding techniques.

SLM and PTS depend strongly on the number of signal representations that should be independent and identically distributed. The SLM approach implies an increase in transmitter complexity due to M full-length (i.e. N-point) IFFTs. While a PTS approach uses a similar number of N-point IFFTs, if the transforms can take advantage of the fact that a large fraction of the input values are zeros, the additional complexity can be kept to the minimum. Nevertheless, in PTS, an optimization is required at the transmitter to best combine the partial transmit sequences. This method, however, requires more redundant bits than SLM to decode the information bits in the receiver, which results in a decrease in spectral efficiency, and therefore is not considered further.

3.5 Summary

In this chapter, the existing methods for performing PAPR mitigation in SISO-OFDM were introduced and classified into three areas, namely, probabilistic techniques, signal distortion techniques and coding techniques. It was found that all these existing techniques involve some form of compromise. The most obvious one was the trade-off between complexity of implementation, data rate loss and BER degradation. Based on the performance comparison and complexity analysis of these schemes, the SLM approach was found to be a very effective technique and conceptually quite straightforward since it lowers the PAPR with relatively small increase in redundancy and without any signal distortion. Therefore, the application and extension of SISO-SLM to MIMO-OFDM will be the focus of this thesis.

Chapter 4

PAPR MITIGATION IN QUASI-ORTHOGONAL SPACE TIME BLOCK CODED MIMO-OFDM SYSTEMS USING SELECTIVE MAPPING

A study of a PAPR reduction scheme for quasi-orthogonal space-time block-coded multi-input multi-output (MIMO) orthogonal frequency division multiplexing (OFDM) systems based on selective mapping (SLM) is presented[1]. In particular, a scheme for four transmit and one receive antennas is considered; the scheme could be easily generalized for multiple receive antennas. The reduction technique is focused upon combining the PAPRs of the transmission blocks from four antennas and exploits the associated antenna diversity gain to mitigate errors in the transmission of the side information (SI) necessary for SLM. Simula-

[1]This work was presented at the LAPC 2008 conference [40].

tion studies are presented which show the CCDFs with and without the combining scheme and bit-error rates of the overall system. Comparisons are also made with SLM-based single-input single-output-OFDM (SISO-OFDM) systems.

4.1 Overview

In Section 3.1.4, it was seen that in SLM the frame to be transmitted is multiplied by a number of preselected phase sequences such that the resulting PAPR is modified and then the mapping which yields the smallest PAPR is the one which is chosen. The receiver must therefore know which out of the candidate phase sequences was actually used, which requires side information (SI) to be sent along with the transmitted signal. For high data rate wireless wideband applications, multiple-input multiple-output (MIMO) transmission combined with OFDM is being considered in a large number of current technology applications. If the PAPR reduction schemes for SISO systems are directly applied to MIMO, the complexity and redundancy increases proportional to the number of transmit antennas, which is not desired. In this work the target is therefore to reduce the additional complexity required in a MIMO system.

The transmission of SI, as explained above, is critical in the SLM scheme, which, when corrupted, leads to a high risk of interpreting all of the transmitted symbols incorrectly. It is thus advisable to protect such information using the diversity gain afforded by MIMO transmission. By employing a MIMO system, multiple spatial channels are created and it is unlikely that all the channels will fade simultaneously. Recent work in [12] is based upon exploiting these advantages. However, this work is limited to two transmit and one receive antennas.

In this chapter, for MIMO-OFDM, (the focus is a multiple-input single-output (MISO) system easily generalizable to a MIMO case), the proposed technique in [12] is extended to increase the available diversity gain and the PAPR performance of a quasi-orthogonal space-time block code (QO-STBC) by using the SLM technique for PAPR reduction. To simplify operation, instead of applying individual SLMs to each antenna, the sequence with the lowest PAPR over four transmit antennas is selected. Using SLM in a MIMO-OFDM system can improve the overall bit-error rate (BER) performance as compared to using SLM in a SISO-OFDM system and increase the reliability of SI at the expense of the overall PAPR reduction gain. The interaction between the feedback necessary for maximum diversity gain in the full rate QO-STBC scheme being exploited and the proposed SLM scheme is also discussed. In the next section, the concept of QO-STBC is presented. Transmit diversity with space-time block coding is explained in Section 4.2. An overview of orthogonal space-time block-codes (OSTBCs) and quasi-orthogonal space-time block codes (QO-STBCs) is given. In Section 4.3, the proposed PAPR mitigation scheme is discussed. Simulation results are provided in Section 4.4. Finally, Section 4.5 gives the chapter summary.

4.2 Transmit Diversity with Space-Time Block Code

The deployment of multiple receive antennas at the mobile station may not be feasible due to size, available power through a battery and cost constraints. On the other hand, the base station is not as restricted in terms of these limitations, this has therefore motivated the research of transmit diversity to provide spatial diversity for the downlink channel using multiple transmit antennas at the base station. In [41], OSTBCs were first proposed for two-transmit antennas by Alamouti and later were extended to a more general number of transmit antennas in the context of general orthogonal designs. A distinct feature of OSTBCs is their low decoding complexity, which renders them attractive when receiver complexity is at a premium. However, the goal of space-time coding is to achieve maximum rate and maximum diversity of $L_t \times L_r$, where L_t and L_r represent the number of transmit and receive antennas respectively. In this section, the Alamouti and QO-STBCs code are briefly reviewed and discussed.

4.2.1 Alamouti Code

A very simple and effective OSTBC coding scheme which achieves full diversity, i.e. there are two uncorrelated paths, and full rate, i.e. two symbols are transmitted over two time slots, for two transmit and one/two receive antennas was introduced by Alamouti [41]. The code matrix for this scheme can be described as follows:

$$\mathcal{G}_{12} = \begin{bmatrix} S_1 & S_2 \\ -S_2^* & S_1^* \end{bmatrix} \tag{4.2.1}$$

where each row represents a time slot and each column represents the transmission from one antenna over time. S_1 and S_2 are complex signals to be transmitted and the operation $(\cdot)^*$ denotes complex conjugate. For the Alamouti scheme described by (4.2.1), at a given symbol period, two symbols are simultaneously transmitted from two antennas over a frequency-flat Rayleigh fading channel. The transmitted symbol from antenna one is S_1 and the symbol transmitted from antenna two is S_2. Then at the next time slot, $-S_2^*$ is transmitted from antenna one and S_1^* is transmitted from antenna two. It should be noted that this code belongs to the class of OSTBCs since the columns of the transmission matrix $\mathcal{G}_{12}$ are orthogonal to each other. In other words, the signal sequences from any two transmit antennas are orthogonal and the transmission matrix satisfies the following identity:

$$\mathcal{G}_{12}\mathcal{G}_{12}^H = \sum_{n=1}^{N} |S_n|^2 \times I \tag{4.2.2}$$

where N is the number of symbols, S_n is the n^{th} complex symbol and I denotes the 2×2 identity matrix.

The orthogonality ensures that full transmit diversity is possible and at the same time, it allows the receiver to decouple the signals transmitted from different antennas and consequently allows simple symbol wise maximum likelihood (ML) decoding [41].

The received signal, at two successive time slots can be written as:

$$\begin{bmatrix} r_1 \\ r_2 \end{bmatrix} = \begin{bmatrix} S_1 & S_2 \\ -S_2^* & S_1^* \end{bmatrix} \begin{bmatrix} h_1 \\ h_2 \end{bmatrix} + \begin{bmatrix} n_1 \\ n_2 \end{bmatrix} \tag{4.2.3}$$

where n_1 and n_2 are independent, zero-mean circularly symmetric, additive white Gaussian noise samples. The channel coefficients, h_1 and h_2, are assumed to remain static over two time slots (symbol periods). Equation (4.2.3) can now be re-written as:

$$\begin{bmatrix} r_1 \\ r_2^* \end{bmatrix} = \underbrace{\begin{bmatrix} h_1 & h_2 \\ h_2^* & -h_1^* \end{bmatrix}}_{\mathbf{H}} \underbrace{\begin{bmatrix} S_1 \\ S_2 \end{bmatrix}}_{\mathbf{x}} + \underbrace{\begin{bmatrix} n_1 \\ n_2^* \end{bmatrix}}_{\mathbf{n}} \tag{4.2.4}$$

From (4.2.4), it should be noted that $\mathbf{H}$ is proportional to a unitary matrix, i.e., $\mathbf{H}^H\mathbf{H} = (\Sigma_{i=1}^2 |h_i|^2) I$, which is due to the fact that the code matrix in (4.2.1) is orthogonal[2]. Assuming perfect channel state information (CSI) is known at the receiver, the transmitted data symbols S_1 and S_2 can be estimated by first combining the received signals linearly according to the following equation:

$$\tilde{\mathbf{S}} = \mathbf{H}^H\mathbf{H}\mathbf{x} + \mathbf{H}^H\mathbf{n} \tag{4.2.5}$$

$$\tilde{\mathbf{S}} = (|h_1|^2 + |h_2|^2)\mathbf{x} + \tilde{\mathbf{n}} \tag{4.2.6}$$

where $\tilde{\mathbf{S}} = [\tilde{S}_1 \ \tilde{S}_2]^T$. Then, to decode S_1, the receiver finds the closest

[2]The Hermitian conjugate of a matrix is the complex conjugate transpose, i.e. $H^H = (H^*)^T$.

symbol to $\tilde{S}_1$ in the constellation. Likewise, the decoding of S_2 relies on the closest symbol to $\tilde{S}_2$ in the constellation. Next, consider the case of more than two transmit antennas, in order to increase the available diversity gain.

4.2.2 Open-loop versus closed-loop QO-STBCs in MIMO-OFDM Systems

OSTBCs discussed in the last section exploit full diversity gain and provide full code rate with low complexity linear ML decoding. Unfortunately, the achievable rate with OSTBCs is relatively low whenever more than two transmit antennas are used with complex constellations. However, in a number of wireless communications applications [42] achieving high transmission rate can be more important than achieving maximal diversity gain. These considerations motivate the development of quasi-orthogonal space-time block codes (QO-STBCs) which, in the open-loop case, trade diversity gain and decoding simplicity for enhancing transmission rate [43] [44]. In [43], the QO-STBCs were defined for the special case of $L_t = 4$ transmit antennas by the following form of transmission matrix:

$$\mathcal{G}_{14} = \begin{bmatrix} \mathcal{G}_{12} & \mathcal{G}_{34} \\ -\mathcal{G}^*{}_{34} & \mathcal{G}^*{}_{12} \end{bmatrix} = \begin{bmatrix} \mathbf{S}_1 & \mathbf{S}_2 & \mathbf{S}_3 & \mathbf{S}_4 \\ -\mathbf{S}_2^* & \mathbf{S}_1^* & -\mathbf{S}_4^* & \mathbf{S}_3^* \\ -\mathbf{S}_3^* & -\mathbf{S}_4^* & \mathbf{S}_1^* & \mathbf{S}_2^* \\ \mathbf{S}_4 & -\mathbf{S}_3 & -\mathbf{S}_2 & \mathbf{S}_1 \end{bmatrix} \tag{4.2.7}$$

where $\mathcal{G}_{pb}$ is Alamouti's code matrix defined in (4.2.1), the operation

$(.)^*$ denotes complex conjugation of $\mathcal{G}_{pb}$ and $\mathcal{G}_{34}$ denotes the 2×2 matrix which contains block symbols $\mathbf{S_3}$ and $\mathbf{S_4}$. Notice that this is in contrast to (4.2.1) where S_1 and S_2 are individual symbols. The form of (4.2.7) with block symbols, is targeted at the OFDM scenario. The transmit matrix $\mathcal{G}_{14}$ corresponds to four transmit antennas transmitting a symbol block of four OFDM symbol intervals. The n^{th} column of this matrix corresponds to the blocks transmitted from the i^{th} antenna at consecutive symbol intervals.

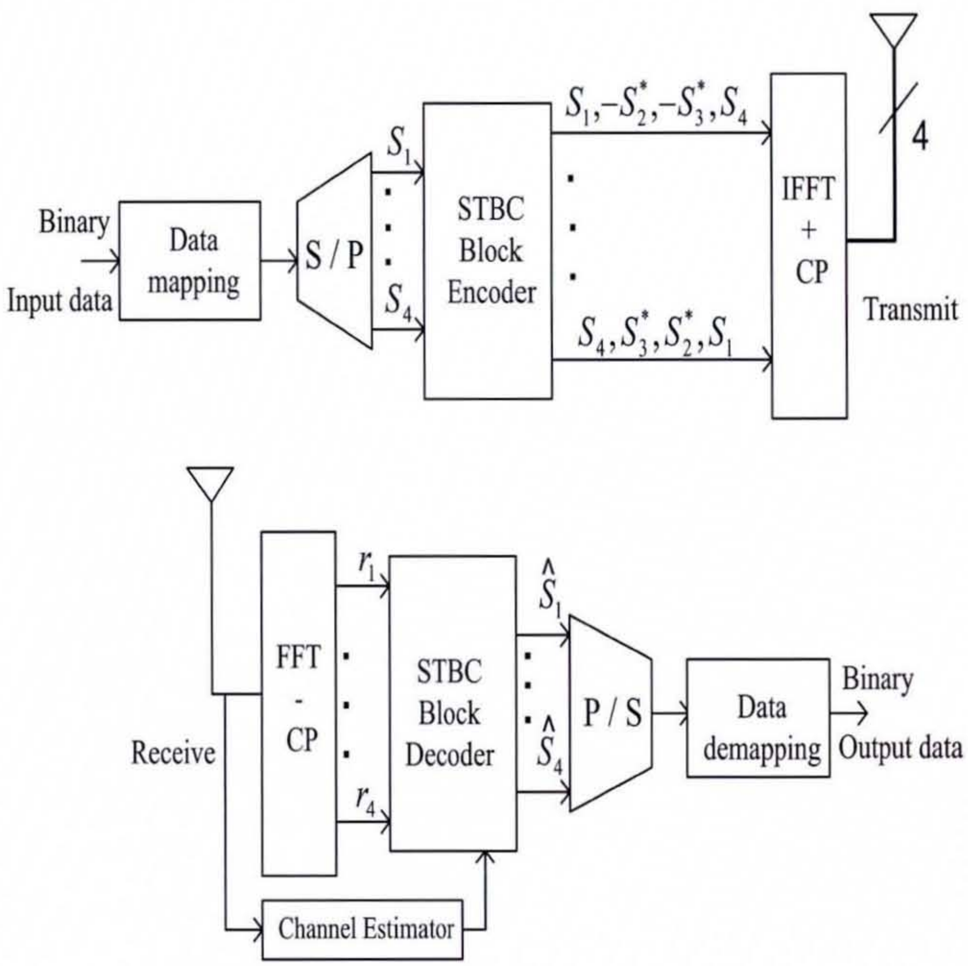

Figure 4.1. Block diagram of the baseband QO-STBC scheme for MIMO-OFDM transmission with four transmit and one receive antennas.

Figure 4.1 describes the block diagram of the open-loop uncoded (in the sense that no other coding, such as convolutive coding with interleaving, is used) QO-STBC MIMO-OFDM transmission system considered in this chapter. Binary input data first go through a mapping system which is typically to form the binary data into a complex quadrature amplitude modulation (QAM) constellation to enhance spectral efficiency. A binary to gray code mapper could also be included to reduce BER but this is not included in this work. $N \times 1$ vectors, consisting of complex valued symbols, are formed through serial-to-parallel conversion and represented by $\mathbf{S}_i, i = 1, ..., 4$. The four data blocks $\mathbf{S}_i$ are then space-time encoded and transmitted over four consecutive block intervals through four antennas using the QO-STBC code matrix in (4.2.7). To eliminate inter-symbol-interference (ISI), a cyclic prefix (CP) of length greater than the length of the channel impulse response is added for each OFDM symbol before the transmission. The addition of the CP also forces the effective channel convolution matrix to be cyclic so that the FFT matrix diagonalizes the channel. It is assumed that the transmitted signal is propagated through quasi-static frequency-selective Rayleigh fading channels, i.e. the channels remain constant over the block interval of the quasi-orthogonal transmission, and is received by one receive antenna. Each channel between the transmit antenna i and the receive antenna is assumed to have L independent multipath (channel taps) where the channel impulse response vector in discrete time is given by $[h_i(0), h_i(1), ..., h_i(L-1)]$. The channel frequency response at the k^{th} frequency subcarrier for a

MIMO-OFDM system can be expressed as:

$$H_i(k) = \sum_{l=0}^{L-1} h_i(l) e^{-j2\pi lk/N} \quad ,0 \leq k \leq N-1 \tag{4.2.8}$$

where $h_i(l)$ is the l-th tap channel impulse response with zero mean complex Gaussian random variable and variance of σ_l^2, where $\Sigma_{l=0}^{L-1}\sigma_l^2 = 1$. At the receiver, the CP is removed and the signals are decoded using CSI obtained through a training-based estimator [43]. The received symbol in the k^{th} subcarrier is therefore written as:

$$\underbrace{\begin{bmatrix} r_1(k) \\ r_2^*(k) \\ r_3^*(k) \\ r_4(k) \end{bmatrix}}_{\mathbf{r}(k)} = \underbrace{\begin{bmatrix} h_1(k) & h_2(k) & h_3(k) & h_4(k) \\ h_2^*(k) & -h_1^*(k) & h_4^*(k) & -h_3^*(k) \\ h_3^*(k) & h_4^*(k) & -h_1^*(k) & -h_2^*(k) \\ h_4(k) & -h_3(k) & -h_2(k) & h_1(k) \end{bmatrix}}_{\mathbf{H}(k)} \underbrace{\begin{bmatrix} c_1(k) \\ c_2(k) \\ c_3(k) \\ c_4(k) \end{bmatrix}}_{\mathbf{x}(k)} + \underbrace{\begin{bmatrix} n_1(k) \\ n_2(k) \\ n_3(k) \\ n_4(k) \end{bmatrix}}_{\mathbf{n}(k)} \tag{4.2.9}$$

At the receiver, the matched filtering is performed in each subcarrier k = 0,..., N-1, as follows:

$$\begin{aligned} \tilde{\mathbf{S}}(k) &= \mathbf{H}^H(k)\mathbf{H}(k)\mathbf{x}(k) + \mathbf{H}^H(k)\mathbf{n}(k) \\ &= \underbrace{\begin{bmatrix} \acute{\gamma}(k) & 0 & 0 & \alpha(k) \\ 0 & \acute{\gamma}(k) & -\alpha(k) & 0 \\ 0 & -\alpha(k) & \acute{\gamma}(k) & 0 \\ \alpha(k) & 0 & 0 & \acute{\gamma}(k) \end{bmatrix}}_{\mathbf{\Delta}} \mathbf{x} + \tilde{\mathbf{n}} \end{aligned} \tag{4.2.10}$$

where $\acute{\gamma}(k) = \sum_{i=1}^{4} |h_i^2(k)|^2$, $\alpha(k) = \Re\{h_1^*(k)h_4(k) - h_2^*(k)h_3(k)\}$ and $\Re\{\cdot\}$ denotes the real part of a complex quantity.

It should be noted that Δ in (4.2.10) is not diagonal; off-diagonal non-zero terms reduce the diversity gain of the code. However, to achieve a full diversity gain in QO-STBC, the off-diagonal terms of $\mathbf{\Delta}$ should be forced to zero. One good solution to eliminate α in (4.2.10) was presented in [45], where the signal transmitted from the third and fourth antennas are rotated by a common phase term $e^{-j\phi_k}$ as follow:

$$\begin{aligned} \alpha(k) &= 2\ \Re\{\{h_1^*(k)h_4(k) - h_2^*(k)h_3(k)\}e^{-j\phi_k}\} \\ &= 2\ \Re\{\chi(k)e^{-j\phi_k}\} \end{aligned} \tag{4.2.11}$$

where the magnitude of the off-diagonal element $\alpha(k)$ is reduced or eliminated. However, this required that the product in (4.2.11) should be a complete imaginary number. It is shown in [46] that this can be achieved if and only if $\phi_k \in [-\pi/2, \pi/2)$.

Mitigation of the PAPR of the time domain signals resulting from such a QO-STBC MIMO-OFDM scheme is next considered.

4.3 The proposed approach

In this section the four antenna space-time block quasi-orthogonal MIMO-OFDM technique is considered with feedback as in [45] to obtain full diversity and full rate performance.

The time-domain OFDM signal, transmitted from the i^{th} transmit antenna is represented algebraically as:

$$s_i[n] = \frac{1}{\sqrt{N}} \sum_{k=0}^{N-1} c_i(k) e^{j2\pi nk/LN} \ , 0 \le n \le LN-1 \tag{4.3.1}$$

where $s_i[n]$, $i = 1, 2, 3, 4$ denote the complex valued time-domain transmitted symbols, $j = \sqrt{-1}$, L is the oversampling factor and $c_i(k)$ is the k^{th} subcarrier of the i^{th} transmit antenna.

It is assumed that the block code matrix in (4.2.7) is transmitted in the form of quadrature phase-shift keying (QPSK) symbols through a frequency selective channel and the signal is received with only one receive antenna. Between each transmitter and the one receive antenna, it is assumed that a multipath channel exists and that the coefficients of that channel are modelled by independent, complex valued, random variables with zero mean and unity variance. It is also assumed that each multipath channel is quasi-static. The PAPR associated with a MIMO-OFDM system can be defined as [4]:

$$PAPR_{MIMO} = \underset{i}{avrg} \left(\frac{\max\limits_{0 \le n \le NL-1} \{|s_i[n]|^2\}}{E\{|s_i[n]|^2\}} \right) \tag{4.3.2}$$

where $avrg[\cdot]$, $\mathrm{E}\{\cdot\}$ and $|\cdot|$ represent respectively the average element, the statistical expected value and the absolute value of the input symbols.

Since the peak power of the time-domain signal is not affected by block complex conjugation and sign-change in the frequency domain, PAPR reduction needs only to be measured on the first period of the OFDM blocks. It is natural to individually apply SLM in Section 3.1.4 to each antenna in QO-STBC. The OFDM symbol, $\mathbf{S}_i$, is mapped to a number of M independent candidate symbols representing the same information. Then, the candidates $[c_i(0), ..., c_i(N-1)]$ are generated by multiplying carrier-wise the original OFDM frame with M phase vectors $\mathbf{b}^{(m)} = [b_0^{(m)}, ..., b_{N-1}^{(m)}]$, $b_k^{(m)} \in \{\pm 1, \pm j\}$. Since there are L_t transmit antennas, this result in ML_t sets of subcarriers vectors. Finally, a set with the minimum average PAPR over L_t transmit antennas is chosen. In order to recover the data at the receiver, SI bits of length $Z = [log_2(M)]$, for each subcarrier, have to be transmitted to indicate which sequence was used in the transmitter. The detection probability of this SI can be given by:

$$P_d = 1 - Z \times \zeta \tag{4.3.3}$$

in which

$$\zeta = (\frac{1-\beta}{2})^D \sum_{d=0}^{D-1} \binom{D-1+d}{d} (\frac{1+\beta}{2})^d \tag{4.3.4}$$

where $\beta = \frac{1}{\sqrt{1+1/SNR}}$ and D represents the number of diversity channels carrying the same SI [4].

In the proposed combined scheme, SI is best transmitted over locations that are evenly distributed in frequency. In this work, QPSK modulation which means that each carries needs log_2Q bits, is used and the OFDM frame is divided into four uniformly separated regions across the frequency range as follows:

$$k_i = \begin{cases} (i-1)\frac{N}{L_t} & \text{if } i \leq \frac{L_t}{4} \\ N - [\frac{\frac{3N}{16}Z}{log_2Q} + \frac{N}{2}] - (\frac{L_t}{2} - i) & \text{if } \frac{L_t}{4} < i \leq \frac{L_t}{4} + 1 \\ N - [\frac{\frac{3N}{8}Z}{log_2Q}] + (L_t - i) & \text{if } \frac{L_t}{4} + 1 < i \leq L_t \\ N - [2Zlog_2Q](L_t - i) & \text{if } i \geq L_t \end{cases} \tag{4.3.5}$$

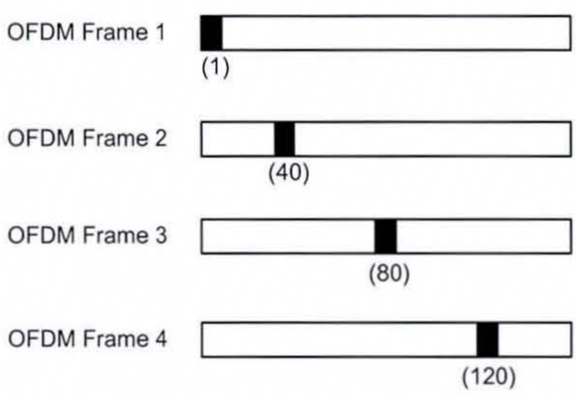

Figure 4.2. Example shows the locations of SI in QO-STBC with $N = 128$, $L_t = 4$, $Z = 2$ and $Q = 4$.

where L_t denotes the number of transmit antennas. An example of this is shown in Figure 4.2. By doing this, the SI is positioned as far apart across frequency as possible to maximize the frequency diversity gain and that same SI is transmitted on all of the antennas, which maximizes the spatial diversity. In the combined SLM approach, the selection among those M random sequences is made according to the average PAPR across the antennas and the corresponding cumulative complementary distribution function (CCDF) of the best sequence is:

$$Pr(PAPR_{MIMO} > \gamma) = [1 - (1 - e^{-\gamma})^{N_s}]^M \qquad (4.3.6)$$

where γ is the threshold of PAPR and M is the phase vector number and $N_s = L_t \times N$. Next, a numerical evaluation of the performance of this approach is considered.

4.4 Simulation Results

The CCDF performance of the scheme was initially considered and the analytical results compared with the numerical results. In particular, Figure 4.3 confirms that, as the possible number of subsequences M changes from 1 to 4, with an oversampling factor of 1; the curve slope is increased. Also, it can be seen that the analytical curves according to (4.3.6) are essentially identical to the simulation results. In this figure, consider when the probability of $PAPR > \gamma = 0.001$ in this case when $M = 1$ the value of $\gamma >$ 10.5 dB. However, when $M = 4$ the value of γ is between 8 and 9.5 dB demonstrating at least a 1 dB reduction.

Figure 4.4 generates a more accurate representation of the true PAPR through oversampling by a factor of 4. Importantly, in the case of QO-STBCs for example, the minimum PAPR threshold that was found is different. In the case of no interpolation for the combined scheme, the minimum PAPR achieved was 9 dB for the combined QO-STBCs. However, with interpolation, the new minimum PAPR changed to 9.5 dB for the same number of antennas. This 0.5 dB difference corresponds to properly finding the peaks in the time-domain signal through the oversampling operation. In Figure 4.5, the BER performance of the complete SLM-based SISO-OFDM systems is shown and compared with the proposed combined closed-loop phase scheme and the open-loop scheme both for four transmit and one receive antennas over frequency selective channels, $N = 128$ and $M = 2$. It is noted that, at BER $= 0.01$ the closed-loop scheme needs E_b/N_o of approximately 8.5 dB while this value increased to at least 14 dB with the SISO-OFDM SLM scheme. Moreover, the overall BER performance matches the perfect SI detection when exploiting four-antenna diversity.

For the final simulation, in Figure 4.6, the probability of detection of SI for both $L_t = 2$ MIMO-STBC and $L_t = 4$ QO-STBCs based on the SLM technique is provided. It can be observed that when $L_t = 2$, both the numerical and the analytical results give a probability of SI detection around 0.95 at $E_b/N_o = 1$ dB and with $L_t = 4$, this probability is increased by approximately 4% confirming the utility of the scheme.

4.5 Summary

In this chapter, a combined SLM approach was proposed for PAPR mitigation in MIMO-OFDM transmission over a four transmit antenna system which exploits closed loop operation with a full rate and full diversity QO-STBC. Performance improvement was demonstrated in terms of comparison with SLM-based SISO-OFDM systems in terms of average BER and probability of SI detection.

It is evident that this proposed scheme is a promising solution for considerably increasing the probability of SI detection. The QO-STBC scheme needs to operate in closed-loop mode in order to have full diversity and full rate. To achieve this, feedback is required from the receiver to the transmitter. When such feedback is used at the transmitter, the transmitted symbols are rotated by a phase value. This operation should not be performed in isolation from the phase rotations that are being applied in terms of the PAPR mitigation scheme. Therefore, the next chapter will be looking at the combination of the feedback together with the PAPR mitigation.

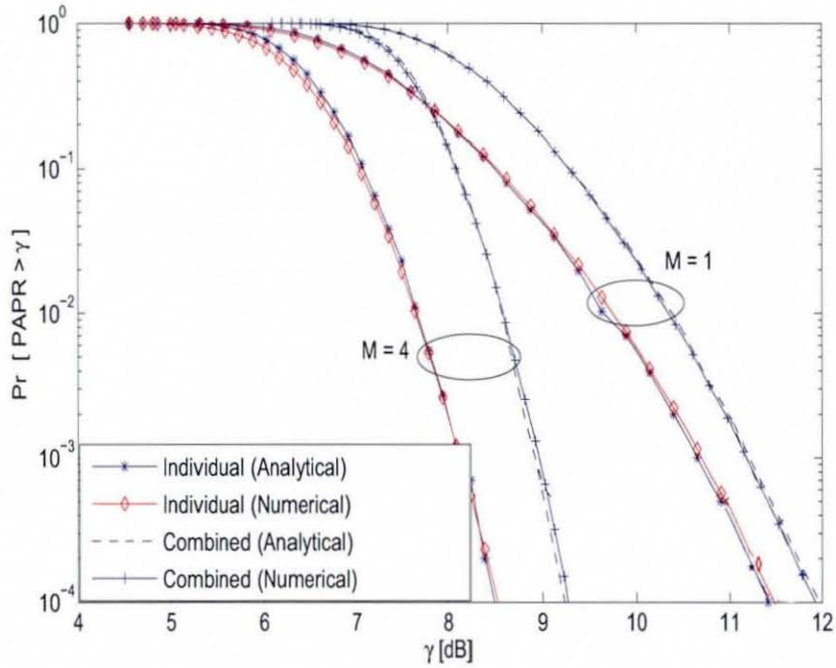

Figure 4.3. CCDF of PAPR, the frame with minimum average PAPR is selected out of M statistically independent frames for both single and combined SLM methods, $L_t = 4$ transmit antennas, $N = 128$, and QPSK modulates each carrier, an oversampling factor of unity.

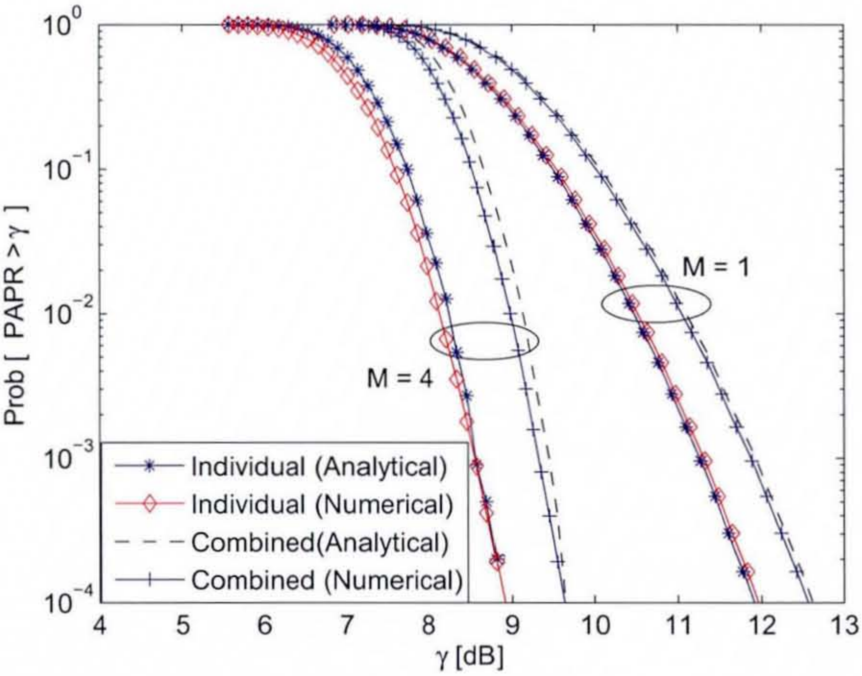

Figure 4.4. CCDF of PAPR, the frame with minimum average PAPR is selected out of M statistically independent frames for both single and combined SLM methods, $L_t = 4$ transmit antennas, $N = 128$, and QPSK modulates each carrier, an oversampling factor of 4.

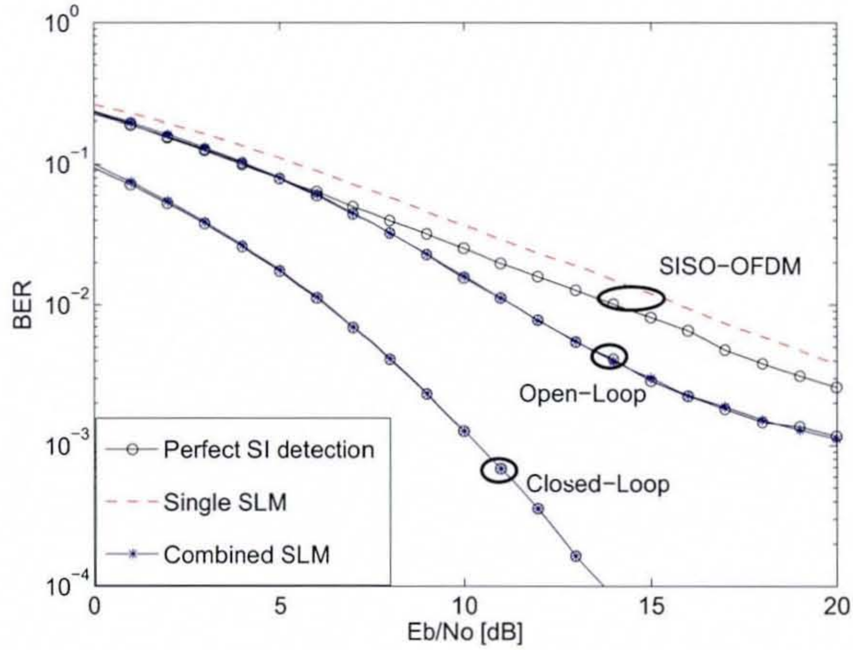

Figure 4.5. BER comparison with respect to side information for both single and combined SLM methods of QO-STBCs with and without feedback, $N = 128$ and $M = 2$.

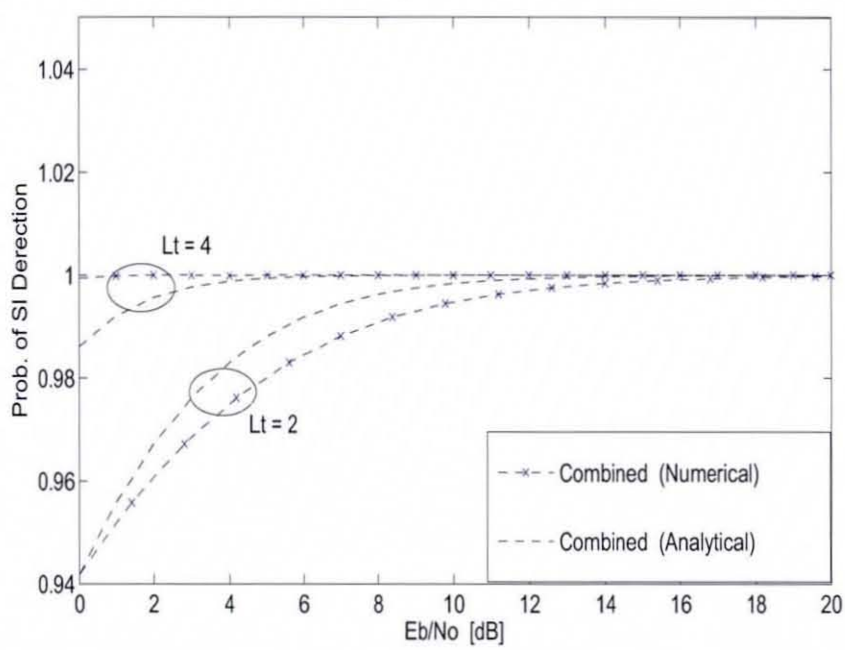

Figure 4.6. Probability of side information detection using SLM method for 2×1 STBC-SLM and a combined 4×1 QO-STBC, $N = 128$ and $M = 2$.

Chapter 5

JOINT SLM AND CLOSED-LOOP QO-STBC FOR PAPR MITIGATION IN MIMO-OFDM TRANSMISSION

In Chapter 4, it was highlighted that a quasi-orthogonal space-time block code (QO-STBC) MIMO-OFDM transmission can attain full diversity and full rate when the third and fourth antennas are rotated by a common phase angle. This however requires N feedback bits for each frequency, k, which imposes too much of an overhead constraint on the uplink channel. This chapter therefore builds upon the work of the previous chapter by practically choosing the feedback angles together with the appropriate sequences within the SLM scheme. The number of bits needed to represent the feedback phase angles will be reduced by exploiting the correlation across frequencies of the required rotation angles[1]. Study of QO-STBC and PAPR mitigation in the context of closed-loop MIMO-OFDM with a realistic amount of feedback is then undertaken. The term 'closed-loop' is used to highlight that channel state information must be fedback from the receiver to the transmitter.

5.1 Overview

The closed-loop quasi-orthogonal space time block coding (QO-STBC) scheme developed by Toker, Lambothoran and Chambers has much attraction due to its full diversity and full rate. This scheme exploits feedback from the receiver to the transmitter by rotating the third and fourth antennas by a common phase angle as described in the previous chapter. However, this technique ignores the effect of increased PAPR introduced by the phase rotations, and the associated demands on the range of linearity of transmission power amplifiers. Moreover, the feedback used for closed-loop operation is impractical. Therefore, the goal of this chapter is to reduce the number of the feedback bits whilst minimizing the PAPR.

Two symbols within an OFDM frame are therefore either used for transmitting selected mapping SI or for PAPR mitigation, thereby retaining the diversity gain of the multiple antennas whilst being able to perform the PAPR mitigation. For an OFDM system with 128 subcarriers and QPSK data symbols, the new scheme shows that the multiple antenna PAPR can be effectively reduced. Furthermore, the BER performance is compared with respect to SI for both the un-quantized and quantized

[1]This work was presented at the Eusipco2008 conference [47]

closed-loop QO-STBC.

The structure of this chapter is as follows. In the next section, background material is presented. Next, in Section 5.3, the PAPR reduction in closed-loop QO-STBC for MIMO-OFDM transmission, in particular the issue of rotating two symbols in the OFDM frame in place of sending useful information, whilst maintaining the diversity gain, is presented. Simulation results are provided in Section 5.4. Practical issues in feedback are introduced in Section 5.5. Finally, Section 5.6 contains the chapter summary.

5.2 Background

In Chapter 4, it was highlighted that a space-time block code for complex symbols with full diversity and full code rate does not exist for more than two transmit antennas. However, the feedback scheme proposed by Jafarkhani and Foschini for QO-STBCs in [43] solved the non-orthogonality by rotating the signals from two antennas before the transmission based on the information provided by the receiver. Assuming that the symbols transmitted from the third and the fourth antennas are rotated by a common phase $e^{j\theta_k}$ and the phase rotation on transmitted symbols is equivalent to rotating the corresponding channel coefficients phases, the new off-diagonal term can be written as:

$$\alpha(k) = 2\,\Re\{\chi(k)e^{-j\phi_k}\} \tag{5.2.1}$$

where $\chi(k) = h_1^*(k)h_4(k) - h_2^*(k)h_3(k)$. In order to eliminate the interference term, $\alpha(k)$, the result of (5.2.1) should be a complete imaginary number. This can be achieved when $\angle\chi(k) - \angle\phi_k = \pm\pi/2$. Therefore, feeding back the exact value of the phase angles with fixed or floating point number representations can require very large feedback overhead. Moreover, in a practical application this may not be possible due to the very limited feedback bandwidth. The number of feedback bits required from the receiver to the transmitter should be kept as low as possible. Assuming a practical scenario that only K bits are allowed for the feedback, the discrete feedback information corresponding to the phase ϕ_k will be an element of the set $\{\phi_k \in \nu = \{\pm\frac{\pi}{2^{K+1}}(2n-1)\}, n = 1, 2, ..., 2^{K-1}\}$ computed as:

$$\phi_k = \arg\min_{\tilde{\phi}_k \in \nu} \Re\{\chi(k)e^{j\tilde{\phi}_k}\} \tag{5.2.2}$$

Figure 5.1 illustrates the phase feedback required for a 64 point OFDM symbol over a particular frequency selective channel of length three. A two level quantized phase $-\pi/4$ and $\pi/4$ is also shown in the same figure. It can be seen that the required phase feedback is a highly correlated waveform in frequency. So instead of feedback of 64 individual frequencies, these are divided into five groups and each group is represented by only one phase angle as shown in Table 5.1, hence the number of feedback bits is reduced significantly, but, of course, the group locations must also be transmitted.

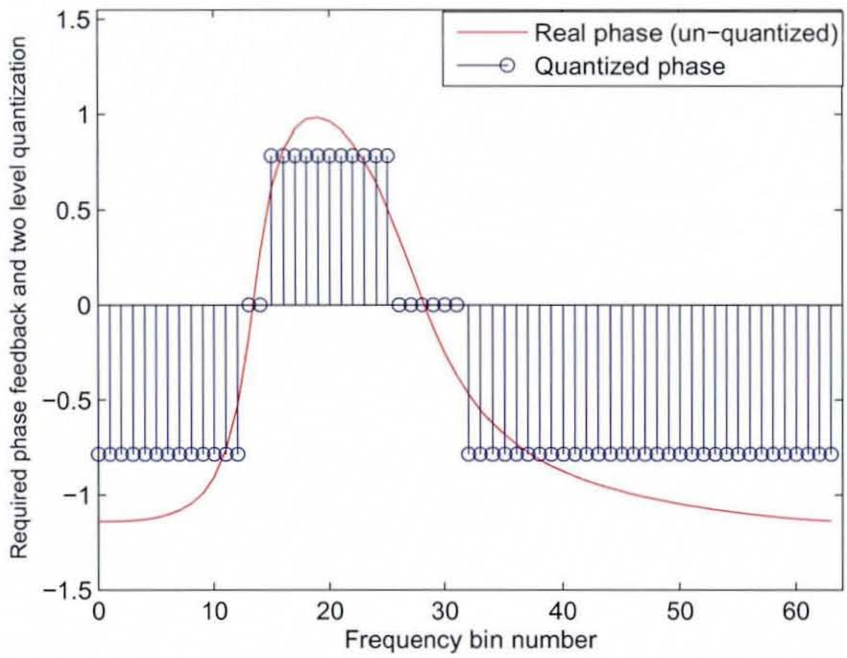

Figure 5.1. Quantized and un-quantized phase angles.

Group no.	Frequency subsets	Phase angle (radians)
1	0 - 14	-0.8
2	15 - 16	0
3	16 - 23	+0.8
4	23 - 28	0
5	28 - 64	-0.8

Table 5.1. Quantization of 64 consecutive subcarriers into five groups in closed-loop QO-STBC required to reduce the feedback overhead.

5.3 PAPR reduction in Closed-Loop QO-STBC

Consider that the block code matrix in (4.2.7) with quadrature phase-shift keying (QPSK) symbols is used to transmit through a frequency selective channel, and the signal is received with only the receive antenna. Between each transmitter and receive antenna, the channel is multipath and the coefficients of the channel are modelled by independent, complex-valued random variables with zero mean and unity variance. Also, consider that each multipath channel is quasi-static over a quasi-orthogonal transmission interval.

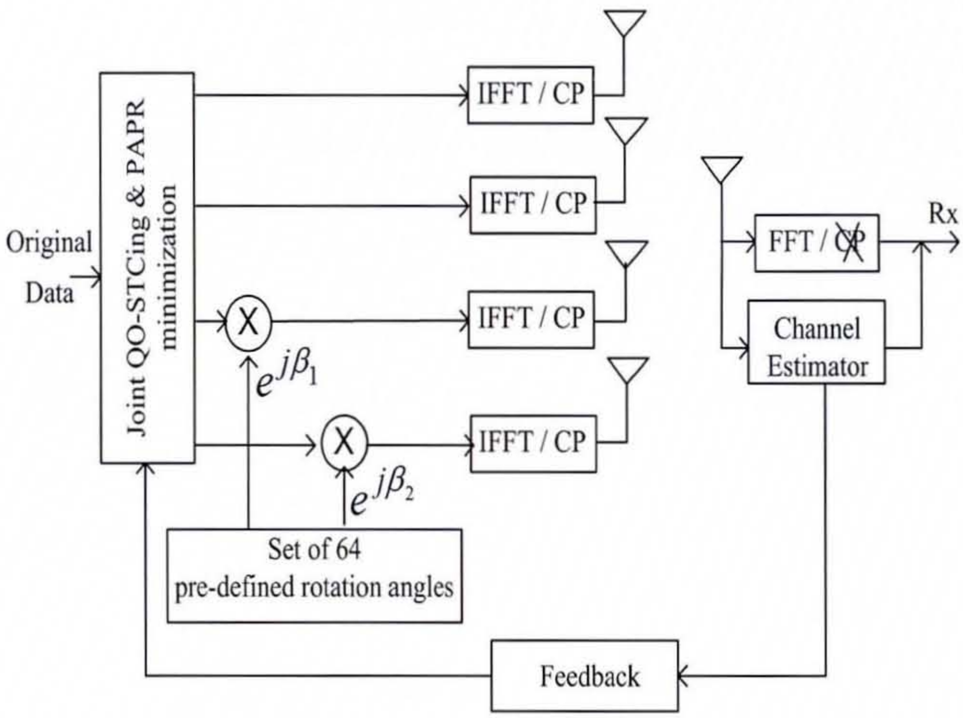

Figure 5.2. Block diagram of the proposed closed-loop joint QO-STBCing and PAPR concept.

The discrete-time samples of OFDM signal $s_i[n], i = 1, ..., 4, n = 0, ..., LN-1$ with N subcarriers can be expressed as:

$$s_i[n] = \frac{1}{\sqrt{N}} \sum_{k=0}^{N-1} c_i(k) e^{j2\pi nk/LN} \ , 0 \leq n \leq LN - 1 \tag{5.3.1}$$

where $j = \sqrt{-1}$, L is the oversampling factor and $c_i(k)$ is the k^{th} subcarrier of the i^{th} transmit antenna.

The PAPR can be calculated as:

$$PAPR_{MIMO} = \underset{i}{avrg} \left(\frac{\max\limits_{0 \leq n \leq NL-1} \{|s_i[n]|^2\}}{E\{|s_i[n]|^2\}} \right) \tag{5.3.2}$$

where $avrg[\cdot]$, $\mathrm{E}\{\cdot\}$ and $|\cdot|$ represent respectively the average element, the statistical expected value and the absolute value of the input symbols.

In a PAPR reduction problem, the peak value of the time-domain signal should be bounded by a specific value $\max[|s_i[n]|] \leq \gamma \ \forall n$. This bound on the time-domain signal after sampling translates easily to the frequency-domain because the IFFT is linear. Stated concisely, without loss of generality, the goal of the new scheme is to use two symbols in the OFDM frame, which had previously been used for SI (see Chapter 4) in the two antenna MIMO-SLM scheme, to rotate the third and fourth antennas by one of a set of pre-defined rotation angles to reduce the PAPR after applying the rotation angles to the other symbols in the OFDM frame necessary in closed-loop QO-STBC scheme. These rotation angles, β_1, β_2, are elements of the set $\{\beta_1, \beta_2 \in \psi = \pi r/8, r = 1, ..., 8\}$ and chosen to satisfy:

$$\{\beta_1, \beta_2\} = \underset{\{\beta_1, \beta_2\} \in \psi}{\arg\min} \ PAPR_{MIMO}(\beta_1, \beta_2) \tag{5.3.3}$$

These rotation angles keep the complexity of the optimization search within bounds, i.e. 64 rotations must be examined when exhaustive search is employed as in this chapter. The value 64 was found by experimentation to be a good compromise between accuracy and complexity.

The SLM method, explained in Chapter 4, is applied in conjunction with the propsed scheme to further reduce the PAPR in the OFDM signals. Note that in the SLM approach all of the M subvectors are assumed to be known to both the transmitter and the receiver. In order to recover the data at the receiver SI bits of length $[\log_2(M)]$ at each subcarrier have to be transmitted to indicate which out of the b^M sequences was used in the transmitter. In this proposed combined scheme, the SI bits are transmitted over two symbols in the OFDM frame. The positions of these two symbols are chosen so as to maximize the frequency diversity across the frame as in [12] and that same SI is transmitted on two antennas which maximizes the spatial diversity. The position of the SI information within the other two antennas is exploited to mitigate the PAPR increase due to the feedback coefficients.

5.4 Simulation results

In this section, a simulation for a complex baseband OFDM system with $N = 128$ subchannels, employing QPSK for four transmit and one receive antennas over a frequency selective fading channel by using 10^5 randomly generated OFDM block symbols is presented.

Figure 5.3 shows evaluation results in terms of the CCDF of implementing the new scheme when applied to closed-loop QO-STBC with an oversampling factor of unity, L = 1. As seen from Figure 5.3, at the probability of 0.001, the new scheme without SLM achieves approximately 0.3 dB PAPR reduction of the threshold, γ, as compared with the closed-loop QO-STBC. However, by combining the SLM approach with both schemes, the PAPR improves by 1.8 dB at the same probability. It can also be seen from Figure 5.3 that the theoretical expressions defined in (4.3.6) are in excellent agreement with the simulation results.

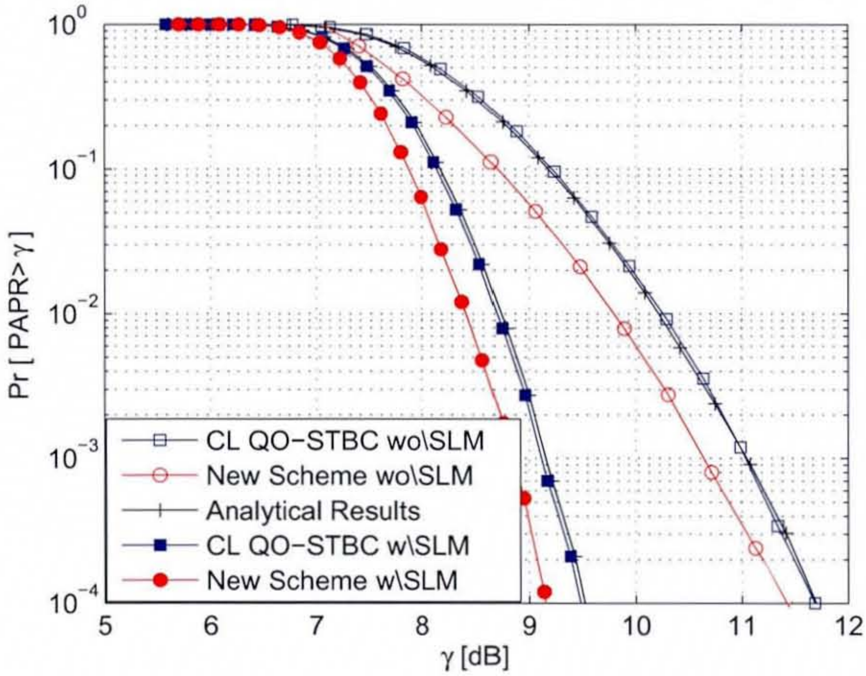

Figure 5.3. CCDF of the PAPR, the frame with minimum average PAPR for the conventional closed-loop QO-STBC technique and the new scheme both combined with the SLM method, $N = 128$, $M = 4$ and with QPSK modulation, oversampling factor of unity.

As already anticipated in Chapter 2, the continuous PAPR has a behaviour that cannot be accurately described by the Nyquist frequency sampled digital signal, L = 1. According to [17] and [27], the presence of peaks in the continuous time-domain signal can be detected with proper confidence when L = 4, see Figure 5.4. The identical notation, as in Figure 5.3, is shown in the curves presented in Figure 5.4, which confirms the proposal. However, the absolute value of γ is increased to the right, supporting that this is a more accurate representation of the performance.

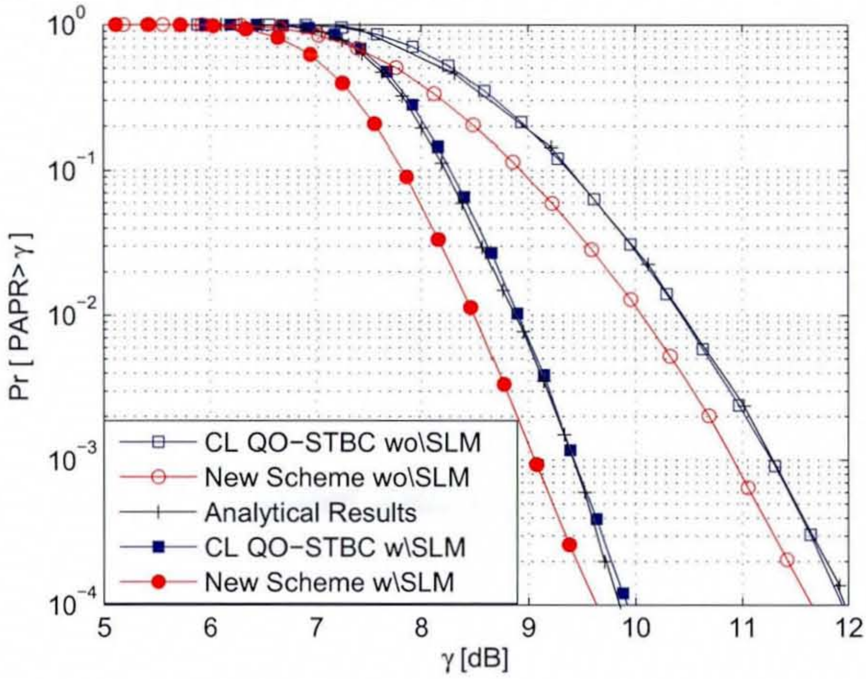

Figure 5.4. CCDF of the PAPR, the frame with minimum average PAPR for the conventional closed-loop QO-STBC technique and the new scheme both combined with the SLM method, $N = 128$, $M = 4$ and with QPSK modulation, oversampling factor of four.

In Figure 5.5 the effect of only transmitting the SI information in two of the four antennas compared with a single antenna is investigated. This shows the overall average bit-error rate (BER) performance of the conventional (un-quantized) closed-loop QO-STBC system with infinite precision feedback and assuming exact SI information is available at the receiver or that it is detected at the receiver. Additionally, for a more practical solution the feedback is quantized to two levels and the same two cases for SI information are compared. The curves for exact and detected SI information are considered in both cases, thereby confirming that transmission of SI information over only two antennas is sufficient in closed-loop QO-STBC. However, if the SI is transmitted from one transmit antenna as in single-input single-output (SISO) system, it is less likely to detect the original signal correctly. Figure 5.5 demonstrates a degradation of approximately 2 dB between the exact and the detected value of SI in SISO-OFDM system.

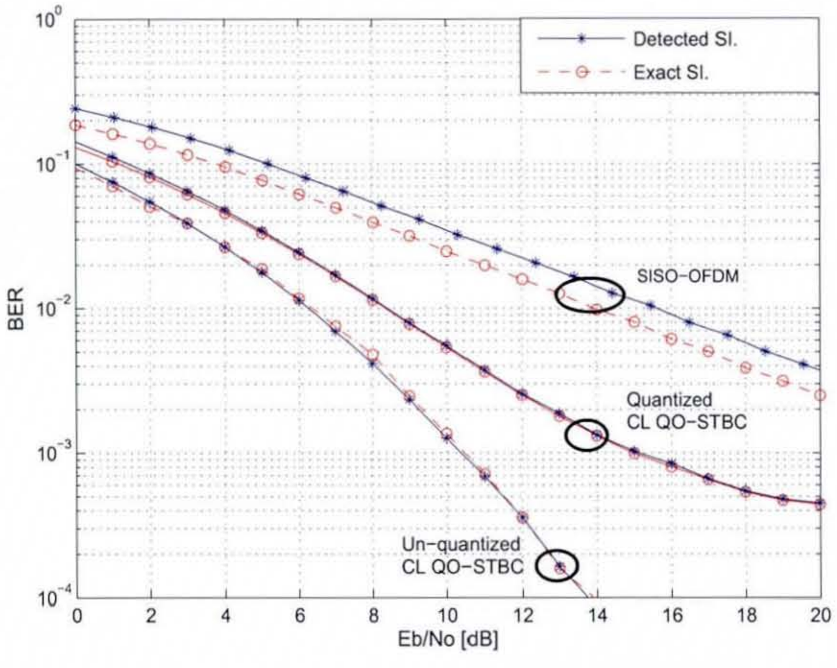

Figure 5.5. BER comparison with respect to side information for conventional closed-loop QO-STBC, quantized closed-loop QO-STBC and SISO-OFDM for $N = 128$ and $M = 4$.

5.5 Practical issues in feedback

One of the major challenges in closed-loop QO-STBC is the use of feedback. For time-division duplex (TDD) systems, the channels in the uplink and the downlink can be assumed to be identical and therefore the feedback issues become straightforward, whereas feedback would be more important in frequency division duplex (FDD) where the information has to be transmitted from the receiver to the transmitter and therefore channel stationarity is a key issue. In practice, by exploiting the strong correlation in the feedback sequence among the subcarriers, the feedback overhead could be decreased [46].

5.6 Summary

Despite the pleasing properties that the closed-loop QO-STBC MIMO-OFDM scheme provides, it, however, does not take PAPR mitigation into account. In this chapter, the occurrence of PAPR over all transmitted antennas in the closed-loop QO-STBC MIMO-OFDM scheme was studied. The proposed technique resolved this problem, with low complexity, by using only two phase rotations in certain frequency bins. Simulation results demonstrated that the proposed algorithm provides a considerable reduction of 2.4 dB at the probability of 0.001 when it is combined with the SLM scheme. Furthermore, the scheme fully utilized the available degrees of freedom produced by employing multiple antennas and embedded a small number of redundancy required for SI detection.

Chapter 6

PAPR MITIGATION IN CLOSED LOOP QO-STBCS USING CARI SCHEME

Closed loop quasi-orthogonal space time block codes (QO-STBCs) have been receiving a great deal of attention as a solution for full spatial diversity and full code rate broadband transmission in four transmit and one receive antenna systems. However, despite the pleasing properties of this approach, it does not consider the effect of high peak-to-average power ratio (PAPR). In this chapter, the aim of the work is to reduce the occurrence of PAPR over all antennas when applied to multiple-input multiple-output orthogonal frequency division multiplexing (MIMO-OFDM) by extending an existing technique called cross-antenna rotation and inversion (CARI) to closed loop QO-STBCs[1]. Additionally, the PAPR is further reduced by including a scrambling algorithm[2]. This new combined approach offers a PAPR that is significantly lower

[1]This work was presented at the IMA 2008 conference [48].

[2]This work was submitted to the Hindawi Advanced in Signal Processing journal [49].

than the original CARI approach. Furthermore, the proposed schemes perform PAPR mitigation whilst maintaining the diversity gain of the multiple antennas. For an OFDM system with 256 subcarriers and quadrature phase shift keying (QPSK) data symbols, the new schemes are shown by simulation study to reduce effectively the multiple antenna PAPR. Moreover, it is shown that by considering only four permutations, the PAPR can be decreased with limited complexity, so that the scheme is more practical. Compared with Chapters 4 and 5, simulation results show that calculating the overall PAPR based on minimum maximum (minimax) is more effective than using the minimum average (miniaverage) criterion.

6.1 Overview

As with single-input single-output OFDM (SISO-OFDM), one of the main disadvantages of MIMO-OFDM is that the signals transmitted from different antennas might exhibit a prohibitively large peak-to-average power ratio (PAPR). In [26], a method was proposed for the reduction of PAPR for STBC MIMO-OFDM, called successive suboptimal cross-antenna rotation[3] and inversion (SS-CARI), in which the input OFDM frame is partitioned into M subblocks of equal size, then subblockwise rotations and inversions across two antennas are performed. Starting from the first subblock, four different OFDM sequence sets are formed where all the other subblocks remain unchanged, then

[3]The term antenna rotation denotes the multiplication of the signal at a particular antenna by a complex phase term, this meaning holds whenever this term is used throughout the remainder of the thesis.

the sequence set which yields the lowest maximum PAPR is selected and by doing this for all M subblocks successively the resulting PAPR shows better performance and similar complexity compared with the simplified SLM scheme. Another suboptimal scheme called random RS-CARI was also proposed in [26] where the sequences for each of the M subblocks are chosen randomly from amongst those used in SS-CARI, for a prescribed number of times P, and the symbol with the best PAPR performance will then be selected for transmission. However, to recover the data, 2M bits of side information (SI) to indicate the proper permutation have to be transmitted to the receiver and this SI is decreased with RS-CARI to $\lfloor \log_2(P) \rfloor$ at the expense of a small reduction in PAPR mitigation. However, if this scheme is directly applied to quasi-orthogonal space-time block codes (QO-STBCs), the complexity would increase proportional to the additional number of transmitting antennas, which is to be avoided.

In this chapter, therefore, the CARI scheme is applied to closed loop QO-STBCs and its complexity is reduced by only considering four possible permutations and therefore the required SI remains the same as the original two optimal CARI schemes. In particular, three methods are examined, successive suboptimal (SS) CARI, random suboptimal (RS) CARI and a new combined approach, scrambling and CARI. These techniques are compared in terms of complementary cumulative density function (CCDF) simulations and the novel scrambling and CARI method yields the best performance.

The rest of this chapter is organized as follows. In Section 6.2 a proposed algorithm based on CARI is introduced for PAPR reduction in closed loop QO-STBCs. Then, a suboptimal scheme, termed random suboptimal (RS) is introduced to reduce computational complexity. Another proposed algorithm, but with remarkably less computational complexity, is presented in Section 6.3. Then, in Section 6.4, simulation results are set out. Finally, Section 6.5 presents the summary of the work.

6.2 SS and RS-CARI in QO-STBCs

This section shows how SS and RS-CARI are applied to closed-loop QO-STBCs and how computational complexity is reduced.

6.2.1 Proposed Algorithm

Consider N subcarriers of the closed loop QO-STBCs defined in Chapter 4 with four transmit and one receive antennas transmitting in the form of quadrature phase-shift keying (QPSK) symbols through a frequency selective baseband channel. Here the generator matrix for QO-STBCs is rewritten to emphasize the block symbols $\mathbf{S_1}$, $\mathbf{S_2}$, $\mathbf{S_3}$, $\mathbf{S_4}$ in the design:

$$\mathcal{G}_{14} = \begin{pmatrix} \mathbf{S}_1 & \mathbf{S}_2 & \mathbf{S}_3 & \mathbf{S}_4 \\ -\mathbf{S}_2^* & \mathbf{S}_1^* & -\mathbf{S}_4^* & \mathbf{S}_3^* \\ -\mathbf{S}_3^* & -\mathbf{S}_4^* & \mathbf{S}_1^* & \mathbf{S}_2^* \\ \mathbf{S}_4 & -\mathbf{S}_3 & -\mathbf{S}_2 & \mathbf{S}_1 \end{pmatrix} \tag{6.2.1}$$

Also, the channel between each antenna and the receiver is considered to be multipath and every multipath channel is assumed quasi-static

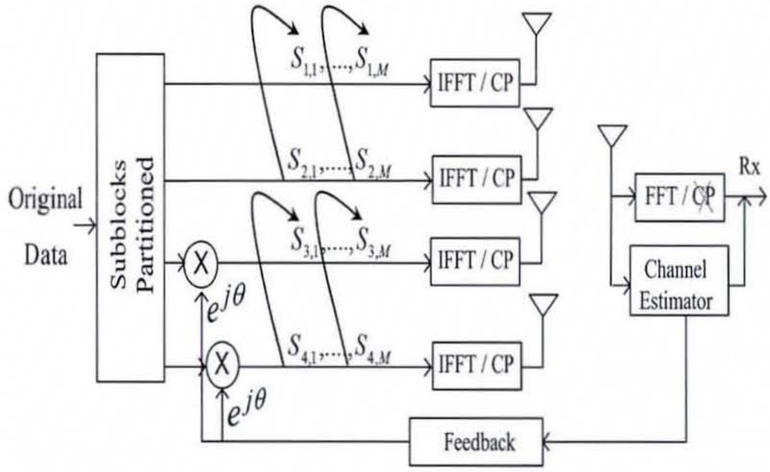

Figure 6.1. Block diagram to mitigate PAPR by combining closed loop QO-STBCs with the CARI scheme; four possible permutations across two pairs of antennas are considered.

over a quasi-orthogonal transmission interval where its coefficients are modelled by independent, complex-valued, random variables with zero mean and unity variance. A simplified block diagram of such a scheme is shown in Figure 6.1. An OFDM data symbol vector is first partitioned into M disjoint subblocks, $\{S_{i,j}\}_{j=1}^{M}$, each of length $K = N/M$. Then, starting from the first subblock, each subblock is swapped and inverted until the lowest maximum PAPR is found and by doing this for all M subblocks successively the PAPR achieved has better performance compared with the simplified concurrent[4] minimax SLM scheme [32]. However, using this scenario would allow many possible rotations and inversion permutations since there are four transmit antennas. Therefore, this complexity is reduced by only considering four possible permutations, i.e. the first subblock has four possibilities denoted as $S_{1,1}, S_{2,1}, S_{3,1}, S_{4,1}$; $S_{2,1}, S_{1,1}, S_{4,1}, S_{3,1}$; $-S_{1,1}, -S_{2,1}, -S_{3,1}, -S_{4,1}$ and

[4]This means combining the PAPRs of the transmission blocks across multiple antennas.

$-S_{2,1}, -S_{1,1}, -S_{4,1}, -S_{3,1}$ and similarly for the other M subblocks, thus, the required SI remains the same as in the original SS-CARI scheme namely, 2M. It is known from Chapters 4 and 5 that the discrete-time samples of OFDM signal $s_i[n], i = 1, ..., 4, n = 0, ..., LN-1$ with N subcarriers, is defined as:

$$s_i[n] = \frac{1}{\sqrt{N}} \sum_{k=0}^{N-1} c_i(k) e^{j2\pi nk/LN} \ , 0 \leq n \leq LN-1 \tag{6.2.2}$$

where $j = \sqrt{-1}$, L is the oversampling factor and $c_i(k)$ is the k^{th} subcarrier of the i^{th} transmit antenna.

Since the performance of the PAPR is calculated by the worst case, the PAPR MIMO-OFDM system is defined as:

$$PAPR_{MIMO} = \max_i \left(\frac{\max\limits_{0 \leq n \leq NL-1} |s_i[n]|^2}{E\{|s_i[n]|^2\}} \right) \tag{6.2.3}$$

where $\max[\cdot]$, $E\{\cdot\}$ and $|\cdot|$ represent respectively the maximum element, the expected value and the absolute value of the input symbols.

Given that $P_{\gamma,o} = 1 - (1 - e^{-\gamma})$, which is the probability that a symbol normalized power exceeds the threshold, γ, then the probability that this happens on N independent subcarriers is:

$$P_\gamma = (P_{\gamma,o})^N \tag{6.2.4}$$

Then, the probability that this happens for M independent alternatives on L_t number of antennas is:

$$Pr(PAPR_{MIMO} > \gamma) = (1 - (1 - e^{-\gamma})^{N_s})^M \tag{6.2.5}$$

where $N_s = N \times L_t$ and L_t is the number of transmit antennas. Here, it should be noted that finding the optimal sequence is still a computationally demanding problem. The RS-CARI scheme introduced in the next subsection is more practical in a closed-loop QO-STBC system since it uses less number of permutations to mitigate the PAPR problem.

6.2.2 Suboptimal Algorithm

In a similar manner, the extension to RS-CARI for four antennas is restricted to the four permutations discussed in Section (6.2.1). Here, the OFDM frame is multiplied by a vector of the same length. This vector is one of the *p-th* rows of the following matrix:

$$\Gamma = \begin{pmatrix} a_{1,1} & a_{1,2} & \cdots & a_{1,M} \\ a_{2,1} & a_{2,2} & \cdots & a_{2,M} \\ \vdots & \vdots & \ddots & \vdots \\ a_{P,1} & a_{P,2} & \cdots & a_{P,M} \end{pmatrix} \tag{6.2.6}$$

where $a_{i,j}$ is a random integer number from 1 to 4, representing the index of the four permutations described in Section (6.2.1). By doing this, the required SI is reduced to $\lfloor \log_2 P \rfloor$. In this case, an optimum PAPR is given by:

$$\tilde{P} = \arg\min_{1 \leq p \leq P}(PAPR^{(p)}_{MIMO}) \tag{6.2.7}$$

To recover $c_i(k)$, it is necessary for the receiver to have a copy of Γ and to determine the vector index based on the lowest PAPR, $\tilde{P}$.

6.3 New Combined Scrambling and CARI Scheme

In this section, a new technique based on CARI is presented. In particular, the reduction technique employs a set of scrambling data before the CARI scheme is applied and then selects the transmitted OFDM symbols to be the ones which have the minimax PAPRs amongst all the transmission symbols from the four antennas. Here, it is claimed that the PAPR reduction can be improved further if the data samples within the subblock are rearranged in a more random pattern before the SS or RS-CARI is applied. In other words, the original data sequence is scrambled by a set of D V-length scrambling sequences, $\{\Omega[i]^{(d)}\}_{i=0}^{V-1}$, where $V = N/M$ and d is an integer such that $d \in [0, D-1]$. This means re-ordering the elements of a subblock such that they are more random in amplitude and thereby the $PAPR$ is likely to be reduced. This is achieved by applying D V-length independent random interleavers to the original data, denoted $int^{(d)}(\cdot)$. Then, the sequence with the lowest $PAPR$ is chosen for transmission. A pseudo-code description of this algorithm is shown below, where $MATLAB$ notation is exploited. Notice that the same scrambling sequences are used for all transmit antennas. Stated concisely when $D = 4$, without loss of generality, the goal of this scheme is to use 4M symbols in total to represent the SI for both the SS-CARI permutation and the choice of interleavers. Equivalently, in the scrambled RS-CARI scheme, $\lfloor 2\log_2(P)]\rfloor$ SI symbols are used, which generally give a smaller value than for the scrambled SS-CARI method.

Pseudo-code of scrambling SS-CARI scheme for closed loop QO-STBCs.

==

d^{th} Interleaver operator as $int^{(d)}(\cdot)$

$S_1^{'} = S_1;\ S_2^{'} = S_2;$

$S_3^{'} = S_3;\ S_4^{'} = S_4;$

for q = 1:M (Down the subblocks)

for d = 1:D (Determining best interleaver for subblock q)

for j = 1:4

$$\tilde{S}_j = [S_{j(1:q-1)}^{'} \ \ int^{(d)} \ \ (S_{jq}^{'}) \ \ S_{j(q+1:M)}^{'}];$$

`end 'j'`

$$PAPR^{(d)} = \max(PAPR(\tilde{S}_1), PAPR(\tilde{S}_2),$$
$$PAPR(\tilde{S}_3), PAPR(\tilde{S}_4));$$

`end 'd'`

$$dopt(q) = \arg\min_{d\in(1,\dots,D)} \left\{PAPR^{(d)}\right\};$$

for j = 1:4 (Store best int output of each subblock)

$$S_{jq}^{opt} = int^{(dopt(q))}(S_{jq}^{'});$$

```
end 'j'
```

Store flipped a cross antenna best outputs:

$$S_{11q}^{opt} = S_{2q}^{opt}; \quad S_{12q}^{opt} = S_{1q}^{opt};$$

$$S_{13q}^{opt} = S_{4q}^{opt}; \quad S_{14q}^{opt} = S_{3q}^{opt};$$

for j = 1:4 (Determining best subblock ordering)

$$\widetilde{S}_j = [S'_{j(1:q-1)} \ (S_{jq}^{opt}) \ S'_{j(q+1:M)}];$$

$$PAPR^{(1,j)} = PAPR(\widetilde{S}_j);$$

$$\widetilde{S}_j = [S'_{j(1:q-1)} \ -(S_{jq}^{opt}) \ S'_{j(q+1:M)}];$$

$$PAPR^{(2,j)} = PAPR(\widetilde{S}_j);$$

$$\widetilde{S}_j = [S'_{j(1:q-1)} \ (S_{1jq}^{opt}) \ S'_{j(q+1:M)}];$$

$$PAPR^{(3,j)} = PAPR(\widetilde{S}_j);$$

$$\widetilde{S}_j = [S'_{j(1:q-1)} \ -(S_{1jq}^{opt}) \ S'_{j(q+1:M)}];$$

$$PAPR^{(4,j)} = PAPR(\widetilde{S}_j);$$

```
end 'j'

for j = 1:4
```

$$PAPR^{(j)} = \max(PAPR^{(j,1)}, PAPR^{(j,2)},$$

$$PAPR^{(j,3)}, PAPR^{(j,4)});$$

```
end 'j'
```

$$xopt(q) = \underset{x\in(1,....,4)}{\arg\min} \left\{PAPR^{(x)}\right\}$$

for j = 1:4 (Forming new frame at the q^{th} stage)

```
if  xopt(q)==1
```

$$S_j^{'} = [S_{j(1:q-1)}^{'} \;\; (S_{jq}^{opt}) \;\; S_{j(q+1:M)}^{'}];$$

```
else  if  xopt(q)==2
```

$$S_j^{'} = [S_{j(1:q-1)}^{'} \;\; -(S_{jq}^{opt}) \;\; S_{j(q+1:M)}^{'}];$$

```
else  if  xopt(q)==3
```

$$S_j^{'} = [S_{j(1:q-1)}^{'} \;\; (S_{1jq}^{opt}) \;\; S_{j(q+1:M)}^{'}];$$

```
else
```

$$S_j^{'} = [S_{j(1:q-1)}^{'} \;\; -(S_{1jq}^{opt}) \;\; S_{j(q+1:M)}^{'}];$$

```
end 'j'
end 'q'
```

$S_1', ..., S_4'$ contain the optimal in the minimax sense frames to be transmitted over the four antennas.

$$SI = \begin{cases} dopt(q) & q = 1 : M \\ xopt(q) & q = 1 : M \end{cases}$$

======================================

The performance of the proposed schemes will be compared and analyzed by means of numerical simulations in the next section.

6.4 Simulation results

In this section, a simulation for a complex baseband OFDM system with $N = 256$ subchannels, employing QPSK for four transmit and one receive antennas over a frequency selective fading channel by using 10^5 randomly generated OFDM block symbols is presented. Complementary cumulative distribution function (CCDF) of PAPR is used to measure the performance which is defined as the probability that PAPR of OFDM symbols exceed a given threshold, γ.

Figure 6.2 illustrates the PAPR reduction performance of the proposed scheme in Section 6.2.1 for M = 4 and M = 16 subblocks. Furthermore, the performance of SLM with the miniaverage selection criterion used in Chapters 4 and 5 and a minimax selection criterion, used in this chapter, are added for comparison. In Figure 6.2, the unmodified OFDM signal has a PAPR which is approximately 11.3 dB at CCDF =

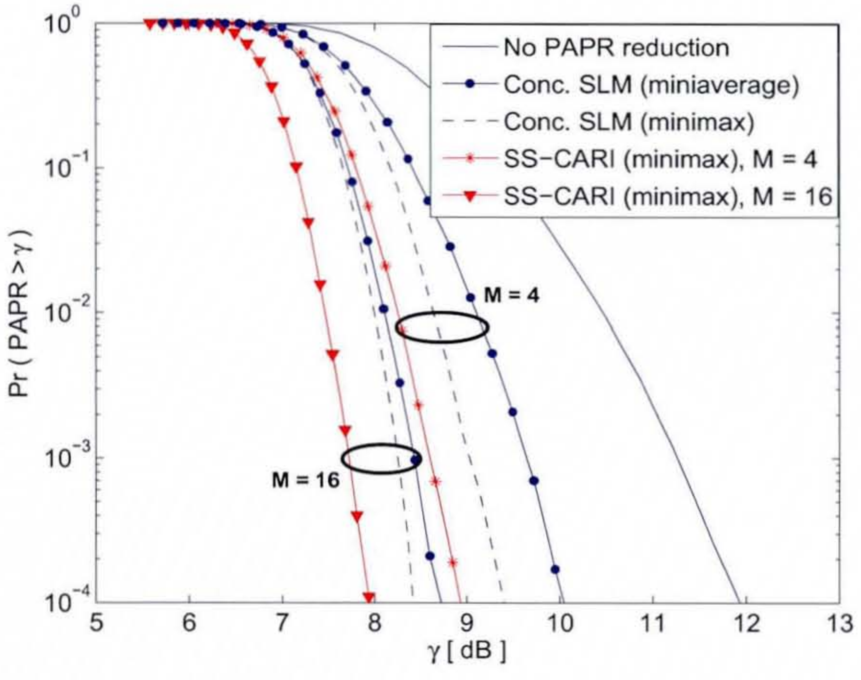

Figure 6.2. CCDF of the PAPR, the frame with minimax PAPR for the conventional closed loop QO-STBC technique and SS-CARI for different values of subblocks M, $N = 256$ with QPSK and an oversampling factor of four.

0.001. For the case with M = 4 and M = 16, at the same probability, the PAPR performance of the concurrent minimax SLM scheme shows an improvement of 2.3 dB and 3 dB respectively compared with the no PAPR reduction. However, this improvement is degraded to 1.6 dB and 2.8 dB when the miniaverage SLM is used. For this reason, in this chapter, the minimax criterion is used. In Figure 6.2, it can also be seen that the SS-CARI achieves a reduction of 2.6 dB and 3.5 dB compared with the no PAPR reduction and better than the minimax SLM scheme by 0.3 dB and 0.5 dB respectively.

The identical pattern as in Figure 6.2 is shown in the curves presented in Figure 6.3. Here, the number of permutations on each M subblocks

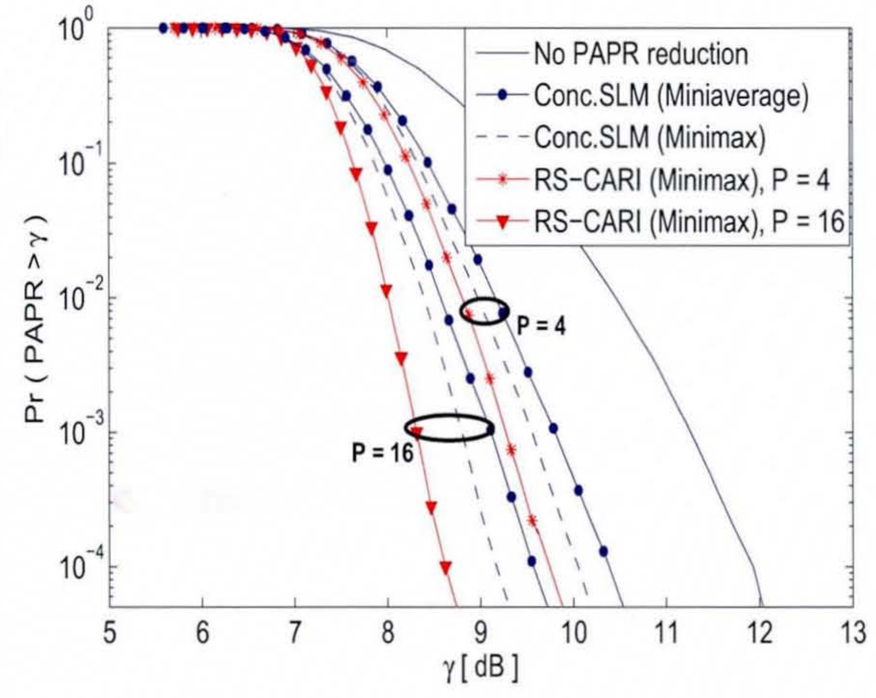

Figure 6.3. CCDF of the PAPR, the frame with minimax PAPR for the conventional closed loop QO-STBC technique and RS-CARI for different values of permutations P, $N = 256$ with QPSK and an oversampling factor of four.

is reduced using random permutation. In Figure 6.3, the unmodified OFDM signal has a PAPR which is approximately 11.3 dB at CCDF = 0.001. Figure 6.3 also shows that the concurrent miniaverage criterion is always outperformed by the minimax criterion. However, the minimax criterion applied on SLM scheme performs worse than RS-CARI scheme due to not utilizing the additional degrees of freedom provided by employing multiple transmit antennas. From this performance comparison, it can be concluded that the absolute value of γ is increased to the right showing less reduction at the expense of lower complexity. Figure 6.4 illustrates the PAPR reduction performance of the proposed scheme in Section 6.3 for M = 4 and M = 16 subblocks with four sets of scrambled data. The performance of the SS-CARI and SLM discussed in Figure 6.2 are also shown for comparison. As seen from Figure 6.4, at CCDF = 0.001, with the help of the new scheme, the PAPR reduction of the transmitted symbols achieved approximately 3.3 dB compared with the no PAPR reduction and better than SS-CARI by 0.7 dB when M = 4. Similarly, at M = 16 and the same probability, the new proposed scheme outperforms the SS-CARI by 0.5 dB. Moreover, the new proposed scheme has larger slope and provided better improvement of approximately 0.3 dB than the minmax SLM when M = 16.

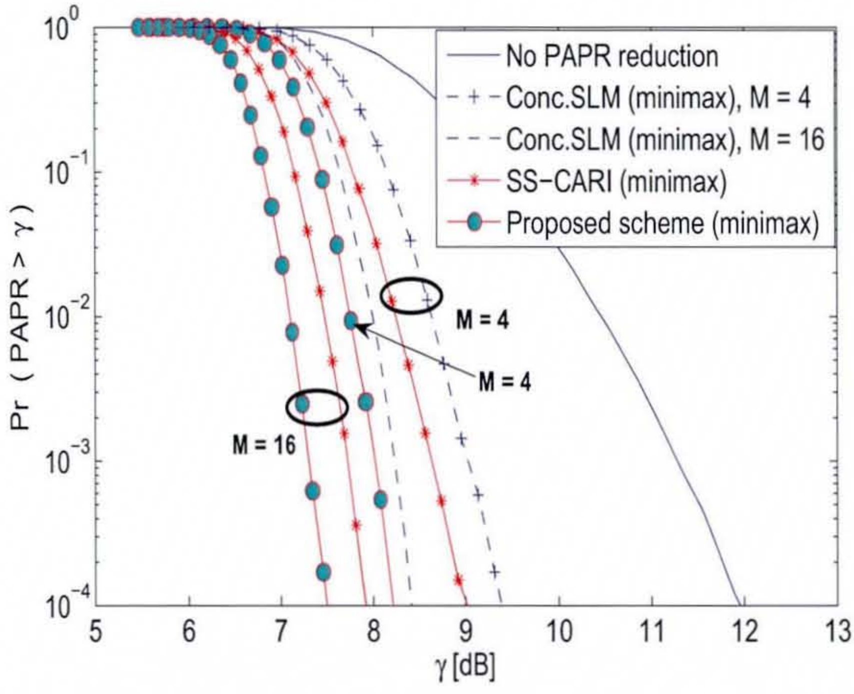

Figure 6.4. CCDF of the PAPR, the frame with minimax PAPR for the conventional closed loop QO-STBC technique, the proposed scheme and SS-CARI for different values of subblocks M, $N = 256$ with QPSK and an oversampling factor of four.

Also, the identical pattern as in Figure 6.4 is shown in the curves presented in Figure 6.5 using four sets of scrambled data along with four sets of random permutation sequences described in Section 6.3. From this figure, it can be seen that the absolute value of γ is increased to the right showing less reduction at the expense of lower complexity. Nevertheless, the performance of the scrambling and CARI scheme still shows better improvement compared with the other schemes, i.e. concurrent SLM and RS-CARI. Taking the example of P = 16 and CCDF = 0.001, the proposed scheme improves the PAPR performance by 3.4 dB compared with the no PAPR reduction and RS-CARI and concurrent SLM by 0.5 dB and 0.9 dB respectively.

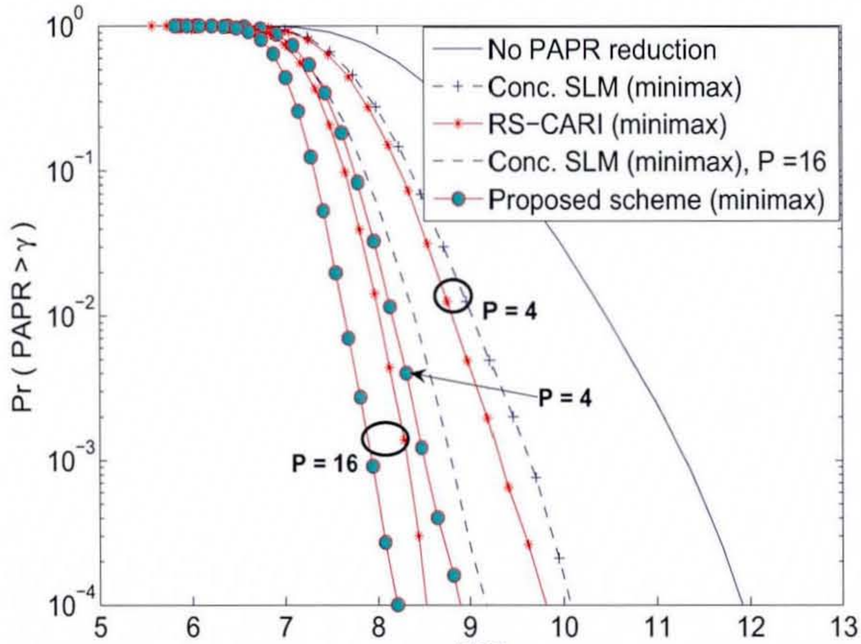

Figure 6.5. CCDF of the PAPR, the frame with minimax PAPR for the conventional closed loop QO-STBC technique, the proposed scheme and RS-CARI for different values of permutations P, $N = 256$ with QPSK and an oversampling factor of four.

6.5 Summary

In Section 6.2, the application of the CARI scheme with closed loop QO-STBCs has been investigated. In particular, the complexity of the CARI scheme was reduced by only considering four permutations per subblock in the context of four antennas. This consideration was also applied to the suboptimal scheme and provided a lower amount of SI while maintaining a similar level of complexity to that shown in the literature [26].

In Section 6.3, a novel algorithm called scrambling and CARI scheme was presented. It has achieved further reduction in PAPR performance than the SS and RS-CARI schemes. However, this reduction is not free. The most significant costs are the D additional IFFT operations, and the D V-length interleaver operations. Moreover, the work in this chapter has shown that measuring the PAPR across multiple antennas with the minimax criterion gives better readings for PAPR reduction than miniaverage criterion used in Chapters 4 and 5.

Now, since the PAPR reduction for point-to-point closed-loop QO-STBC MIMO-OFDM has been extensively investigated in Chapters 4, 5 and 6, the next chapter will look at the PAPR mitigation in the context of co-operative networks and will suggest a practical method in order to tackle this problem.

Chapter 7

A STUDY OF SLM PAPR MITIGATION IN A BROADBAND MULTI-HOP NETWORK

In this chapter, a selective mapping (SLM) algorithm is proposed to reduce the peak-to-average power ratio (PAPR) of OFDM transmission over cooperative networks[1]. In particular, the scheme is applied at the source node and, through the intermediate relay stages, the side information (SI) is transmitted. Otherwise, applying the scheme at both the source and relays would add more complexity. Simulation results show a comparison between the two methods and verify that the degradation in the end-to-end bit error rate (BER) is relatively small but proportional to the number of relay stages.

[1]This work has been submitted to the EUSIPCO'09 conference [50].

7.1 Overview

One of the well-known reasons for quasi-orthogonal space time block coding (QO-STBC) is to exploit diversity gain and thereby increase the robustness of the link in a multi-path fading environment. The diversity gain relies upon the antennas providing uncorrelated links [51]. In point-to-point multi-input multi-output (MIMO), the difficulty is that the antennas are likely to be relatively close to each other due to the mobile station space limitation. To tackle this problem, researchers have suggested a new form of diversity using what is called a virtual antenna array (VAA) or cooperative MIMO [6]. Such a scenario enables single antenna mobiles in a multi-user environment to share their antennas and generate a virtual MIMO channel that allows them to achieve transmit diversity. The mobile wireless channel also suffers from path loss [6] which is proportional to the link length between the two nodes. The principle of a VAA is to have an array of spatially distinct single antenna elements connected with shorter links to combat the deleterious effect of path loss. Moreover, forming a VAA group is very likely to guarantee that the channels are uncorrelated. Lastly, if the relay nodes themselves can work with a single antenna, that is much cheaper than having one node with four antennas and all the associated electronics. MIMO combined with orthogonal frequency division multiplexing (OFDM) systems are regarded as one of the most important candidates for next generation wireless systems. This is due to the fact that OFDM offers high spectral efficiency, robustness to multi-path fading and its ability to efficiently handle frequency selective fading channels without resorting to complex channel equalization schemes. A major limitation of MIMO-OFDM systems is that the transmitted signal amplitude varies widely and causes a very high PAPR when the input sequence is highly correlated. As mentioned in Chapter 2, a high PAPR requires that the power amplifier and the digital-to-analog (D/A) converter have a large dynamic range to avoid amplitude clipping, thus leading to the high power consumption and component cost of the system. Otherwise, the amplitude clipping would introduce a substantial amount of distortion. Considering the seriousness of high PAPR, several techniques have been proposed [2], [32] and [27] such as clipping, SLM and partial transmit sequence (see Chapter 3) to alleviate the power efficiency problem. SLM is the most attractive of these techniques as it can reduce the PAPR with no distortion and relatively small complexity. Note that applying SLM separately on each node of a cooperative network adds more complexity and makes this scheme impractical. In this chapter, it is therefore shown that SLM can be included in a decode-and-forward (DAF) cooperative network for PAPR reduction with relatively low complexity. It is proposed to implement the SLM scheme at the source node and forward the SI through the relay stages. Otherwise, applying the scheme at both the source and the relay stages increases the complexity and makes it unsuitable for practical application. Simulation results show the comparison between the two schemes and confirms that the degradation in end-to-end bit error rate is relatively small but proportional to the number of relay stages.

The layout of this chapter is as follows. Section 7.2 describes the proposed relaying system model for SLM implementation in a cooperative network. In Section 7.3, simulation results are given. Finally, Section 7.4 is the chapter summary.

7.2 Proposed Relaying System Model

A VAA network using a DAF approach, which consists of one source, one destination and four relay nodes within both stages each equipped with one antenna, is considered as in Figure 7.1. These virtual antennas are assumed to have perfect collaboration, synchronization and also perfect channel state information (CSI) at each stage of the network. CSI is easier to obtain with time-division duplex (TDD) transmission as the channels in the uplink and downlink are essentially symmetric [6]. The cooperative transmission procedure of the proposed scheme operates as follows: the transmission of information data from source to destination goes through two stages where the relay terminals are set to work in the DAF mode. Basically, the SLM scheme explained in Section 3.1.4 is applied to the original data, where the OFDM symbol, $\mathbf{C}$, is mapped to a number of M independent candidate symbols representing the same information. Then, the candidates $[c_i(0), ..., c_i(N-1)]$ are generated by multiplying carrier-wise the original OFDM frame with M phase vectors $\mathbf{b}^{(m)} = [b_0^{(m)}, ..., b_{N-1}^{(m)}]$, $b_u^{(m)} \in \{\pm 1, \pm j\}$. Next, the combination with the lowest PAPR along with the SI is transmitted to the relay nodes R_i, i=1,...,4. The PAPR at the source node is defined as:

$$PAPR = \frac{\max_{0 \le n \le NL-1} |s_i[n]|^2}{E\{|s_i[n]|^2\}} \tag{7.2.1}$$

where $s_i[n]$, and in the source node $i = 1$, max[·], E{·} and $|\cdot|$ represent respectively the discrete-time samples of the i^{th} transmit antenna of the OFDM signal, the maximum element, the expected value and the absolute value of the input symbols.

Note that the discrete-time samples of the OFDM signal are expressed as:

$$s_i[n] = \frac{1}{\sqrt{N}} \sum_{k=0}^{N-1} c_i(k) e^{j2\pi nk/LN} \ , 0 \le n \le LN-1 \tag{7.2.2}$$

where $j = \sqrt{-1}$, L is the oversampling factor and $c_i(k)$ is the k^{th} subcarrier of the i^{th} transmit antenna ($i = 1$ at the source node and $i =$ 1,...,4 at the relay stage).

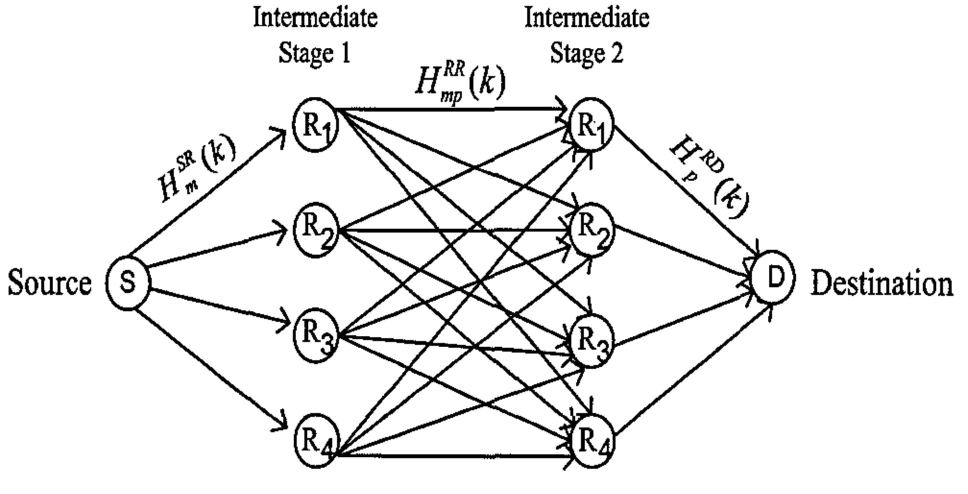

Figure 7.1. Three-link DAF cooperative network which consists of one source, one destination and four relay nodes within both stages, at the $k-th$ carrier.

It is assumed that the channel satisfied quasi-static fading assumption, in which the fading coefficients are constant within one transmission block, but change independently from one block to another. It is also assumed that the fading channels between the source and each relay, between the intermediate stages and between the last intermediate stage and the destination are independent. Moreover, it is assumed that the transmission channels through all relays are uncorrelated. Denoting the channel transfer function of the subcarrier k from the source, S, to the m^{th} relay as $H_m^{SR}(k)$, from the m^{th} relay to the p^{th} relay as $H_{mp}^{RR}(k)$, from the p^{th} to the destination as $H_p^{RD}(k)$. With the frequency domain representation of the multipath channels, $H_m^{SR}(k) = \sum_{l=0}^{L} h_m^{SR}(l)e^{-j2\pi lk/N}$, $H_{mp}^{RR}(k) = \sum_{l=0}^{L} h_{mp}^{RR}(l)e^{-j2\pi lk/N}$ and $H_p^{RD}(k) = \sum_{l=0}^{L} h_p^{RD}(l)e^{-j2\pi lk/N}$. At the source N symbols at each carrier frequency $c_i(k)$, $k = 0, ..., N-1$ are transmitted from the source to the first intermediate stage, such that the received signal at m^{th} relay:

$$y_m^R(k) = H_m^{SR}(k)c_i(k) + n_m(k) \tag{7.2.3}$$

where $n_m(k)$ is zero mean complex Gaussian random variable with the variance of σ_N^2.

At the relays maximum likelihood decoding is applied and a new vector, $y_m = [y_1[0], ..., y_1[N-1]]$, is formed. This block of data is then encoded with a STBC scheme between the first and the second intermediate stage. The same scenario is repeated from the second intermediate stage to the destination.

Clearly, the retransmitted signal again suffers from large PAPR which has to be reduced. In this case, implementing SLM again would effectively reduce the PAPR at the intermediate stage. However, the downside of this is that it adds $(M-1)$ extra[2] set of computations and the power cost associated with the implementation of $(M-1)$ IFFTs. Therefore, the objective of this study is to mitigate the PAPR of the signal after the intermediate stage(s) by reducing the computational complexity to only one IFFT at each node. This, however, can be performed by decoding the SI transmitted from the source and choosing the corresponding phase sequence at stage 1. Next, multiply the OFDM symbols at each relay antenna by the decoded phase sequence in which the scheme across these antennas shares the same SI. Using MIMO-SLM can improve the overall BER performance and increase the reliability of SI offered by the MIMO system. In this case, at the intermediate stage, the PAPR is calculated based upon the worst case:

$$PAPR_{MIMO} = \max_{i} \left(\frac{\max_{0 \le n \le NL-1} |s_i[n]|^2}{E\{|s_i[n]|^2\}} \right) \tag{7.2.4}$$

At stage 2, the same scenario is repeated again. Finally, at the receiver, the received signal is mapped to the original data according to the final SI received. Similarly, to recover the original data OFDM sequence, $\lfloor \log_2 M \rfloor$ bits are needed to provide the SI.

[2] M is number of independent candidate symbols in SLM scheme, see Chapter 3, Section 3.1.4.

7.3 Simulation results

In this section, a simulation comparison between two structures of VAA networks is performed: one compromises of one source node, one destination node and one intermediate relay stage and the other network has one source node, one destination node and two sets of intermediate relay stages. This simulation is for a complex baseband OFDM system employing QPSK with $N = 128$ subchannels. In both structures, it is assumed that there is a perfect collaboration and synchronization between the network nodes at each stage and the closed loop QO-STBCs with decode and forward is used at these intermediate relay stage(s). The performance of the PAPR reduction scheme for these multi-hops networks was tested by a Monte Carlo simulation with 10^5 randomly generated OFDM block symbols.

The complementary cumulative distribution function (CCDF) of PAPR is used to measure the performance which is defined as the probability that PAPR of OFDM symbols exceeds a given threshold γ:

$$CCDF = Pr(PAPR > \gamma) \tag{7.3.1}$$

In Figure 7.2, the CCDF of the PAPR is evaluated before and after applying the SLM scheme at both the source node and the relay stages. In this figure, it can be seen that in the absence of the SLM scheme, both the source node and the relay stage have a PAPR of approximately 11.3 dB at the probability of 0.001. However, once the SLM is applied at either the source or the relay, the PAPR reduces dramatically to

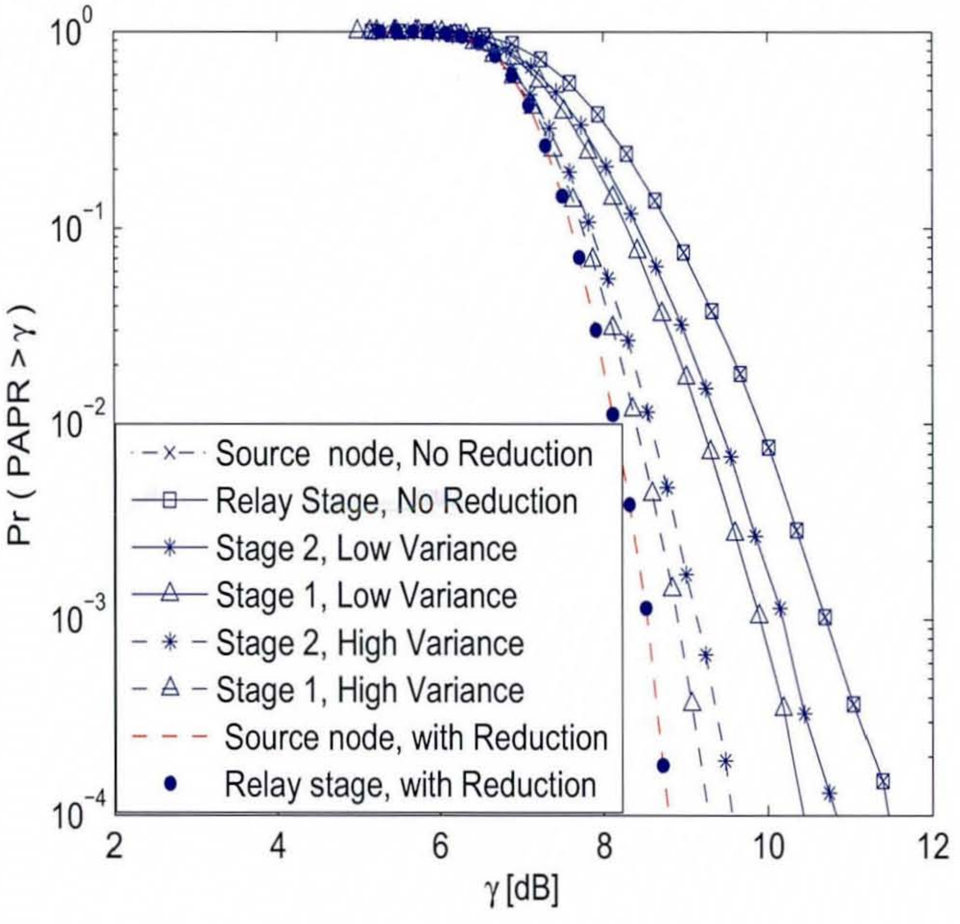

Figure 7.2. CCDF of the PAPR, the frame with minimum PAPR at the source node and minimax PAPR at the intermediate relay stages for $M = 4$, $N = 128$ with QPSK and the Nyquist oversampling factor.

approximately 8.8 dB at the same probability for both nodes. This is because the OFDM signal is very sensitive to phase shifts in the frequency-domain. Notice that the PAPR at the relay stage is measured based on the minimum maximum (minimax) criterion.

The second test was performed when the SLM scheme was only applied at the source node at a fixed value of SNR and the noise variance was the only factor changed. In Figure 7.2, it can also be seen that once the noise is raised to a higher value, for example SNR = 30, the PAPR performance degraded towards the right recording 9.2 dB for the first relays group and 10.2 dB for the second relays at the probability of 0.001. Here, as one can see the degradation is worse in the second link as it suffers from a larger noise. On the other hand, this performance improves moving to the left when the noise variance decreased to 15 dB showing a value of 8.8 dB and 9.2 dB, at the same probability, for the first and the second relay group respectively. So, as the number of intermediate stages is increased, as expected, the degradation becomes worse.

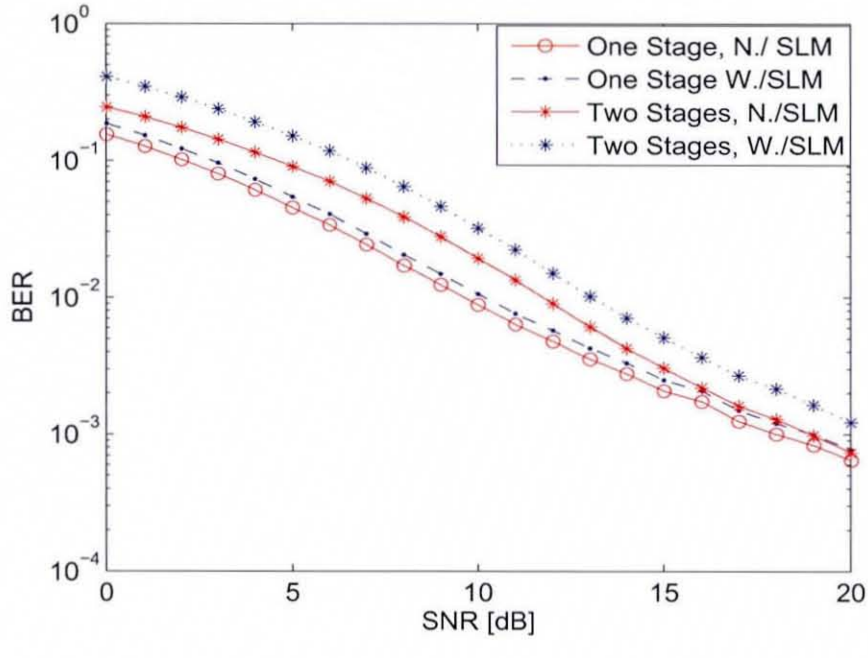

Figure 7.3. BER comparison between three and four-stages network with and without SLM for QPSK, N = 128 and M = 4 (The slight fluctuation in BER is due to simulation length).

This, however, provides a good indication that the PAPR within a cooperative network can be reduced by only reducing the signal peak at the output of the source with no need for this to be performed at the relay stage. This, however, reduces the computational complexity and can offer more practical method to mitigate PAPR in cooperative networks.

The end-to-end bit-error rate (BER) simulation for the aforementioned network structures is given in Figure 7.3. In this figure, the BER performance, for each structure, with and without the use of the SLM scheme at the intermediate stage(s) is depicted. In the case of using one intermediate stage structure, there is no difference in BER performance before and after applying SLM. This means that the SI can be detected correctly at the destination node, thanks to diversity.

Clearly once the number of intermediate stages is increased to two, its performance becomes worse, compared with the one stage VAA structure, at lower SNR. Here, interestingly, when the complexity is reduced, i.e SLM scheme is merely applied at the source node, the SNR penalty is only 2 dB. From this figure, it can be concluded that the BER performance is degraded as the number of intermediate stages is increased. This is due to the fact that the noise is proportional to the link length which, however, leads to wrong detection of SI at the final destination.

7.4 Summary

The PAPR reduction in the context of a one and two-stage virtual antenna multi-hop network using the SLM scheme has been studied. It has been observed that when the noise variance in the link is large then the likelihood that the error in the SI at the receive node is going to increase leading to an incorrect sequence for reducing the PAPR and vice versa. Likewise, if there is a mistake on receiving the SI, the received signal at the final destination will have a large BER. This is due to the fact that the received signal with the wrong phase rotation causes a large BER.

Chapter 8

CONCLUSIONS

8.1 Summary of the thesis

Orthogonal frequency division multiplexing (OFDM) has become a popular technique for high speed data transmission in frequency-selective radio channels [52] [53]. It has been adopted in different wireline and wireless communication standards such as high-bit-rate digital subscriber lines (HDSL), asymmetric digital subscriber lines (ADSL), very high-speed digital subscriber lines (VHDSL), digital audio broadcasting (DAB), and high-definition television (HDTV) [54].

In OFDM, intersymbol interference is prevented by adding a guard interval, which allows multipath effects to be mitigated using a simple equalizer on a frequency-by-frequency basis. This simplifies the design of the receiver and leads to inexpensive hardware implementations. One disadvantage of using OFDM is that its time-domain signals suffer from large envelope variations. Such variations, quantified by the peak-to-average power ratio (PAPR), can be a problem for certain devices such as digital-to-analog converters (D/A) and power amplifiers (PAs) in the transmitter. In particular, realization of an amplifier with a large linear range of operation can be expensive. If a high PAPR signal passes through an amplifier with a nonlinear response, it may suffer significant out-of-band radiation leading to spectral regrowth and in-band distortion causing an increase in the bit-error rate (BER) and performance degradation [1]. The drawbacks and problems of high PAPR were explained in detail in Chapters 1 and 2.

For high data rate, wireless, wideband applications, multiple-input multiple-output (MIMO) transmission combined with OFDM is being considered in a large number of current technology applications such as WiFi/WiMax [9]. However, as with SISO-OFDM, one of the main disadvantages of MIMO-OFDM is that the signals transmitted from different antennas might exhibit a prohibitively large PAPR. Unfortunately, most of the techniques proposed to mitigate the PAPR are limited to specific situations such as only for single-input single-output (SISO) systems. Therefore, this thesis evaluated the PAPR techniques used in SISO systems and proposed four methods for PAPR mitigation in MIMO systems.

Chapter 3, provided a survey study of PAPR reduction techniques available in the literature for SISO-OFDM system. These techniques were classified into three areas; probabilistic techniques, clipping and filtering and coding techniques. The basic idea of the probabilistic techniques is to generate a set of statistically independent symbols either in the time or frequency-domains by modifying the data sequence and selecting the symbol with lowest PAPR for transmission. To recover the original data, the receiver has to know which candidate data block was used, which requires sending of side information (SI) along with the transmitted signal. Thus it is very important for the receiver to receive the SI correctly, since an error in the SI leads to a high risk of wrongly interpreting all of the transmitted symbols. By employing a MIMO system, the available degrees of freedom produced by additional transmit antennas could be utilised and transmit the SI more effectively and with no error.

Clipping and filtering is the simplest method as it combats the high peaks directly by distorting the signal prior to the amplifier. As explained above, however, this causes in-band distortion and out-of-band radiation.

Coding techniques limit the set of possible signals that can be transmitted. Only those signals with a low PAPR are chosen. Analysis revealed that if half of the possible code words were permissible then that could achieve a reduction in PAPR of 4.58 dB and if a quarter were used the reduction could be 6.02 dB. In fact, if the overall word length is eight or possibly ten, the method is computationally feasible but by the time the word length reaches sixteen or sixty four it is impractical to go through this as it would need an exceedingly large look-up storage table. However, another way to perform this scheme would possibly be to use different types of coding, either the Golay code or the Reed-Muller code. But the price for that is the extra redundancy, and therefore the reduction in code rate. For example, if the frame length is very large, say N = 256 to guarantee that the PAPR is going to be low, it might be necessary to operate at a redundancy rate of half or less. A comparison between these classification techniques was given in detail in Chapter 3, Section 3.4.

The reason for these classifications was to give researchers and engineers a guide-line into the correct choice of method depending on their constraints. Moreover, it allows new methods to be added according to the objective of the method, BER degradation and useful data rate loss. Here, it should be mentioned that these methods do not cover all the techniques studied during the last three decades. This is, however, firstly due to the huge quantity of work presented on this subject and secondly, that they share the same principles and thus can be grouped into three areas.

From this survey, the probabilistic techniques were chosen to be the most effective for comparing with the other two families of PAPR reduction. This is because probabilistic techniques are distortionless techniques and have little cost in transmission efficiency. This, however, encouraged the mitigation of the PAPR in the work in this thesis to be based on using the same principle without distorting the original signal. A focus on quasi-orthogonal space-time block codes (QO-STBCs) as an example for MIMO-OFDM was undertaken since they provide high capacity, full code and full diversity when the closed loop feedback is applied.

In Chapter 4, a study of a PAPR reduction scheme for QO-STBCs MIMO-OFDM systems based on selective mapping (SLM) was presented. Instead of applying individual SLM to each antenna, the sequence with the minimum average (miniaverage) PAPR over four transmit antennas was selected. Using SLM in a MIMO-OFDM system can improved the overall bit-error rate (BER) performance as compared to using SLM in a SISO-OFDM system and increased the reliability of SI. Simulation revealed that when this scheme is used, the PAPR is improved by 24.3 %, at probability of 0.001 and M = 4, compared with the no PAPR reduction (M = 1). In terms of BER performance, it was observed that, at BER = 0.001 the closed-loop scheme needed SNR of approximately 11 dB while this value increased to at least 17 dB with the SISO-SLM scheme. Furthermore, the probability of detection of SI for both $L_t = 2$ MIMO-STBC and $L_t = 4$ QO-STBCs, where L_t is the number of transmit antennas, based on the SLM technique was provided. This simulation illustrated that when $L_t = 2$, both the numerical and the analytical results give a probability of SI detection around 0.95 at SNR = 1 dB and with $L_t = 4$, this probability is increased by approximately 4 % confirming the utility of the scheme.

In Chapter 5, a new technique for PAPR reduction in the context of closed-loop QO-STBCs with a realistic amount of feedback was studied. This technique was based upon rotating two symbols in the OFDM frame in place of sending useful information in combination with the SLM method, so that the miniaverage PAPR over all four transmit antenna decreased whilst maintaining the diversity gain. Furthermore, in this work, the number of feedback bits needed to represent the feedback phase angles reduced by exploiting the correlation across frequencies of the required rotation angles. Using a set of 64 rotation angles to rotate two symbols in the third and fourth antennas, at the probability of 0.001 and without using SLM, the new scheme achieved only 3.5 % PAPR reduction of the threshold, γ, as compared with the no PAPR reduction. However, by combining the SLM approach, the PAPR achieved 20.5 % at the same probability.

In Chapter 6, three techniques based on cross-antenna rotation and inversion (CARI) were presented for the reduction of PAPR for the closed loop QO-STBCs, one called a successive suboptimal cross-antenna rotation and inversion (SS-CARI). The principle of this technique was to partition the input OFDM frame into M subblocks of equal size, then, subblockwise, four permutations of rotations and inversions across pairs of two antennas were performed. Starting from the first subblock, four different OFDM sequence sets were formed where all the other subblocks remain unchanged, then the sequence set which yielded the minimum maximum (minimax) PAPR was selected and, by doing this for all M subblocks successively, the resulting PAPR, at the probability of 0.001, showed a reduction of 23 % and 31 % for M = 4 and 16 respectively compared with the no PAPR reduction.

Another suboptimal scheme called random RS-CARI was also proposed in this chapter; where the sequences for each of the M subblocks were chosen randomly from amongst those used in SS-CARI, for a prescribed number of times P, and the symbol with the minimax PAPR performance was selected for transmission. In this case, the computational complexity was reduced but the PAPR reduction is degraded to 17.7 % and 25.7 % instead of 23 % and 31 %. Moreover, a comparison between the minaverage criterion used in Chapters 4 and 5 and the minimax criterion used in this chapter was performed. It was observed that the minimax criterion outperforms the minaverage by 0.7 dB with the optimal scheme and 0.3 dB with the suboptimal scheme.

The third algorithm proposed in this chapter was to employ a set of scrambling data before the CARI scheme was applied and then the transmitted OFDM symbols were selected as being the ones which have the minimax PAPRs amongst all the transmission symbols from the four antennas. This achieved better reduction than SS and RS-CARI scheme. It showed a PAPR reduction of 35 % and 30 % instead of 31 % and 25.7 % recorded, respectively, by SS and RS-CARI scheme. This scheme takes advantage of the fact that changing the signal phase in the frequency domain leads to a good PAPR reduction. The pseudo-code for this algorithm was presented in this chapter.

In Chapter 7, the application of SLM PAPR mitigation in a broadband multi-hop network in the case of having one and two intermediate stage(s) was studied. This study discussed two different ways of minimizing the PAPR in a decode and forward virtual antenna multi-hop network; once by applying the SLM technique only on the source node and the other one by applying this technique on both source and relay stage(s). Simulation results demonstrated that when the noise variance in the link was large then the likelihood was that the error in the SI at the receive node would increase, leading to a wrong sequence for reducing the PAPR and vice versa. It has also been shown that a mistake on receiving the SI, leads to a large BER on the received signal at the final destination.

8.2 Overall conclusions and future work

From this research, it is clear that when an algorithm for PAPR reduction is designed, the following criteria should be taken into account:

1. High PAPR reduction capability: The PAPR reduction algorithm should have a high PAPR reduction capability, with as little usage of side information as possible.

2. Minimal computational complexity: The PAPR reduction algorithm should be computationally efficient. Both time and hardware stipulations for the PAPR reduction should be kept to a minimum. Generally, complex techniques display better PAPR reduction.

3. No redundancy: The loss in data transmitted as a result of side information should be avoided or at least be kept to a minimum. Usually, there exists a trade off between the loss in transmitted data and distortion of the signal.

4. Minimal performance deterioration: Blind techniques suffer from distorted signals, which lead to degradation in BER, without reducing throughput. On the other hand, non-blind techniques experience reduced throughput without distorting the signal.

5. No spectral regrowth: spectral regrowth is a very significant aspect of the PAPR reduction technique since it affects the neighbouring channels, which then causes interference. Therefore, clipping techniques are not desirable, even if they show marked PAPR reduction.

6. Power control: In the case of wireless communications, the power of the transmit signal should be kept constant.

7. Cost saving with high efficiency: the cost saving in power amplifiers and digital-to-analog converters offered by the efficiency of the PAPR reduction technique is a critical factor in designing the appropriate PAPR reduction method.

These are the most important criteria demonstrated by this research. However, it may not be possible to meet all the requirements of an ideal PAPR reduction algorithm for a given situation and a trade-off between PAPR reduction and other factors, such as overall cost, error performance, complexity, and efficiency, should be sought.

Two topics that have resulted from this research which may be considered worthy of further exploration and development:

(i) Although the PAPR reduction algorithms proposed in Chapter 5 can be used with low complexity, by using two phase rotations in certain frequency bins taken from a set of 64 possibilities, it would be interesting to develop a more sophisticated PAPR reduction algorithm which examines the optimal way of finding the values of $\{\beta_1, \beta_2\}$, so that whatever the data samples and feedback values, the PAPR always remains minimum.

(ii) The PAPR reduction in the context of a decode and forward virtual antenna multi-hop network using the SLM scheme has been explored in Chapter 7. This has demonstrated that the degradation in side information is proportional to the number of intermediate stages. It would be interesting to analyze that degradation as a function of the number of hops.

BIBLIOGRAPHY

[1] S. Litsyn, *Peak Power Control in Multicarrier Communications.* Cambridge University Press, 2007.

[2] Li. Xiaodong and L. J. Cimini, "Effect of Clipping and Filtering on the Performance of OFDM," *IEEE Transactions on Wireless Communications*, vol. 3, pp. 1634–1638, 1997.

[3] T. S. Rappaport, *Wireless Communications: Principles and Practice.* Prentice Hall., 1996.

[4] J. G. Proakis, *Digital Communications.* New York: McGraw-Hill, 1989.

[5] W. Mohr and W. Konhäuser, "Access Network Evolution Beyond Third Generation Mobile Communications," *IEEE Commun. Mag.*, vol. 38, no. 12, pp. 122–133, 2000.

[6] M. Dohler, E. Lefranc and H. Aghvami, "Space-time block codes for virtual antenna arrays," *Personal, Indoor and Mobile Radio Communications, 2002. The 13th IEEE International Symposium.*, vol. 1, pp. 414–417, 2002.

[7] M. Dohler, *Virtual Antenna Arrays.* Ph.D. thesis, University of London, United Kingdom, 2004.

[8] R. van Nee and R. Prasad, *OFDM for Wireless Multimedia Communications.* Artech House, Boston, 2000.

[9] H. Yagoobi, "Scalable OFDMA Physical Layer in IEEE 802.16 WirelessMAN," *Intel Technology Journal*, vol. 08, no. 3, pp. 201–212, 2004.

[10] ETSI, *Radio Broadcasting Systems: Digital Audio Broadcasting (DAB) to mobile, portable and fixed receiver.* European Telecommunication Standard ETS., 1997.

[11] ETSI, *Digital Video Broadcasting (DVB): Framing structure, channel coding and modulation for digital terrestrial television.* EN 300 744.

[12] Y. L. Lee, Y. H. You, W. G. Joen, J. H. Paik, and H. K. Song, "Peak-to-average power ratio in MIMO-OFDM systems using selective mapping," *IEEE Commun. Lett.*, vol. 3, no. 12, pp. 575–577, 2003.

[13] S. Darlington, "On Digital Single-sideband Modulators," *IEEE Transactions on Circuit Theory*, vol. 17, no. 3, pp. 409–414, 1970.

[14] L. J. Cimini, "Analysis and Performance Evaluation of a Digital Mobile Channel Using Orthogonal Frequency Division Multiplexing," *IEEE Transactions on Communications*, vol. 33, no. 7, pp. 665-675, 1985.

[15] E. Costa, M. Midrio and S. Pupolin,, ""Impact of Amplifier Nonlinearities on OFDM Transmission System Performance," *IEEE Comm. Letters*, vol. 3, no. 2, pp. 37–39, 1999.

[16] N. Chen and G. Tong, "Peak-to-Average Power Ratio Reduction in OFDM with Blind Selected Pilot Tone Modulation," *IEEE Transactions on Wireless Communications*, vol. 5, no. 8, pp. 845–848, 2006.

[17] J. Tellado, *Multicarrier modulation with low PAPR: Applications to DSL and Wireless.* Massachusetts, USA: Kluwer Academic Publishers, 2000.

[18] A. V. Oppenheim and J. R. Buck, *Discrete-time signal processing.* Upper Saddle River, NJ, USA: Person Education, Inc., 1999.

[19] M. Friese, "Multitone signals with low crest factors," *IEEE Trans. Commun.*, vol. 45, pp. 1338–1344, 1997.

[20] W. Rudin, "Some theorems on Fourier Coefficients," *Proc. Amer. Math* , no. 10, pp. 855-859, 1959.

[21] S. Boyd, "Multitone signals with low crest factors," *IEEE Trans. Circuits Syst.*, vol. 33, pp. 1018–1022, 1986.

[22] M. R. Schroeder, "Synthesis of low-peak-factor signals and binary sequences with low correlation," *IEEE Trans. Inform. Theory*, vol. 16, pp. 85-89, 1970.

[23] S. Narahashi and T. Nojima, "New phasing scheme of N-multiple carriers for reducing peak-to-average power ratio," *Electron. Lett.*, vol. 30, pp. 1382–1383, 1994.

[24] M. S. Baek, M. J. Kim, Y. H. You and H. K. Song, "Semi-blind channel estimation and PAR reduction for MIMO-OFDM system with

multiple antennas," *IEEE Trans. Broadcast*, vol. 50, no. 4, pp. 414–424, 2004.

[25] H. Lee, D. N. Liu, W. Zhu and M. P. Fitz, "Peak power reduction using a unitary rotation in multiple transmit antennas," *in Proc. IEEE Int. Conf. on Commun*, vol. 4, pp. 2407–2411, 2005.

[26] M. Tan, Z. Latinovic and Y. Bar-Ness, "STBC MIMO-OFDM Peak-to-average power ratio reduction by Cross-Antenna Rotation and Inversion," *IEEE Commun. Lett.*, vol. 9, pp. 592–594, 2005.

[27] A. D. S. Jayalath and C. Tellambura, "Adaptive PTS approach for reduction of peak-to-average power ratio of OFDM signal," *Electronic Letters*, vol. 36, no. 14, pp. 1226–1228, 2000.

[28] S. H. Muller and J. B. Huber, "A comparison of peak power reduction schemes for OFDM," *Pr. IEEE GLOBECOM'97*, vol. 1, pp. 1–5, 1997.

[29] C. Tellambura, "Phase optimisation criterion for reducing peak-to-average power ratio in OFDM," *Electronic Letters*, vol. 34, no. 2, pp. 169–170, 1998.

[30] C. Tellambura, "Upper bound on the peak factor of N-multiple carriers," *Electronic Letters*, vol. 33, pp. 1608–1609, 1997.

[31] C. Van Eetvelt, G. Wade and M. Tomlinson, "Peak-to-average power reduction for OFDM schemes by selective scrambling," *Electronic Letters*, vol. 32, no. 21, pp. 1963–1964, 1996.

[32] R. W. Bauml, R. F. H. Fischer, and J.B. Huber, "Reducing the peak-to-average power ratio of multicarrier modulation by selected mapping," *Electronics Letters*, vol. 32, no. 22, pp. 2056–2057, 1996.

[33] A. E. Jones, T. A. Wilkinson and S. K. Barton, "Block coding scheme for reduction of peak to mean envelope power ratio of multicarrier transmission schemes," *Electronics Letters*, vol. 30, no. 25, pp. 2098–2099, 1994.

[34] A. E. Jones, and T. A. Wilkinson, "Minimisation of the Peak to Mean Envelope Power Ratio of Multicarrier Transmission Schemes by Block Coding," *IEEE Proc. Vehic. Tech. Conf.*, vol. 2, no. 20, pp. 825–829, 1995.

[35] R. D. J. Van Nee, "OFDM Codes for Peak-to-Average Power Reduction and Error Correction," *IEEE Trans. Signal Processing*, pp. 740–744, 1996.

[36] M. J. E. Golay, "Complementary Series," *IRE Trans. Information Theory*, vol. IT-7, pp. 82–87, 1961.

[37] R. Sivaswamy, "Multiple Complementary Codes," *IRE Trans. Information Theory*, vol. IT-24, no. 5, pp. 8–10, 1978.

[38] R. L. Frank, "Polyphase Complementary Codes," *IRE Trans. Information Theory*, vol. IT-26, no. 6, pp. 82–87, 1980.

[39] L. J. Cimini and N. R. Sollenberger, "Peak-to-average power ratio reduction of an OFDM signal using partial transmit sequences," *IEEE Commun. Lett.*, vol. 4, no. 3, pp. 86–88, 2000.

[40] F. S. Alharbi and J. A. Chambers, "Peak-to-average power ratio mitigation in quasi-orthogonal space time block coded MIMO-OFDM systems using selective mapping," *Antennas and Propagation Conference, LAPC 2008. Loughborough*, vol. 17, pp. 157–160, 2008.

[41] S. M. Alamouti, "A simple transmit diversity technique for wireless communications," *IEEE J. Select. Areas Commun.*, vol. 16, no. 12, pp. 1451– 1458, 1998.

[42] A. Goldsmith, *Wireless Communications.* Cambridge University, 2005.

[43] H. Jafarkhani, "A quasi-orthogonal space-time block code," *IEEE Trans. Commun.*, vol. 49, pp. 1–4, 2001.

[44] C. B. Papadias, G. J. Foshini, "A space-time coding approach for systems employing four transmit antennas," *IEEE ICASSP.*, vol. 4, pp. 2481–2484, 2001.

[45] C. Toker, S. Lambotharan, and J. A. Chambers, "Closed-Loop Quasi-Orthogonal STBCs and Their Performance in Multipath Fading Enviroments and When Combined With Turbo Codes," *IEEE Trans. Commun.*, vol. 3, no. 6, pp. 1890–1896, 2004.

[46] C. Toker, S. Lambotharan, "Closed-Loop Space Time Block Coding Technique for OFDM based Broadband Wireless Access Systems," *IEEE Trans. Commun.*, vol. 51, no. 3, pp. 765– 769, 2005.

[47] F. S. Alharbi and J. A. Chambers, "A combined SLM and closed-loop QO-STBC for PAPR mitigation in MIMO-OFDM transmission,"

EUSIPCO 2008-16th European Signal Processing Conference, Lausanne, Switzerland, August 2008.

[48] F. S. Alharbi and J. A. Chambers, "PAPR mitigation in closed-loop QO-STBCs using the cross-antenna rotation and inversion scheme," *8th International Conference on Mathematical in Signal Processing, Cirencester, UK,* December 2008.

[49] F. S. Alharbi and J. A. Chambers, "A new scrambled SS-CARI scheme for PAPR mitigation in closed-loop QO-STBC-MIMO-OFDM systems," *submitted to the Hindawi Advances in Signal Processing journal,* March 2009.

[50] F. S. Alharbi and J. A. Chambers, "A study of SLM PAPR mitigation in a broadband multi-hop network," *submitted to the 17th European Signal Processing Conference, Glasgow, Scotland,* March 2009.

[51] H. Bölcskei and A. Paulraj, "Space-frequency coded broadband OFDM systems," *Proc. IEEE WCN, Chicago* , vol. 1, no. 39, pp. 1–6, 2000.

[52] G. Foschini, "Layered space-time architecture for wireless communication in fading enviroment when using multi-element antennas," *Bell Labs Technical Journal.*, vol. 1, pp. 41–59, 1996.

[53] H. Yang, "A road to future broadband wireless access: MIMO-OFDM based air interface," *IEEE Commun. Mag.*, vol. 43, pp. 53–60, 2005.

[54] W. Y. Zou and Y. Wu, "COFDM: An overview," *IEEE Trans. Broadcasting*, vol. 41, pp. 1–8, 1995.